BIOGEOCHEMICAL AND ECOLOGICAL IMPACTS RESULTING FROM BEETLE-INDUCED FOREST MORTALITY

by

Brent Brouillard

A thesis submitted to the Faculty and Board of Trustees of the Colorado School of Mines in partial fulfillment of the requirements for the degree of Doctor of Philosophy (Civil and Environmental Engineering).

Golden, Colorado

Date: ________________

Signed: ______________________________
Brent Brouillard

Signed: ______________________________
Dr. Jonathan Sharp
Thesis Advisor

Signed: ______________________________
Dr. Eric Dickenson
Thesis Advisor

Golden, Colorado

Date: ________________

Signed: ______________________________
Dr. John E. McCray
Professor and Head
Department of Civil and Environmental Engineering

ABSTRACT

Over the last two decades, increasing temperatures and drought conditions have caused unprecedented bark beetle infestation across western North America. As forest die-off ensues, several aspects of the hydrologic cycle are altered due to canopy loss, altered evapotranspiration, and decreased water uptake by infested trees. Additionally, the cessation of root exudates along with the decay of enhanced litterfall following tree death alters biogeochemical cycling. These shifts may alter water quality or produce nutrient feedbacks into the atmosphere and hydrosphere. While modeling and field investigations have begun to elucidate these responses, questions still exist regarding whether a certain level of infestation is required to produce these secondary effects along with perceptions of increased fire risk that drive forest management policies. This work focuses on the ecological and biogeochemical shifts that occur following beetle infestation by investigating 1) shifts in aromatic carbon loading and subsequent disinfection byproduct (DBP) formation potential in beetle-impacted watersheds, 2) alterations in fire severity following mountain pine beetle infestation, and 3) how geochemical responses within soil horizons are influenced as a function of localized tree mortality severity.

Analysis of quarterly municipal monitoring data from 2004-2014 from six municipalities in the Rocky Mountain region of Colorado containing varying levels of beetle infestation were analyzed. Watersheds containing >50% areal infestation were found to have significantly increasing total organic carbon and DBP concentrations, with increases continuing nearly one decade after initial infestation. Alarmingly, DBP concentration trends at high-impact sites were found to exceed regulatory maximum contaminant levels during the final two years of analysis (2013-2014). Focused surface water sampling at each municipality further revealed elevated carbon loading and aromaticity in beetle-impacted sites, increasing DBP formation potential particularly during precipitation events. This additional sampling supports the hypothesis that degrading tree material along with elevated groundwater tables may be impairing surface waters used for human consumption following extensive beetle infestation.

The relationship between mountain pine beetle infestation and fire severity was analyzed from 2000-2014 across the Western United States. Maps delineating zones of beetle-impacted lodgepole and ponderosa pine forest were overlain with remote sensing fire severity data products providing validation across a range of ecoregions and fire conditions. Results demonstrate a decline in fire risk following beetle infestation with beetle-impacted forests burning 65-77% and 90-94% as severely compared to unimpacted controls; respectively, for lodgepole and ponderosa pine. Forest management decisions should be wary in removing beetle-impacted forests to mitigate fire threats as these actions may not reduce fire risk and can have unintended impacts to water quality.

Finally, as the severity of beetle infestation within a forest may impact biogeochemical response, near surface horizons (litter, organic, and mineral soil) were sampled below live and beetle-killed lodgepole pine trees surrounded by varying extents of tree mortality to investigate potential compensatory effects from surviving trees. While some edaphic parameters were significantly different between green and grey phase trees (water content, pH, soil respiration) many biogeochemical signatures tracked with the extent of surrounding tree mortality (carbon aromaticity, C:N ratio, ammonium). Furthermore, the proportion of ammonium in the total nitrogen pool primarily increased once surrounding tree mortality exceeded 40%, demonstrating compensatory effects from surrounding live trees when infestation levels are minimal. Declining C:N ratios and an elevated proportion of ammonium indicate an enrichment of nitrogen in this N-limited ecosystem which may promote regrowth after forest disturbance.

TABLE OF CONTENTS

LIST OF FIGURES

LIST OF TABLES

ACKNOWLEDGMENTS

What a wild ride these last five years at Mines has been. I vividly remember driving to Grand Lake when I was in high school and seeing the vast amount of forest impacted by bark beetles. I never thought that ten years later I would be investigating the water quality impacts following this infestation or trying to answer everyone's main concern about whether this tinderbox of dead trees would increase fire severity. But here I am, and I have so many people to thank for their support along the way.

My family has always pushed me to search for opportunities and I am so grateful of their continued support toward my educational endeavors. Thanks to my friends for providing someone to lean on and for getting me outside during our many camping, fishing, snowboarding, and biking trips. One of the best parts about CSM is the quality of their graduate students. Not only have my peers in the CEE department and Hydrology program provided invaluable assistance during my PhD research, but they have also become well-respected friends. I would also like to thank the National Science Foundation for funding the research conducted in this Thesis under Grant No.'s WSC-1204787 and CBET-1055396.

A special thanks goes out to my committee members for valuable insights and contributions to this thesis. Thank you Dr. Spear for making me think outside of the box about microbiology and adding a perpetual sense of humor to the lab. I'd like to thank Dr. Hogue for teaching two of my favorite classes I took in the hydrology program (Watershed Modeling and Snow Hydrology). Dr. Dickenson has been an incredible co-advisor. The bulk of my second chapter would not have occurred without your invaluable assistance. Thank you for strengthening my passion for water quality/water resources and for the opportunity to work at SNWA. Most of all, thank you Dr. Sharp for being an incredible advisor. During my time at Mines you taught me how to think critically about research and helped drastically improve my writing abilities. You gave me freedom to explore different avenues within my research topics while providing the appropriate amount of guidance when needed. Thank you for allowing me the opportunity to join your lab and always being an advocate for your students.

CHAPTER 1

INTRODUCTORY REMARKS

Recent drought and warmer temperatures associated with climate change have increased the magnitude and scale of forest mortality (Williams et al., 2010), with continued widespread conifer loss predicted in the coming decades (McDowell et al., 2015). These land cover disturbances can impact hydrologic and biogeochemical cycles, as well as alter water quality and quantity making source waters more difficult to treat (*Agriculture, Hydrology and Water Quality*, 2002; Mikkelson et al., 2013a; Smith et al., 2011; Tong and Chen, 2002). For instance, forest fires and flood events are natural disturbances that rapidly alter surface waters, leading to an increase in nutrient content, suspended solids, and sediment loading in adjacent streams and storage reservoirs (Burke et al., 2013; Smith et al., 2011; Whitworth et al., 2012). Alternatively, anthropogenic disturbances such as timber harvesting can also impact organic carbon, major ions, and nitrate concentrations in proximal waters (Kalbitz et al., 2004; Likens et al., 1970; Vitousek et al., 1979). Studying shifts in vegetation response and biogeochemical cycling after forest disturbances can help predict and address nutrient flux in analogously impacted systems.

A large portion of the forest mortality occurring across North America can be attributed to bark beetle infestation. Although indigenous, bark beetles have impacted millions of hectares of evergreen forest across the western United States and Canada over the last two decades due to warming temperatures and drought conditions (Park Williams et al., 2012; Raffa et al., 2008; Williams et al., 2010). Analogous infestations are also occurring in coniferous regions of Europe (Štursová et al., 2014) and Asia (Tokuchi et al., 2004) as well as deciduous portions of North America (Herms and McCullough, 2014). The focus of this thesis will be investigating the biogeochemical and ecological shifts that occur following beetle-infestation in the Rocky Mountains and Western United States.

As beetle-induced tree mortality occurs, shifts in aqueous carbon cycling have been shown to alter water quality in municipal watersheds (Mikkelson et al., 2013b). This may create the need to more actively manage source waters or expand technologies used in drinking water treatment facilities. The second chapter of this thesis focuses on water quality effects associated with this type of forest disturbance. We hypothesized that surface waters in beetle-impacted watersheds display higher carbon loading and more aromatic carbon character compared to control watersheds, which subsequently increases disinfection byproduct formation potential. However, we predicted that these shifts in water quality only occur in watersheds experiencing a certain level of beetle infestation.

As beetle-induced tree mortality occurs, alterations to the hydrologic and biogeochemical cycle alter water quality (Figure 1.1). Initially within the first year of infestation, tree death occurs and water uptake ceases, increasing water tables particularly during the summer and fall (Bearup et al., 2014; Penn et al., 2016). Additionally, production of root exudates ceases causing a decline in organic carbon inputs into the soil (Moore et al., 2013; Štursová et al., 2014). After the tree stops transpiring, needles turn red and fall to the ground in a comparatively rapid pulse (1 to 3 years post-infestation). Eventually roots decompose and the tree falls to the forest floor (Mikkelson et al., 2013a). Deposits of needles and other tree components after forest die-off contain high molecular weight compounds such as lignin and cellulose that are recalcitrant in character

(Šturšová et al., 2014; Weintraub et al., 2007). Annual litterfall rates double for several years after infestation (Kaňa et al., 2012) leading to elevated organic pools in upper soil horizons beneath impacted trees (Huber et al., 2004; Kaňa et al., 2012) which may change the composition of surface and ground water sources.

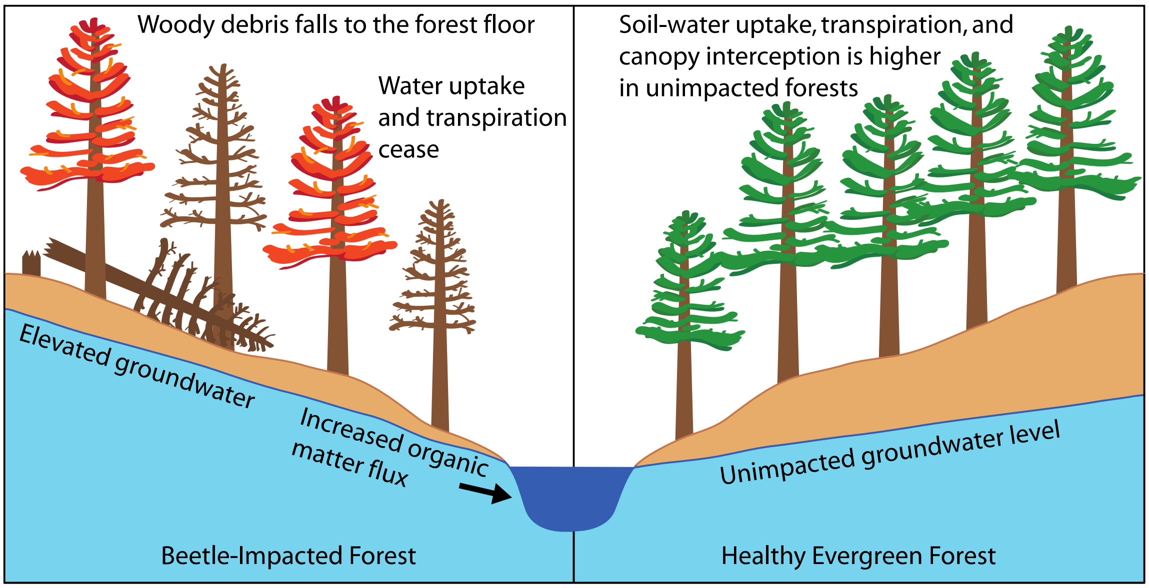

Figure 1.1: A conceptual diagram depicting hydrologic and biogeochemical shifts associated with bark beetle infestation (Brouillard et al., 2016).

These waters can experience increases in disinfection byproduct (DBP) formation during drinking water treatment as added chlorine comes into contact with humic and fulvic fractions of natural organic matter. Resultant DBPs including trihalomethanes (THMs) and haloacetic acids (HAAs) (Grünwald et al., 2002; Jung and Son, 2008; Nikolaou and Lekkas, 2001) are regulated by the Environmental Protection Agency's (EPA) Stage 1 and 2 Disinfection Byproduct Rules and are known carcinogens (*Comprehensive Disinfectants and Disinfection Byproducts Rules (Stage 1 and Stage 2): Quick Reference Guide*, 2010; Richardson and Postigo, 2011). A recent investigation revealed elevated total organic carbon (TOC) levels in beetle-impacted municipal water sources compared to control municipalities, while median effluent DBP concentrations were tenfold higher in beetle-impacted municipalities compared to control municipalities (Mikkelson et al., 2013b).

To further elucidate these changes, water quality was investigated in six municipal watersheds within the Colorado Rocky Mountains that contained varying degrees of beetle infestation. Historical TOC and DBP data from 2004-2014 was first compared to level of impact. Although this historical regulatory data allowed analysis of altered water quality parameters across a timeframe associated with the expansion of beetle infestation within each watershed, this dataset contained uncertainties related to variable water treatment operation, sample timing, and other collection biases. To help alleviate these uncertainties, surface water sampling at the intake of each of the six water treatment facilities were collected for ~1.5 years to gain additional insights into the drivers of increased DBP formation potential including aromatic carbon content, seasonal variations, and hydrologic shifts.

When the findings from chapter two were presented to water utility managers and various stakeholders at American Water Works Association events, many of the participants were mainly concerned about increased wildfire severity following beetle infestation and the secondary impacts to water quality associated with fire events. To address these concerns, chapter three investigates whether increased fire severity is visible following mountain pine beetle infestation across the Western United States. We hypothesized that fire severity would decline in beetle-impacted forests due to reduction in fuel loads associated with canopy loss.

Wildfire frequency has increased over the last two decades due to drought and warmer temperatures (“A burning issue for insurers?,” 2013; Park Williams et al., 2012; Westerling, 2006; Williams et al., 2010) which has sizeable implications for property damage and human health impacts. Societal concern regarding fires has heightened in part due to increased development in the wildland-urban interface (“A burning issue for insurers?,” 2013; Calkin et al., 2014) with total economic losses from fire in the US doubling from $6.8 billion from 1992-2001 to $13.7 billion from 2002-2011 (Haldane, 2013). Beetle infestation has also caused a striking visual of expansive red and grey phase forests, which has raised questions from the public regarding correlations between the vast amount of dead fuel from beetle-induced tree mortality and subsequent shifts in fire danger.

Specifically, questions exist about whether shifts in surface and canopy fuels from beetle-induced tree mortality lead to increased burn severity (Hicke et al., 2012). Burn severity is traditionally defined as the qualitative assessment of soil heating, consumption of litter, duff, and the organic layer beneath vegetation, and the mortality of underground plant parts (“Glossary of Wildland Fire Terminology,” 2014). In chapter three, burn severity is evaluated based on the effects of fire on above-ground biomass. Within one year following beetle infestation, needles turn red. Increases in ignition, torching potential, and crown fires have been predicted due to lower foliar moisture, non-fiber carbohydrate, and crude fat content which increase flammability (red phase, Figure 1.2) (Hicke et al., 2012; Jolly et al., 2012; Page et al., 2012). Approximately three to four years after tree mortality, needles and twigs drop to the forest floor (grey phase, Figure 1.2) (Hicke et al., 2012). This decreases canopy fuel loads and lowers crown fire risk;

however, elevated forest floor fuels may increase ground fire severity while vegetation regrowth or increased tree fall may provide ladder fuels that carry fire into the crown, possibly counteracting lower crown fire risk due to decreased canopy bulk density (Hicke et al., 2012; Jenkins et al., 2014).

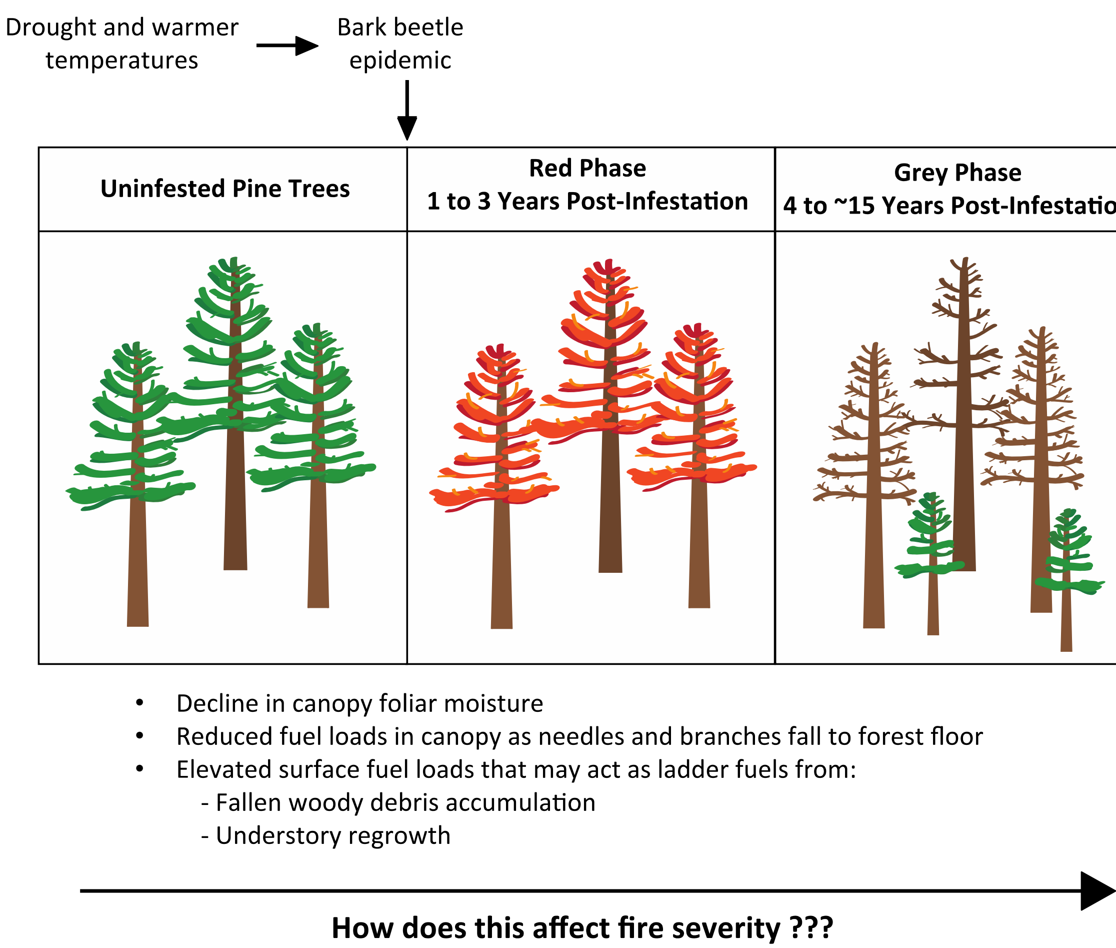

Figure 1.2: Alterations to forest structure and fuel loads following beetle infestation that may affect fire severity.

Although recent studies have begun to elucidate the links between beetle infestation and wildfires (Bebi et al., 2003; Harvey et al., 2014; Hoffman et al., 2013; Lynch et al., 2006; Meigs et al., 2015; Schoennagel et al., 2012; Simard et al., 2011), there is a range of conflicting viewpoints regarding the effects of beetle impact on fire behavior and empirical observations are lacking. It is clear that beetle infestation alters fuel loads. Stand-level fire behavior models suggest that these shifts change fire behavior (Hoffman et al., 2013; Jenkins et al., 2014; Schoennagel et al., 2012; Simard et al., 2011), yet it is uncertain if these fuel loads lead to observable changes in observed fire severity. Retrospective studies using discrete fire localities have reported varying effects of beetle outbreaks on fire behavior (Harvey et al., 2014; Kulakowski and Velben, 2007; Lynch et al., 2006). Additionally, beetle infestations in previous fire-related studies do not always compare in size, extent, and severity to the current outbreak or the fires analyzed were limited in number providing results for a limited set of fire conditions or infestation stage (Meigs et al., 2016). These uncertainties emphasize the importance of validating model results and expanding conclusions found through discrete fire analysis by conducting large-scale, spatial and temporal analysis of observed landscape disturbance trends. Yet to date, few studies have taken this approach to evaluate the impacts bark beetle infestation has on fire risk. A recent study that utilized this approach contradicted the expectation for increases in burned mountain pine beetle (MPB) area following infestation; specifically, no differences were found in expected and observed wildfire burn area during three peak fire years across the Western US (Hart et al., 2015). Additionally, recent work conducted in the US Pacific Northwest found that fire severity within MPB and western spruce budworm impacted forests reduced subsequent fire severity (Meigs et al., 2016).

In chapter three, the links between fire severity and beetle infestation are analyzed from 2000-2014 across the Western United States. Zones of mountain pine beetle infestation were overlain with fire severity maps to determine if fire severity increased with this form of forest disturbance. Severity analysis was conducted in both lodgepole and ponderosa forests using three different remote sensing fire severity products (dNBR6, dNBR, and RdNBR). Over 600 forest fires were analyzed covering a range of topography and ecoregions to address public concern and contribute to the growing body of research evaluating the links between beetle infestation and fire severity.

Chapter four focuses on evaluating whether biogeochemical response below beetle-infested trees is dictated by the severity of surrounding tree mortality (dead trees/total number of trees). For this chapter, we hypothesized that biogeochemical signatures remain stable until a certain threshold level of beetle infestation occurs, due to compensatory effects from surrounding live trees. Inspiration for this research question came from the results in chapter two where shifts in water quality were only found in high-impacted watersheds (>50% areal infestation) along with prior work where edaphic parameters were altered under trees in a severely infested forest (85% mortality) while parameters were comparatively stable between green and grey trees in another forest that experienced lower beetle-induced tree mortality (Mikkelson et al., 2015). Biogeochemical cycling in montane and subalpine forest soils has important implications for water quality, ecosystem resilience, and atmospheric feedbacks to a warming climate (Jandl et al., 2007; Lal, 2005). This work can elucidate when and where these responses occur following beetle infestation. While a critical component in climate forecasting (Falkowski et al., 2000), knowledge gaps exist in this are due to the highly heterogeneous, interdependent, and biological variances in natural systems (Schimel and Bennett, 2004). In extreme instances, bark beetle-induced tree mortality has the potential to change forests from carbon sinks to sources, potentially intensifying climatic feedback loops that will persist after impact (Kurz et al., 2008; Wear and Coulston, 2015).

Furthermore, in some watersheds, large-scale beetle-induced forest disturbances have been shown to affect water quantity and quality (Bearup et al., 2014; B. M. Brouillard et al., 2016; Mikkelson et al., 2013b) while altering terrestrial carbon (C) and nitrogen (N) cycling (Mikkelson et al., 2013a; Morehouse et al., 2008; Norton et al., 2015; Trahan et al., 2015).

Soil biogeochemical parameters such as N and C pools, pH, and water content are affected by tree mortality after bark beetle infestation; however, there is significant variability in the magnitude of these responses (Mikkelson et al., 2013a). After bark beetles infest and kill a tree, C and N inputs to the soil system are altered (Figure 1.3). Initially, as transpiration ceases and photosynthesis stops, root exudates are no longer excreted and a source of labile C in the subsurface is lost (Grayston et al., 1997). After several years in the dead "red" phase, beetle-killed trees progress to the grey phase, during which there is a large increase in recalcitrant organic matter input as needles and coarse woody material fall from dead trees (Edburg et al., 2012). Needle litter from beetle-killed trees is also N-enriched relative to naturally-senesced litter (Griffin et al., 2011; Morehouse et al., 2008) potentially increasing the terrestrial contribution to the subsurface N-pool. These litter inputs then decay and transformed compounds are leached and transported over time from the litter horizon downward through the organic and mineral horizons.

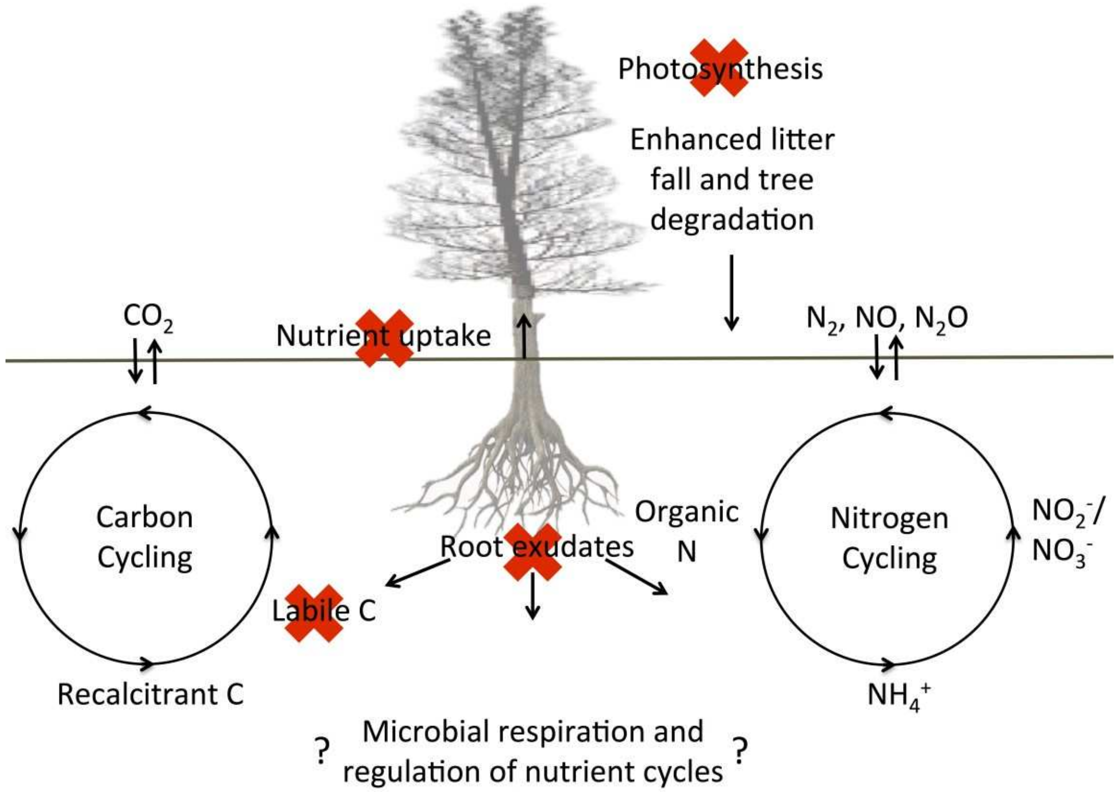

Figure 1.3: Conceptual diagram demonstrating shifts in carbon and nitrogen cycling and associated processes that cease (marked with red x) following beetle-induced tree mortality.

Altered inputs of C and N along with speciation shifts following beetle-induced tree mortality can create notable secondary effects that have implications for altered gaseous and aqueous flux to the atmosphere and hydrosphere. For example, the flux of greenhouse gases such as CO_2 may decline as root respiration ceases, heterotrophic respiration from root-associated microbial communities declines, or shifts to abiotic processes and changing C-N pools occur (Barrena et al., 2013). Similarly, increases in aqueous outputs such as nutrients and dissolved organics may have downstream effects on ecological processes and drinking water quality. In addition to the prior mentioned findings where mountain pine beetle-impacted watersheds in the Colorado Rocky Mountains were linked to increased organic carbon and disinfection byproduct formation potential at downstream water treatment plants (B. M. Brouillard et al., 2016; Mikkelson et al., 2013b), bark beetle-impacted forests in the comparatively nitrogen rich soils of the Czech Republic have been linked to increased nitrate runoff, threatening water sources with eutrophication (Huber, 2005; Zimmermann et al., 2000).

To investigate whether the level of tree severity impacts biogeochemical response in chapter four, we sampled near surface soil horizons (litter, organic layer, and mineral soil) beneath green (n=7) and grey (n=31) phase lodgepole pine trees located in the Colorado Rocky Mountains. Eight-meter radius plots were established around each sample tree and the numbers of surrounding dead and live trees were counted. The severity of tree mortality was then calculated in each plot and compared to a suite of biogeochemical parameters (pH, water content, soil respiration, C and N species). Sampling was conducted over two subsequent summers for temporal reproducibility and to investigate whether biogeochemical shifts occur during different moisture regimes.

CHAPTER 2

WATER QUALITY FOLLOWING EXTENSIVE BEETLE-INDUCED TREE MORTALITY: INTERPLAY OF AROMATIC CARBON LOADING, DISINFECTION BYPRODUCTS, AND HYDROLOGIC DRIVERS

Modified from a paper published in *Science of the Total Environment*[1]

Brent M. Brouillard[2,3,4], Eric R.V. Dickenson[5], Kristin M. Mikkelson[2,3], Jonathan O. Sharp[2,3]

Abstract

The recent bark beetle epidemic across western North America may impact water quality as a result of elevated organic carbon release and hydrologic shifts associated with extensive tree dieback. Analysis of quarterly municipal monitoring data from 2004-2014 with discretization of six water treatment facilities in the Rocky Mountains by extent of beetle impact revealed a significant increasing trend in total organic carbon (TOC) and total trihalomethane (TTHM) production within high (~>50% areal infestation) beetle-impacted watersheds while no or insignificant trends were found in watersheds with lower impact levels. Alarmingly, the TTHM concentration trend in the high impact sites exceeded regulatory maximum contaminant levels during the most

[1] Reprinted with permission from *Science of the Total Environment* (2016) 572:649-659 and all co-authors.
[2] Department of Civil and Environmental Engineering, Colorado School of Mines
[3] Hydrologic Science and Engineering Program, Colorado School of Mines
[4] Principal researcher and author of this manuscript
[5] Water Quality Research and Development Division, Southern Nevada Water Authority

recent two years of analysis (2013-14). To evaluate seasonal differences, explore the interplay of water quality and hydrologic processes, and eliminate variability associated with municipal reporting, these treatment facilities were targeted for more detailed surface water sampling and characterization. Surface water samples collected from high impact watersheds exhibited significantly higher TOC, aromatic signatures, and disinfection byproduct (DBP) formation potential than watersheds with lower infestation levels. Spectroscopic analyses of surface water samples indicated that these heightened DBP precursor levels are a function of both elevated TOC loading and increased aromatic character. This association was heightened during precipitation and runoff events in high impact sites, supporting the hypothesis that altered hydrologic flow paths resulting from tree mortality mobilize organic carbon and elevate DBP formation potential for several months after runoff ceases. The historical trends found here likely underestimate the full extent of TTHM shifts due to monitoring biases with the extended seasonal release of DBP precursors increasing the potential for human exposure. Collectively, our analysis suggests that while water quality impacts continue to rise nearly one decade after infestation, significant increases in TOC mobilization and DBP precursors are limited to watersheds that experience extensive tree mortality.

2.1 Introduction

The research conducted in chapter two focuses on water quality shifts following beetle infestation. Although prior work has demonstrated that altered carbon cycling in infested forests increased TOC and subsequent DBP formation for municipalities reliant on source waters from beetle-impacted watersheds (Mikkelson et al., 2013b), questions still exist regarding shifts in organic carbon character and aromaticity following beetle infestation as well as the timeframe associated with these shifts. Furthermore, extensive forest mortality alters hydrologic processes that may impact water quality. Trees no longer transpire within one growing season following infestation, decreasing vegetative water uptake from the subsoil (Hubbard et al., 2013). The resulting loss of needles and canopy cover also decreases interception, changing soil moisture and snowmelt patterns (Biederman et al., 2012; Mikkelson et al., 2013a). These alterations to the hydrologic cycle have been found to increase groundwater contributions to streams in the summer and fall months, change hydrologic flow paths, and create a lag in timing between annual peaks in TOC and DBP precursors that typically occur during spring runoff (Bearup et al., 2014; Mikkelson et al., 2013b; Penn et al., 2016). Previous historical analysis was limited to quarterly TOC and DBP data collected by treatment facilities for regulatory compliance (*Comprehensive Disinfectants and Disinfection Byproducts Rules (Stage 1 and Stage 2): Quick Reference Guide*, 2010; Mikkelson et al., 2013b). This constraint obscures questions relating to seasonal timing and hydrologic drivers of water quality, differences in treatment operation, confounding variability in the blending of surface and groundwater, delineation of groundwater capture zones (Bakker and Strack, 1996), and groundwater residence times that can mitigate water quality impacts associated with land cover change (Baker et al., 2000; McGuire et al., 2005). These limitations inhibit the kind of predictive understanding necessary to inform long-term management and technological evolution following forest disturbance.

Further investigation into water quality impacts following tree mortality can elucidate the timing and degree of organic matter loading in impacted watersheds along with changes in its structure. Noting the above limitations, our study analyzed additional historical water quality data coupled to a surface water sampling campaign conducted from 2013-2014 that was designed to improve the resolution and interpretation of water quality impacts with further delineation of degree and timeframe of beetle impact. The objective of this work was to evaluate differences in organic carbon loading, character, and DBP precursors derived from montane catchments with varying degrees of beetle impact while delineating seasonal hydrologic shifts and drivers of these water quality parameters. The data presented here provides an example of how land cover change can alter biogeochemical cycling of carbon and associated shifts in seasonal water quality, which may be of interest to water providers and stakeholders experiencing beetle mortality or analogous watershed disturbances.

2.2 Materials and Methods

2.2.1 Watershed Classification

Beetle-impacted and control watersheds utilized by municipalities for drinking water in the Rocky Mountain region of Colorado were considered for analysis in this study. Historical water properties, water treatment practices, and soil characteristics are detailed in prior work (Mikkelson et al., 2013b). Municipal sources that utilized surface water were further considered for water quality analysis (Table SI-1). After removing one municipality that obtained surface water from irregular sources (a reservoir and a spring fed stream), six municipalities were selected for historical analysis and the expanded sampling campaign (Figure 2.1, page 17).

Temporal quantification of beetle infestation was quantified within each delineated watershed using ArcGIS software and United States Forest Service (USFS) Aerial Detection Survey data from 1994-2013. This provides shapefiles of tree mortality with the associated damage causal agent. Only USFS shapefiles with bark beetles or disease complexes associated with beetle impact (5 needle pine decline, subalpine fir mortality, true fir pest complex, and pinyon pine mortality) listed as their damage causal agent were included in the analysis (*Areas with tree mortality from bark beetles*, 2014). The 2001 and 2011 National Land Cover Datasets (NLCD) were also used to determine the various land cover types in each watershed. The infestation shapefiles were then clipped by the evergreen and mixed forest land cover types found through the NLCD to ensure infestation areal accuracy.

After the infestation analysis, watersheds were labeled as either high, moderate, or low impact as of 2013 (Figure 2.1, page 17) depending on the areal percent of each watershed infested with bark beetles to allow historical and averaged seasonal trends to be easily depicted and characterized. Watersheds with less than 20% infestation area were considered low impact and were used as healthy controls (Aspen and Carbondale), watersheds with 20-40% infested area were considered moderate impact (Gypsum and Glenwood Springs), and watersheds with greater than 40% infested area were considered high impact (Granby and Steamboat).

2.2.2 Long-Term Trends

Historical trend analysis of TOC and DBP concentrations was conducted beginning in 2004 with the introduction of expanded EPA regulatory monitoring requirements through 2014 to allow characterization prior to and following beetle infestation and build upon previous published historical analyses (Mikkelson et al., 2013b). Historical water quality data were collected primarily from the Colorado Department of Public Health and Environment. Any missing data were collected directly from water-treatment facility archives. Data were quality checked and boundaries were established as follows: (1) TOC concentrations that were 250% greater than the average monthly value were removed (limited to Granby in October, 2004) to correct for sample bias or extreme weather events and (2) recorded TOC and DBP concentrations below detection levels were reassigned to analytical detection thresholds of 0.5 mg/L for TOC and 1 ug/L for DBPs.

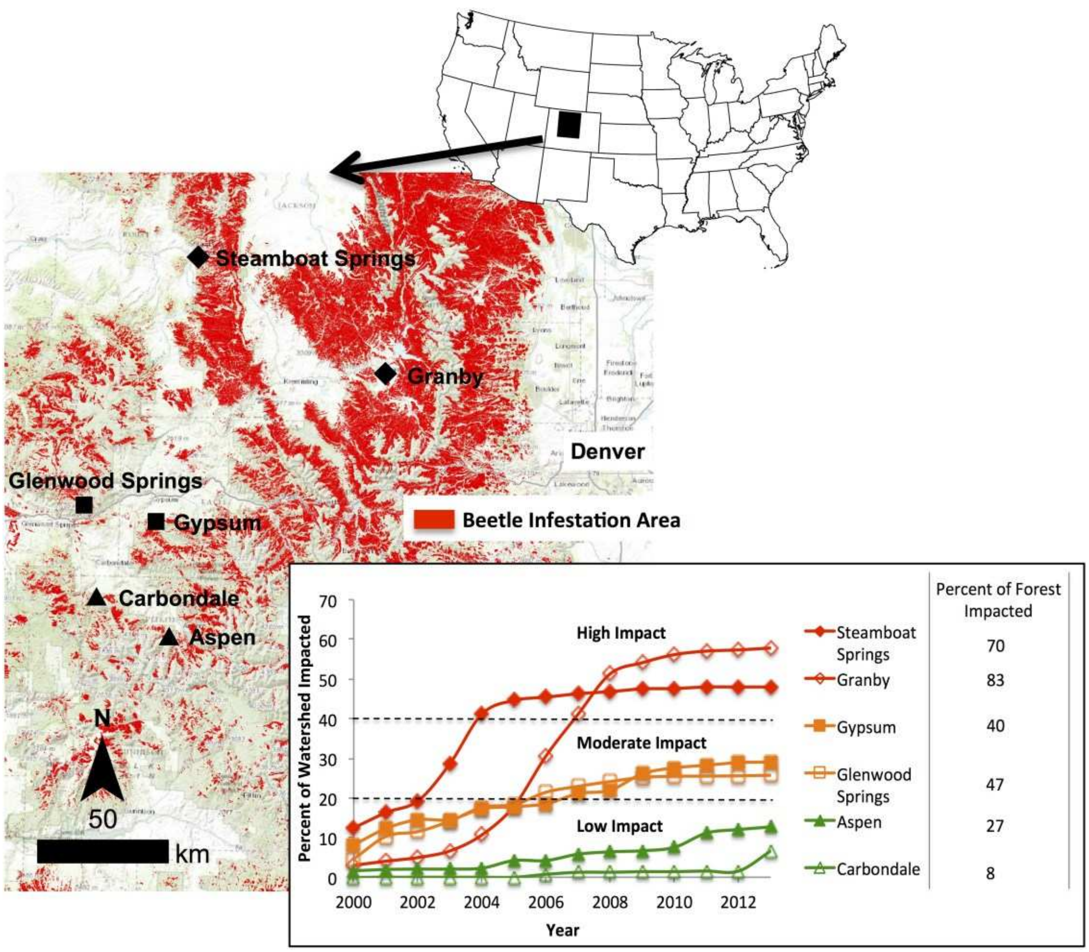

Figure 2.1: Map of beetle infestation and the 6 sample locations analyzed in the study with diamonds denoting high beetle impact, squares denoting moderate impact, and triangles representing low impact watersheds. The inset depicts beetle infestation temporal trends from 2000-2013 for the analyzed watersheds delineated into the three infestation bins. The percent of forested area within each watershed impacted by bark beetles as of 2013 (as opposed to total area) is provided to the right of inset legend.

2.2.3 Influent Water Collection

Aqueous samples were collected at municipal surface water intakes or sampling nozzles prior to the application of water treatment processes within 8 hours of one another for all six water treatment facilities during each sampling date. Samples were collected in amber glass bottles approximately monthly at each municipality during the snow-free window of May 2013 through December 2013 and more frequently during runoff events for improved water quality resolution. Four additional samples were taken from each municipality in the snow-free portion of 2014 as additional time points prior to, during, and after runoff. During winter months, samples were not collected as water characteristics (TOC, DBP formation potential) were stable and because of weather-related access issues. Once collected, samples were shipped overnight on ice for laboratory analyses.

2.2.4 Water Quality Analyses

Influent water samples were tested for TOC, total nitrogen (TN), DBP formation potential, UV, and fluorescence. TOC and TN were analyzed using a Shimazdu TOC-V_{CSH} with a TNM-1 unit after acidification using 0.1 M HCL. The DBP formation potential test was performed using Standard Method 5710b. Samples were chlorinated at various concentrations using a sodium hypochlorite dosing solution, buffered to a pH of 7 with phosphate (10 mM final concentration), and left at room temperature (approximately 21^{o}C). After seven days, free chlorine was measured and samples with a concentration closest to 3-5 mg/L (optimal for analysis by ensuring complete DBP formation) were then quenched. Chloroform, bromoform, bromodichloromethane, and dibromochloromethane were measured using a purge and trap gas chromatography-mass spectrometer system, which were summed and reported as total trihalomethanes (TTHM) (U.S. EPA Method 524.2). Concentrations of monobromoacetic acid, dibromoacetic acid, monochloroacetic acid, dichloroacetic acid, and trichloroacetic acid were analyzed using liquid-liquid extraction followed by a gas chromatography-electron capture detector system (U.S. EPA Method 552.2), and were summed and reported as five haloacetic acids (HAA5). DBP concentrations were measured prior to the addition of chlorine during the early sampling events and concentrations were found to be below detection limits.

UV spectroscopy was conducted using a PerkinElmer Lambda 45 UV/VIS spectrometer. Total specific UV absorbance (TSUVA) or the carbon-normalized aromaticity was calculated by dividing UV absorbance at 254 nm by TOC concentration which can indicate the degree of disinfection byproduct formation potential of a water sample (Kitis et al., 2001, 2004; Lu et al., 2009). Excitation emission matrices (EEM) were also collected using a scanning fluorometer (PTI QM4) for excitation wavelengths from 240 to 470 nm in 2.5 nm steps and emission wavelengths from 280 to 580 nm in 1 nm steps. UV correction was conducted by running DI water blanks in conjunction with each sample to remove Raman scattering. The resulting EEMs were then carbon normalized and used to provide additional information on organic matter character. Specific peak intensities in the A and C regions were calculated. These peaks are associated with humic-like fluorescence with Peak C correlating with hydrophobicity, aromaticity, and THM formation potential (Bieroza et al., 2009; Coble, 1996; Kalbitz et al., 1999). Fluorescence index (FI) was calculated from the ratio of intensities at emission wavelengths 470 and 520 nm (both at an excitation wavelength of 370 nm), which has been used to distinguish sources of aquatic fulvic acids (McKnight et al., 2001). Fluorescence regional integration (FRI) of 5 regions within the EEMs was also conducted to further quantify carbon character signatures (Chen et al., 2003). Additional information regarding carbon character analysis can be found in the supplementary information.

2.2.5 Hydrologic Data

Stream discharge data were collected during the ice-free season for 3 watersheds that contained United States Geological Survey (USGS) gauges (Aspen, Granby, and Steamboat). The gauge for Steamboat was located at the water quality sampling point while the other two gauges were located either upstream or downstream of the sampling location. Monthly precipitation rates and monthly average temperatures from 2004-2014 and 30-year normals were collected from the National Climatic Data Center. Gauges closest to the watershed sampling points were selected for analysis. While a gauge collecting 30-year normals for Carbondale was not identified, climatic data for Glenwood Springs and Aspen likely reflects general trends in Carbondale due to their proximal nature (within 30 km).

2.2.6 Statistical Analyses

Linear regression was utilized to determine historical trends in TOC, DBPs, and climate data from 2004-2014 in accordance with prior approaches (Mikkelson et al., 2013b). All historical water quality and climate data utilized to investigate long-term trends were decomposed using moving averages to smooth seasonal differences. The Mann-Kendall test was then utilized to determine if decomposed trends were significantly different from zero (R Core Team, 2015). Friedman Tests were used to determine significant differences between high, moderate, and low impact sites for each water quality parameter investigated during the sampling campaign. A post-hoc Wilcoxon test was then used to evaluate significant differences between two bins and compared high to moderate, high to low, and moderate to low impacted sites for all collected samples. Mann-Whitney tests were utilized to determine significance between 2013-2014 climate data and 30-year normals. Pearson correlations were used to determine correlations between UV_{254}, TSUVA, and DBP formation potential. P-values $<$ 0.05 were considered significant throughout the study.

2.3 Results and Discussion

2.3.1 Decade-Long Trend Toward Impaired Water Quality

Quarterly regulatory monitoring data collected by water treatment facilities from 2004 through 2014 were used to better understand temporal impacts of large-scale beetle-induced forest mortality on water quality (Figure 2.2). Initially identified in a prior study that contrasted impacted versus control regions (Mikkelson et al., 2013b), watersheds were further discretized into 3 impact level bins. In conjunction with temporal evolutions of beetle impact, this provides the ability to query associations between potential thresholds of infestation, water quality shifts, and watershed hysteresis. This analysis also included 3 additional years of data from 2012-2014 as well as filled gaps in missing TOC concentration data for all watersheds from 2006-2008. Both high impact watersheds exceeded 40% areal infestation by bark beetles during the 2004-2007 time period with areal infestation in each watershed reaching approximately 50% or higher by 2008 (Figure 2.2). This corresponds to enhanced needle drop between 2006 and 2009 (three years post infestation) allowing trends to be analyzed prior to and following infestation.

Moderate impacted sites contained between 26-29% areal infestation with low impact sites containing <13% infestation.

Results indicate a statistically significant increasing trend of 0.04 mg TOC L^{-1} yr^{-1} for the high impact watersheds while a similar trend in the moderate and low impact sites was not found. High impact sites also displayed a significant increase of 2.37 ug TTHM L^{-1} yr^{-1} while an increasing trend in watersheds with less beetle infestation was not observed. Alarmingly, the slope for TTHMs has gotten steeper with time since 2008 while the extended analysis through 2014 reveals that the increasing TTHM trend in the high impact sites has continued for nearly a decade after initial peak tree mortality. This observation highlights the long-term effects associated with recalcitrant needle and woody debris degradation and water quality shifts associated with this form of forest disturbance. The long-term extent and timeframe of water quality shifts with beetle infestation is still unknown; therefore, continuing water quality monitoring as depicted here is important in elucidating how long these effects will last. HAA5 analysis was also conducted but results were inconclusive due to unavailable data (Gypsum, Carbondale, Glenwood Springs) during portions of the analysis period or sample error (4 quarterly samples were below or near the detection limit of 1 ug/L for Granby while the majority of samples contained at least 15 ug/L).

Analysis of the three infestation bins, while limited in number, alludes to the interpretation that water quality impacts may not be altered until a high level of tree mortality occurs (~> 50% areal infestation), with possible mitigating factors keeping water quality stable in lower impact watersheds. If water quality continues to exceed regulatory levels, alternative water sources or enhanced treatment techniques may need to be adopted to decrease DBP precursor levels and formation. Collectively, results demonstrate continuing increases in organic carbon loading and DBP precursor levels associated with beetle-induced forest mortality well after maximal infestation and suggest a heightened TTHM response in the heavily impacted watersheds beyond that observed in a prior 2004-2011 analysis (Mikkelson et al., 2013b).

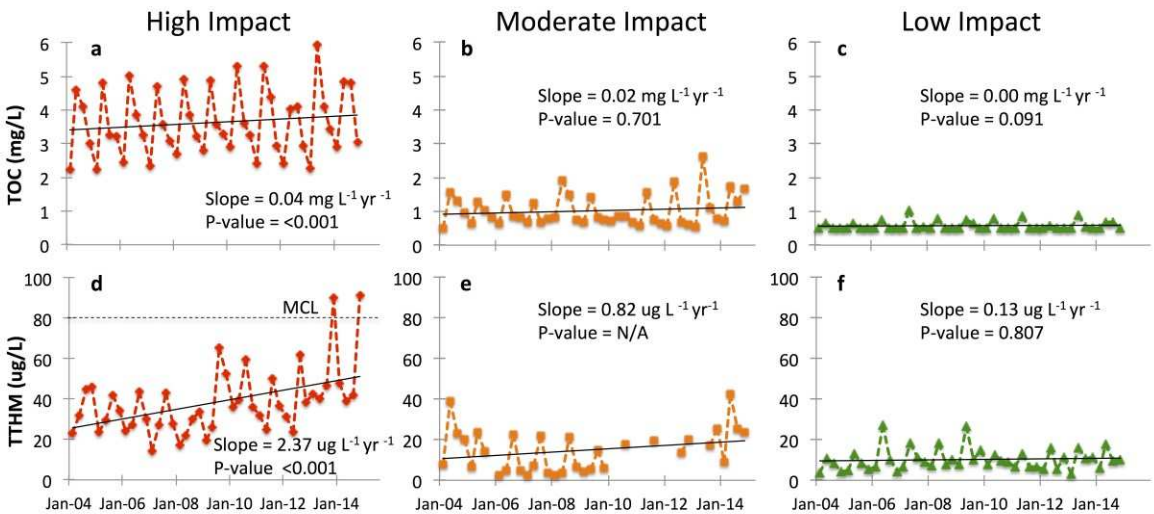

Figure 2.2: Compiled water quality data obtained from from six water treatment facilities reveals an increasing trend in high impact watersheds compared to lower impacted facilities. Panels depict water quality data from 2004-2014 where **a-c.** display binned TOC concentrations and **d-f.** portray binned TTHM concentrations in high (red diamonds), moderate (orange squares), and low impact (green triangles) watersheds with a regulatory TTHM maximum contaminant level (MCL) of 80ppb (*Comprehensive Disinfectants and Disinfection Byproducts Rules (Stage 1 and Stage 2): Quick Reference Guide*, 2010). P-values were found through the Mann-Kendall test after decomposition with significance demonstrating a departure from a slope of zero. Trends for individual watersheds revealed similar results and can be found in Table SI-2.

Importantly, during the most recent two years (2013-14) the trend analysis for the high impact sites exceeded the maximum contaminant level (MCL) of 80 ug TTHM L^{-1} (Figure 2.2d). Discreet analysis of each of these impact sites reveals that Steamboat Springs exceeded TTHM and HAA5 MCLs during 3 quarters while Granby exceeded the TTHM MCL during one quarter between 2011-2014 (Table A.2). This increasing trend is particularly alarming as water municipalities are only required to sample for DBPs once each quarter and can select a sampling date within this window; hence municipal reporting contains an inherent bias that may not accurately capture seasonal fluctuations in water quality. For example, the average quarter 2 and quarter 3 sampling dates for all municipalities in this study from 2004 to 2013 was May 14th and August 17th. When evaluating the high impact sites only, the average second quarter sampling date shifted almost two weeks earlier to May 3rd. The water quality data collected in the following portion of this study showed TOC and DBP formation potential peaked with runoff in early to mid-June in both years analyzed (Figure 2.3). Therefore, by collecting quarterly water quality data prior to and after runoff, municipalities are not capturing maximal peaks in TOC and DBP formation in their water treatment systems. Hence, trends obtained from municipal data may underestimate the increase in water quality impacts from beetle infestation or other analogous shifts in land cover, demonstrating the importance of more frequent monitoring.

Although this data mining approach provides long-term data allowing TOC and TTHM shifts with beetle infestation to be investigated, several caveats exist that limit interpretation. As with many large datasets collected from multiple participants, not all data during the analysis period was available for all watersheds. Granby, Steamboat, and Aspen had complete quarterly datasets for DBPs; however, Gypsum, Glenwood Springs, and Carbondale moved to a reduced monitoring schedule in the later half of the analysis period, only recording values once a year. This prevented the calculation of a TTHM p-value for the moderate impact sites. Besides missing data, Carbondale and Gypsum TOC concentrations were typically below detection limits. These municipalities rely primarily on groundwater sources that are occasionally blended with surface waters, which lower TOC concentrations and DBP precursor levels as seen here. Groundwater may also mitigate detection of water quality shifts due to longer residence times and unclear delineation of supply capture zones. Elevated aromatic carbon character may also increase DBP production, but data evaluating carbon structure are not typically analyzed by these treatment facilities and were unavailable.

2.3.2 Carbon Loading and Aromatic Character

Due to these limitations with the water provider data, an independent sampling campaign was conducted in the six identified watersheds from 2013-2014 to increase the resolution of TOC and DBP data. The goal was to better understand TOC properties and potential for DBP formation as well as to allow a more refined temporal analysis so that hydrologic drivers of water quality could be investigated. Only surface waters were analyzed and carbon character analyses were conducted to determine if differences in aromatic structure exist in watersheds with variable beetle-induced tree mortality. The additional sampling campaign also alleviates inherent uncertainties in the historical analysis associated with variable water treatment operation, ground versus surface water sources, sample timing, and other collection biases.

Results from two concurrent snow-free seasons (~1.5 years) of surface water sampling and characterization aided in the interpretation of surface water property shifts associated with beetle infestation. High impact watersheds exhibited the most elevated organic carbon loading with average TOC concentrations 3 to 5 times higher than the moderate and low impact sites (Figure 2.3a, page 27). Moderate impact watersheds displayed TOC concentrations that resided between those found in high and low impact sites. The smallest TOC concentrations were found in low impact watersheds with concentrations typically below 1 mg L^{-1}. Although nitrate concentrations are often significantly elevated after forest disturbances such as timber harvest (Burns and Murdoch, 2005; Feller and Kimmins, 1984), the total nitrogen concentrations in this study were often below the detection limit (0.2 mg-N/L). This supports findings of a minimal stream water nitrate response following beetle infestation in Colorado (Rhoades et al., 2013) and highlights the unique nature of this type of disruption when contrasted with timber harvest, windfall, fire or other abrupt forest disturbance (Adams et al., 2012).

In addition to increased organic carbon loading in impacted watersheds, the deposition of needle and tree material to the forest floor after beetle-induced forest mortality (Kaňa et al., 2012; Mikkelson et al., 2013a) may change the structure and aromaticity of carbon transported to surface water sources used by municipalities (Beggs and Summers, 2011). After infestation, fallen needles and woody material continue to degrade which may increase leachate TSUVA, specific humic peak intensities, and lignin-associated carbon further elevating aromatic structure (Beggs and Summers, 2011; Kalbitz et al., 2006; Yavitt and Fahey, 1986). To investigate this phenomenon, TSUVA was calculated to provide a carbon-normalized value of UV absorbance to evaluate differences in aromatic structure. Averaged TSUVA values were 150% higher in the high impact sites compared to moderate and low impact watersheds, which tended to overlap throughout most of the study (Figure 2.3a, Figure A1b). The increased TSUVA in surface waters exhibited here at the catchment scale in high impacted watersheds supports prior findings of elevated soil digest TSUVA found below trees in beetle infested forest plots when contrasted with uninfested controls (Kaňa et al., 2015).

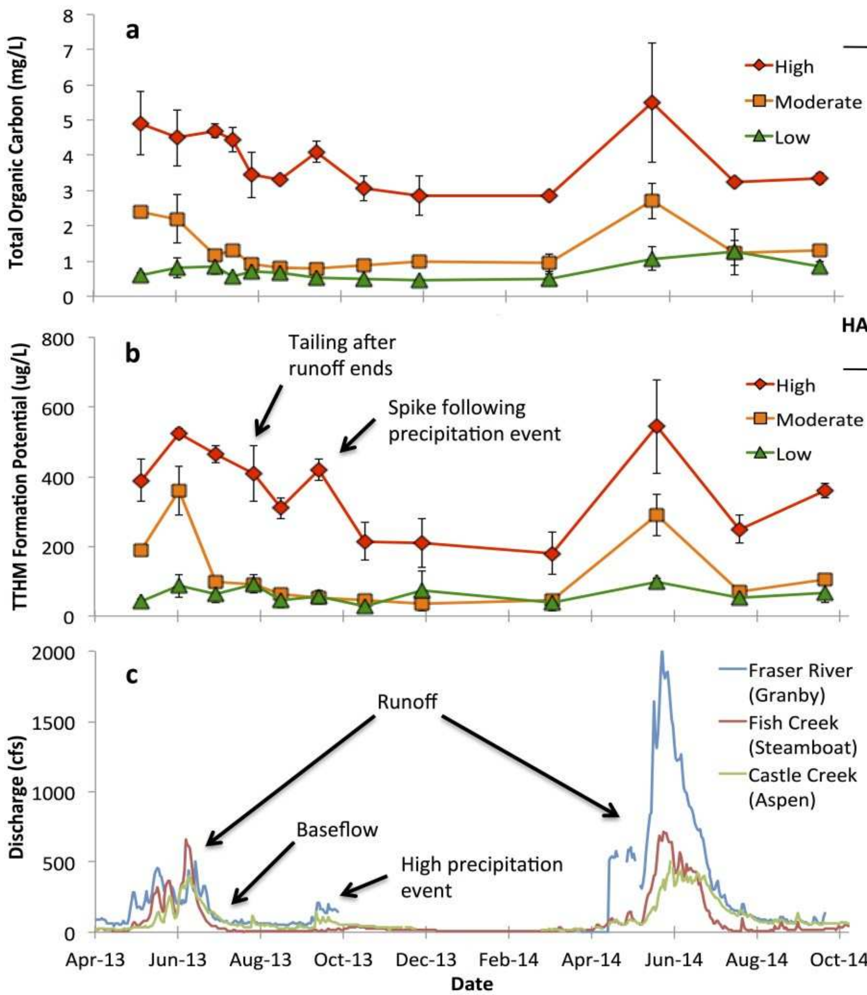

Figure 2.3: Increases in organic carbon concentration, aromatic content, disinfection byproduct formation potential, and relationship to stream discharge are apparent when contrasting high, moderate, and low bark beetle-impacted watersheds (red diamonds, orange squares, and green triangles respectively). Panels display **a.** total organic carbon concentration **b.** total trihalomethane (TTHM) formation potential and **c.** discharge flow rates for two high impact watersheds (Granby, Steamboat) and one low impact watershed (Aspen). Water quality points represent the average value of the two watersheds in each infestation bin with error bars denoting sample values. Averaged total specific ultraviolet absorbance (TSUVA) and five haloacetic acid (HAA5) formation potential across the sampling period are shown to the right of panels **a** and **b** with their corresponding standard deviations. Additional plots displaying water quality parameters for each individual watershed are shown in Figure A.1.

Analysis of EEM results further confirms that elevated aromatic character is found within beetle-impacted watersheds compared to healthy controls (Table 2.1).

Averaged FI values were inversely proportional to impact, ranging from a high of 1.42 for Aspen to a low of 1.28 in Steamboat Springs. These results are consistent with terrestrially derived fulvic acids compared to microbially derived sources that typically have FI values around 1.9 (McKnight et al., 2001). The high impact watersheds also exhibited elevated carbon-normalized fluorescence in peak A and peak C specific intensities along with the humic and fulvic acid-like fluorescence regions. Averaged humic-like peak intensities were 18 to 54% and 22 to 45% higher in the peak A and C regions, respectively, for the high impact watersheds compared to the low impact watersheds. Similarly, the averaged regional fluorescence in the high impact sites was elevated by 35-75% in the fulvic acid-like region and 17-47% in the humic acid-like region compared to the low impact watersheds. The moderately impacted watersheds displayed peak intensity and regional fluorescence values that were between the high and low impact watersheds.

Table 2.1: Fluorescence index (FI), carbon normalized specific peak intensity, and carbon normalized fluorescence regional integration (FRI) results. Units are RU L mg_c^{-1} for peak intensities and FRI.

			Specific Peak Intensity		FRI	
			Humic-Like		Fulvic Acid-Like	Humic Acid-Like
Treatment Facility	**Impact Level**	**FI**	**Peak A**	**Peak C**	**Region 3**	**Region 5**
Steamboat Springs	High	1.28 ± 0.04	0.232 ± 0.080	0.073 ± 0.022	0.066 ± 0.021	0.020 ± 0.006
Granby		1.35 ± 0.05	0.292 ± 0.108	0.080 ± 0.025	0.085 ± 0.029	0.022 ± 0.007
Gypsum	Moderate	1.39 ± 0.06	0.216 ± 0.086	0.065 ± 0.021	0.062 ± 0.022	0.018 ± 0.006
Glenwood Springs		1.41 ± 0.04	0.217 ± 0.093	0.070 ± 0.022	0.063 ± 0.023	0.020 ± 0.006
Carbondale	Low	1.39 ± 0.04	0.189 ± 0.076	0.060 ± 0.019	0.052 ± 0.018	0.017 ± 0.005
Aspen		1.42 ± 0.04	0.196 ± 0.094	0.055 ± 0.020	0.053 ± 0.022	0.015 ± 0.006

2.3.3 Disinfection Byproduct Formation Potential

As most municipalities located in beetle-impacted regions of the Rocky Mountains use chlorine as a disinfectant during drinking water treatment, differences in DBP formation potential were also analyzed for the collected water samples. The uniform potential test (Standard Method 5710b) was employed to evaluate the formation potential of THMs and HAAs as a more absolute measurement of DBP precursor concentrations free from individual municipality management, sampling time, or water treatment biases (Figure 2.3b). Chlorinated species dominated this analysis (chloroform, dichloroacetic acid, trichloroacetic acid) with concentrations of brominated DBP species typically falling below detection limits. Waters from high impact sites produced both TTHM and HAA5 concentrations that were typically 3 to 6 times higher than the formation potentials found in the moderate and low impact watersheds. HAA5 formation potentials were typically higher than TTHM formation potentials during the sampling period but both DBPs displayed similar temporal trends for each infestation bin.

To evaluate the importance of aromatic structure on the formation potential of DBPs, correlation plots were created between TSUVA and DBP formation potential for all samples collected (Figure A.2). Positive correlations between DBP formation potential and TSUVA were found which is typical during aromatic analysis (Jung and Son, 2008) and confirms the validity of elevated DBP formation from increased aromaticity in our study watersheds (R^2 = 0.58, p-value<0.001). This correlation also indicates that elevated aromatic character seen in the high impact sites increases DBP precursors throughout the year. The matching trends between TOC and DBP formation potential (Figure 2.3) indicate that temporal variations in TOC loading in impacted watersheds drives the seasonal fluctuations seen in DBP precursor levels.

Statistical tests were also performed for the parameters analyzed during surface water sampling to determine if significant differences exist across infestation bins (Table 2.2). All water quality parameters were found to be significantly different when contrasting all bins using the Friedman test. When analyzing across two bins, significant differences between high-moderate and high-low were further revealed for TOC, UV_{254}, TSUVA, HAA5, and TTHM formation potential using a post-hoc Wilcoxon test. The post-hoc Wilcoxon test also found significant differences between the moderate and low bins for TOC and UV_{254}. These statistical analyses were also performed for Granby and Steamboat Springs individually to ensure that binning the sites together didn't affect the significant results found.

Table 2.2: Statistical differences between infestation bins for all water quality parameters analyzed were found through the Friedman and the post-hoc Wilcoxon tests with bold values indicating significant p-values.

Parameter Tested	Friedman Test		Post-hoc Wilcoxon Test p-values		
	p-value	chi-squared	High-Moderate	High-Low	Moderate-Low
TOC	**< .001**	44.087	**< .001**	**< .001**	**< .001**
UV 254	**< .001**	40.783	**< .001**	**< .001**	**< .001**
TSUVA	**< .001**	31.565	**< .001**	**< .001**	1.000
HAA5 FP	**< .001**	32.818	**< .001**	**< .001**	.300
TTHM FP	**< .001**	35.182	**< .001**	**< .001**	.130
FI	**< .001**	23.645	**.001**	**< .001**	1.000
Specific Peak A	**.001**	13.875	.620	.110	1.000
Specific Peak C	**< .001**	18.375	.900	.055	.543
FRI Region 3	**< .001**	19.625	.507	.055	.328
FRI Region 5	**.007**	9.875	1.000	.091	.507

Collectively, these results support the hypothesis that watersheds experiencing bark beetle-induced forest mortality produce an elevated concentration of organic carbon that also contains more aromaticity than unimpacted forests. The elevated TOC concentrations, increased aromatic signature, and TTHM formation potential in impacted watersheds supports historical data archived by municipalities presented both here and previously (Mikkelson et al., 2013b), while bringing strong insights into unanswered questions about this trend. For instance, HAA5 formation potential in collected influent surface water was higher than TTHM formation potential and was significantly different between bins (Figure 2.3b, Figure A.2 c-d). This contrasts with historical HAA5 concentrations reported by municipalities which were lower than TTHMs and were not found to increase significantly with beetle infestation (Mikkelson et al., 2013b), which could be explained by the removal of humic-like HAA precursors (Hua and Reckhow, 2007) during water treatment prior to chlorination. Unlike the historical analysis of municipal data, the collected surface water samples were untreated waters. Therefore, the HAA5 formation potential in high impact sites is likely elevated compared to TTHM formation potential (Figure 3) due to the enhanced levels of humic-like substances as well as wood-derived lignin phenols which are more important precursors for HAA formation (Hua et al., 2014). Additionally, the differences in HAA formation between historical and sampled results could occur from bias in the formation potential test from high chlorine dosing, which may preferentially create reactions forming HAAs that would not otherwise occur from chlorine dosing at lower concentrations typical at water treatment facilities. This supports effective practitioner judgment at these municipalities and illustrates the importance of minimal dosing in decreasing DBP production.

2.3.4 Climatic and Vegetative Differences Between Watersheds

Several climatic factors such as precipitation and temperature along with differences in vegetation could contribute to the variations in historical and sampled water quality; however, these variables were analyzed and beetle-induced forest mortality is still the most probable cause. Trends in temperature and precipitation from 2004-2014 were typically insignificant (Table 2.3). Any significant trends found were expected to limit shifts in water quality rather than induce them. Additionally, monthly temperatures and precipitation in each watershed during the 2013-2014 sampling campaign, which was when TTHM trends exceeded MCLs, were not found to be significantly different from their respective 30-year normals.

Table 2.3: Precipitation and temperature trends from 2004-2014 and P-values comparing monthly precipitation and temperature data for 2013 and 2014 to 30-year normals.

	Historical Climate Trends				Climate Differences Between Sample Year and 30-yr Normals			
Watershed	Precipitation Slope ($mm\ yr^{-1}$) and P-value		Temperature Slope ($mm\ yr^{-1}$) and P-value		2013 Precipitation P-value	2014 Precipitation P-value	2013 Temperature P-value	2014 Temperature P-value
Steamboat Springs	-1.42	<0.001	-0.01	0.418	0.126	0.889	0.952	0.976
Granby	-1.13	<0.001	N/A[1]	N/A[1]	0.667	0.873	N/A[1]	N/A[1]
Gypsum	-0.29	<0.001	0.04	0.169	0.889	N/A[1]	0.928	0.928
Glenwood Springs	0.04	0.066	N/A[1]	N/A[1]	0.509	0.126	N/A[1]	N/A[1]
Aspen	0.22	0.708	-0.07	<0.001	0.889	0.401	0.667	0.795

Climatic data were either unavialable or contained missing data[1]
Historical P-values were calculated from the Mann-Kendall test following decomposition
2013 and 2014 P-values were calculated using the Mann-Whitney test

In headwater catchments similar to the watersheds analyzed here, organic matter primarily originates from terrestrial vegetative sources (Hood et al., 2005); therefore, ecological differences may play a role in water quality and were also investigated (Table 2.4). Barren land cover was elevated in the low impact watersheds, comprising 26-44% of the total watershed area compared to the moderate and high impact sites, which contained less than 4% barren land. This may explain why TOC concentrations in the low impact control sites were consistently lower and displayed limited seasonal peaks than watersheds with more pronounced beetle infestation both when evaluating historical results and during the surface water sampling campaign. Although this vegetative difference between the healthy controls and more impacted sites confines interpretation, the vegetative area was similar between the high and moderate impact watersheds (89 to 99% vegetated: area without barren land, perennial snow/ice, or development) yet clear differences in historical and sampled TOC concentrations and DBP precursor levels were found. More detailed analysis of climatic and vegetative differences between watersheds is presented in the Supplemental Information.

Table 2.4: Land cover percentages for each watershed.

Watershed	Evergreen Forest	Deciduous & Mixed Forest	Shrub, Herbaceuous, & Pasture	Wetlands	Developed	Barren Land & Perennial Snow
Steamboat Springs	53.3	15.1	21.1	9.1	0.2	0.4
Granby	67.7	1.8	16.2	3.6	1.7	9.0
Gypsum	40.8	31.5	24.0	0.5	0.0	3.1
Glenwood Springs	35.8	17.9	43.6	2.3	0.0	0.2
Carbondale	27.6	19.6	9.2	0.0	0.0	43.6
Aspen	28.5	17.5	25.2	2.4	0.0	26.3

2.3.5 Hydrologic Connection to Organic Carbon Fluctuations

Carbon transport from its vegetative source to water municipality intakes is dependent on runoff and precipitation events (Dawson et al., 2008; Xu and Saiers, 2010). As such, we investigated the impact altered hydrologic processes have on water quality after tree dieback. Following beetle-induced tree mortality, transpiration ceases and canopy interception of precipitation declines as needles and branches fall to the forest floor (Mikkelson et al., 2013a; Pugh and Gordon, 2013). This causes a decline in subsurface water demands and an increase in soil moisture (Adams et al., 2012), which have been found to increase late summer groundwater contributions in beetle-impacted watersheds and subsequently increase water table levels (Bearup et al., 2014; Penn et al., 2016). Natural organic matter concentrations are elevated in soil profiles closer to the ground surface and decline with depth and distance from their vegetative source (Mei et al., 2012; Michalzik and Matzner, 1999; Neff and Asner, 2001). Additionally, aromatic and hydrophobic organic carbon is generally less mobile and therefore concentrated in higher soil profiles (Jardine et al., 1990). These hydrophobic fractions tend to stay in the upper soil layers during average soil moisture conditions and remobilize during precipitation events (Jardine et al., 1990). It follows that higher water table levels potentially mobilize pools of organic matter with higher aromatic content and decrease the degradation potential of mobile aqueous carbon due to shorter subsurface residence times (Mei et al., 2012).

This potential mechanism may partially explain the elevated TOC and aromaticity in surface waters associated with beetle-induced forest mortality (Graphical Abstract). Peaks in TOC and DBP formation potential at the impacted sites occurred during both seasonal runoff events captured in the study (Figure 2.3). During the first snowmelt-driven event, DBP formation potential peaked at the moderately impacted sites with runoff (early June 2013) and dropped down to a value similar to the low impact watersheds when discharge returned to baseflow conditions the following month. The DBP formation potential in high impact sites also peaked concurrently; however, DBP formation potential did not decline as rapidly and displayed a tailing effect, not reaching the lowest concentrations until the late summer and fall months. This tailing event may be indicative of increased mobilization resulting from elevated groundwater contributions and changing flow paths. TOC concentrations and DBP precursor levels reach an annual low point in the fall as colder temperatures decrease debris degradation (Davidson and Janssens, 2006), rainfall precipitation switches to snowfall, and water flow through the vadose zone declines.

The spike in DBP formation potential during mid-September 2013 in the high impact sites (Figure 2.3b, Figure A.1) also revealed the importance of rainfall events in mobilizing organic carbon. This spike coincided with a historic precipitation and flooding event that occurred east of the analyzed watersheds in the front range of Colorado (Brennan and Aguilar, 2013). After comparing 30-year normal rainfall rates to their observed monthly totals, results indicated that all studied watersheds experienced rainfall rates that were approximately double the 30-year average during September 2013 (Table A.5). USGS gauges also saw a rise in discharge during this time period. Importantly, even though all watersheds experienced a pulse of water during this large precipitation event, TOC and DBP formation potential spiked only within the high impact sites indicating elevated mobilization of excess carbon in high impact watersheds. Although empirical (Bearup et al., 2014) and modeling (Penn et al., 2016) studies have demonstrated rising water tables following beetle infestation, future studies can target this hydrologic mechanism to further elucidate its effect on water quality while answering more detailed inquiries related to variable subsurface carbon pools, seasonal timing and degree of water table variation following beetle infestation, and quantification of water quality shifts related to elevated hydrologic flow paths.

2.3.6 Water Quality Management and Environmental Implications

From a public health and regulatory perspective, municipal monitoring has revealed that DBP concentrations are now exceeding regulatory limits at high impact sites (Figure A.1), and our analysis of this historical data in complement to our more rigorous surface water characterization suggests that biases in collection are likely underestimating the extent of this challenge. Watershed monitoring and management could be used to help municipalities understand and predict influent water quality properties to enhance water treatment efficacy, offer cost effective alternatives, and provide safer water for human consumption (Foran et al., 2000; Postel and Thompson, 2005). To be proactive in watershed protection, municipalities could conduct additional water quality sampling during runoff or precipitation events that mobilize contaminants of concern, particularly if their watershed is beetle-impacted. Implementing increased monitoring may also help better inform operators of the timing of contaminant loading within their watersheds, help predict when future contaminant spikes may occur, and aid in the selection of water treatment techniques that alleviate water quality impacts. For instance, the strong correlation in these watersheds indicates that monitoring UV_{254} could provide real time water quality characterization particularly during hydrologic events to aid in predicting DBP formation potential (Figure A.2) or provide insight into when alternative disinfection processes could best be utilized.

It is possible that high impact water treatment facilities may need to consider alternative waters during high flow events or retrofit or expand existing treatment technologies if increases in DBP formation continue to surpass regulatory MCLs. Treatment technologies such as coagulation, filtration through granular activated carbon, or alternative disinfectant strategies such as chloramination can also lower TOC concentrations and DBP production (Bond et al., 2011; Xie, 2003). Municipalities may also mitigate the effects caused from watershed disturbances through source strategies such as blending surface and groundwater particularly during higher risk windows. Because groundwater contains lower levels of organic carbon in the Rocky Mountain Region (Bauch and Bails, 2004; Thurman, 1985) and can help protect against threats from land cover change or anthropogenic surface contamination (Custodio, n.d.; Metcalf and Robbins, 2013), municipalities that rely solely on surface water sources are more susceptible to water quality shifts toward MCL concentrations. Diversification to include a mix of surface and groundwater sources can provide safeguards against unanticipated water quality shifts as well as provide a low organic carbon groundwater source for blending or bypass during hydrologic events. Furthermore, groundwater can provide additional water during times of peak water demand which usually occurs in the summer months (Kenney et al., 2008) when TOC concentrations in surface waters are elevated.

The findings disseminated within our study reveal how shifts in biogeochemical cycling associated with ecological disturbances can have secondary effects on water resources altering TOC loading and DBP precursor levels. Although expanded tree fall will occur and increased TOC loading could continue with subsequent degradation of tree biomass, mitigating factors may begin to alleviate this concern. As regrowth of saplings and other vegetation occurs, increased transpiration may return groundwater contribution and water table depth to pre-infestation levels alleviating the changes associated with hydrologic flow paths (Bearup et al., 2014). Additionally, microbial communities have been found to shift in beetle-impacted forests (Mikkelson et al., 2016b) with a larger abundance of saprotrophic taxa that may increase the utilization and degradation of woody material and decrease aromatic TOC loading into surface water sources (Štursová et al., 2014). Forest lands are an important source for safe and reliable drinking water globally; however, natural disturbances are predicted to create large changes in forested regions under a changing climate (Furniss, 2011; Williams et al., 2010). In extreme instances, extensive forest die-off can also have global consequences when forests switch from a carbon sink to a carbon source (Kurz et al., 2008; Schwalm et al., 2012). As such, understanding the shifts in biogeochemical cycling that occur following land disturbance is imperative in safeguarding these vital water sources while enabling more informed water resources management.

2.4 Conclusions

The water quality analyses presented here reveal that increased TOC loading and aromatic content from beetle-infested watersheds is reaching surface waters used by drinking water treatment facilities. This results in elevated DBP precursor levels particularly during rainfall and snowmelt events when organic carbon is mobilized. Additionally, while DBP precursors are typically elevated during runoff, concentrations in high impact sites may stay elevated for months afterward due to altered hydrologic flow paths and increased TOC mobilization. TTHM concentrations in drinking water following municipal water treatment and chlorination have continued to rise for nearly a decade after peak initial tree mortality demonstrating the long-term effects on water quality associated with this type of forest disturbance. Furthermore, this trend obtained from municipal data likely underestimates the full extent of water quality shifts due to collection biases. Alarmingly, these historical TTHM concentrations collected from municipal distribution systems for regulatory compliance monitoring have begun to exceed the regulatory drinking water MCL of 80 ug/L at sites hardest hit by bark beetle infestation. While clear differences in water quality were found between three infestation level bins (Figure 2.2 and 2.3), differences between the high versus moderate impact watersheds provide the most compelling contrast due to their ecological similarities and reveal a trend of heightened TOC mobilization following runoff and precipitation in the high impact sites. Watersheds experiencing beetle mortality are located in forested mountainous catchments with pristine water quality, typically requiring minimal surface water treatment (Mikkelson et al., 2013b). Therefore, small fluctuations in TOC at these municipalities are more detrimental than fluctuations for water providers with more extensive treatment techniques at their disposal. Our analysis also suggests that water quality is stable until a certain infestation threshold is exceeded (~>50% watershed areal impact) enabling the identification of regions where water resources are most likely to be adversely affected. If these trends continue, high impact sites may need to adopt enhanced water quality monitoring, alternative treatment techniques, or utilize different water sources to reduce TOC levels and DBP production to protect human health.

CHAPTER 3

MOUNTAIN PINE BEETLE INFESTATION REDUCES FIRE SEVERITY IN WESTERN UNITED STATES PINE FORESTS

Modified from a manuscript submitted for publication

Brent M. Brouillard[1,2], Kristin M. Mikkelson[1,3], Jonathan O. Sharp[1,3]

Abstract

Natural and anthropogenic land cover shifts are occurring across the globe due to drought and warming temperatures. During these landscape transformations, the secondary effects that arise from these disturbances must be evaluated to determine ecological and human health impacts. For instance, unprecedented bark beetle-induced tree mortality has caused shifts in forest structure that have been perceived by the public as a heightened wildfire threat. As such, we evaluated the relationship between mountain pine beetle-induced tree mortality and fire severity from 2000-2014 across Western North American forests. Zones of beetle infestation were overlain with fire severity maps to determine if forest fire severity increased in association with this climate change-exacerbated phenomenon. Severity analysis was conducted on >600 forest fires using three different remote sensing fire severity data products (dNBR6, dNBR, and RdNBR) to provide a high degree of validation across different conditions within the study

[1] Department of Civil and Environmental Engineering, Colorado School of Mines
[2] Principal researcher and author of this manuscript
[3] Hydrologic Science and Engineering Program, Colorado School of Mines

domain. Results collectively demonstrate that contrary to public perception, forest fires burn less severely in the red and subsequent grey phases of mountain pine beetle infestation when contrasted with unimpacted forests. This decreasing trend in burn severity with beetle infestation was most pronounced in lodgepole pines but also occurred for ponderosa pine forests. Fire severity was 65-77% as severe in red and grey phase lodgepole forests compared to uninfested controls, while fire severity in ponderosa pine was 90-94% as severe in both phases of infestation when contrasted with controls. These findings contribute to a growing body of research indicating that forest fire effects associated with beetle infestation are of less importance than impacts on climatic feedbacks and water resources. The conclusions presented here indicate that future forest management and policy decisions should be cautious in removing beetle-infested forests as tree mortality may act as a natural buffer that reduces fire severity.

3.1 Introduction

Chapter three focuses on determining whether fire severity is altered following mountain pine beetle infestation in the Western United States. While recent work has begun to illustrate that beetle infestation does not increase fire risk to the degree intuited by the public, further elucidation can limit uncertainty and aid in forest management and policy decisions. For instance, although discrete retrospective studies and regional spatial analyses have begun to evaluate how grey and old phase beetle kill impacts burn severity, it is difficult to evaluate the impacts of recent beetle infestation in the red phase due to the short time frame (1-3 years post infestation) before red needles fall from the canopy to the forest floor. To collect sufficient data to analyze the differences in burn severity between red phase trees and control forests, large spatial analyses over peak infestation regions and timeframes need to be conducted. Similarly, while regional analysis of pre-fire insect effects on burn severity have been conducted in the US Pacific Northwest (Meigs et al., 2016), the majority of fires analyzed contained western spruce budworm while only 19 fires contained MPB infestation prior to burning with the majority being in the old phase (Figure 3.1). As MPB is the dominant form of insect infestation across Western North America, further elucidation of the effects this type of insect infestation have on burn severity is needed, particularly during the earlier phases of infestation. Additionally, host tree species, notably lodgepole and ponderosa pine that are infested by MPB, contain variable fuel and canopy dynamics and grow in a range of environments (*2008 Report: The Health of Colorado's Forests*, 2008; Graham and Jain, 2005; Jenkins et al., 2014). These differences in host species may create differences in burn severity following beetle-induced mortality.

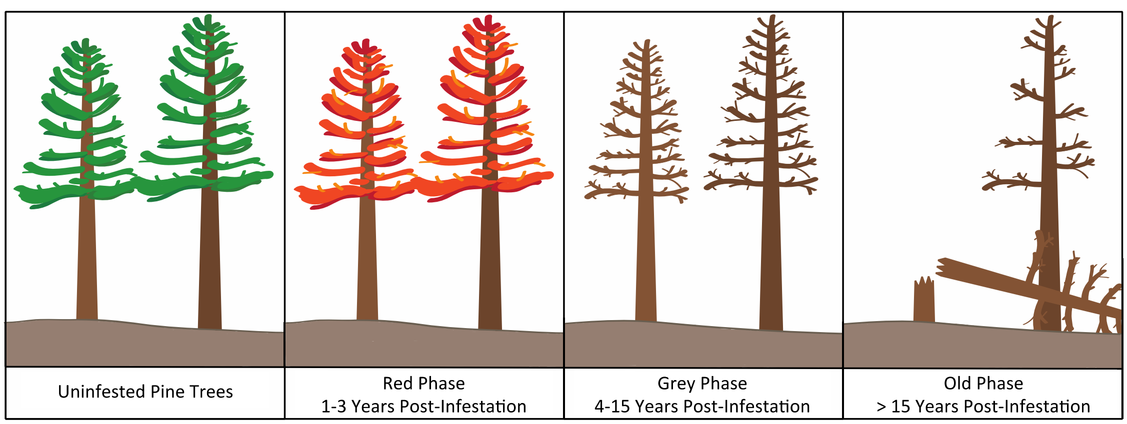

Figure 3.1: A conceptual timeline of beetle-induced tree mortality typically seen in the Western US region and used in this study; however, phase timing may be different in other regions (Štursová et al., 2014).

In this study we evaluate the impacts of MPB infestation on fire burn severity for 15 consecutive years beginning before the recent infestation and ending after the epidemic peaked across the Western US. The areal extent of the study includes the majority of MPB domain within the US, extending the analysis of previous studies to determine if decreased fire severity following beetle infestation is specific to the US Pacific Northwest or is applicable to a broader set of eco-regions. Additionally, this broader regional analysis allows the links between fire severity and MPB infestation to be analyzed during the early stages of beetle infestation (red phase), which are lacking in prior studies. Therefore, fire severity results were analyzed for the red and subsequent grey phases of infestation and were broken down by tree species to analyze differences in burn severity between MPB hosts (lodgepole and ponderosa pine).

3.2 Methods

3.2.1 Data Collection and Processing

<u>Forested Data Layers</u>

The evergreen-forested area analyzed in this study was first determined from the 2001 National Land Cover Dataset (NLCD), which provides land classifications across the United States and is mapped at a 30 m grid size (Homer et al., 2007). This layer provided a foundation of coniferous forests in the Western US, but MPB primarily attacks lodgepole and ponderosa pine species. Therefore, the National Gap Analysis Program (GAP) was then used to determine regions of lodgepole and ponderosa pine. Forest cover classes utilized in Hart et al. (Hart et al., 2015) were employed to delineate these two tree species in GAP. Due to potential ecological differences, fuel abundance, and potential variations in burn behavior, the evergreen forest layer was further subdivided into these two specific host species, which were studied separately. After collecting the appropriate subclass data for each host species type from GAP, the GAP layers were overlain on the NLCD evergreen forest layer and clipped to produce the lodgepole and ponderosa pine layers utilized in the study and produce agreement between the two data sources (Hart et al., 2015). These layers represent potential areas where MPB beetle infestation could occur. The unimpacted control layers were then created by erasing regions that contained MPB infestation, tree harvesting, or fire layers in any years prior to the observation year. The collection and processing steps for these disturbance types are further discussed below.

<u>Disturbance Data Layers</u>

The extent of bark beetle impact for each year from 2000-2014 was found using the United States Forest Service (USFS) Aerial Detection Survey (ADS), which has been frequently used to delineate areas of beetle impact in preceding studies (Bearup et al., 2014; Hart et al., 2015; Mikkelson et al., 2013b; Park Williams et al., 2012). This dataset provides a geographic inventory of tree mortality, insect infestations, and disease activity for forests throughout the United States. It includes information on the extent of affected areas and damage causal agents. For the purpose of this study, only areas listed with MPB as their primary damage causal agent (DCA coded as 11006) were considered. Once we filtered for the damage causal agent, areas of overlap in different years were clipped to ensure that mapped infestation reflected the original time point of infestation and that no area was double counted. The ADS polygon data was then rasterized to a 30 m grid size to match that of the wildfire and forest cover data. To provide an additional level of accuracy that ensured beetle-infested areas from the ADS aligned with MPB host species, beetle-infested regions were subsequently clipped by the lodgepole and ponderosa pine forest data layers. Tree harvest data were also collected from LANDFIRE when available from 1999-2012 to ensure control host species layers were not impacted by anthropogenic disturbance.

To enable temporal insights relating to different stages of tree mortality, maps of red and grey phases of infestation were created for each observation year from 2000-2014. Infestation maps were broken down into bark beetle phases of red (observation year and infestation 2 years prior) and grey (infested 3 or more years prior to observation year) for each fire year analyzed based on when a pixel was first classified as impacted (Hart et al., 2015). ADS data usually misses the initial year of infestation as needles typically have not changed color; therefore, impacted forests analyzed in the study became impacted the year before the observation year with the red phase beginning during the observation year (Hart et al., 2015). For example, when evaluating burn severity in wildfires occurring in 2010, the areas that were initially demarked as infested in the detection survey in 2008-2010 were considered red phase and those first labeled as infested between 2000-2007 were considered grey phase.

<u>Fire Data Layers</u>

Fire data were obtained from Monitoring Trends in Burn Severity (MTBS). MTBS is a product of the United States Geological Survey and the USFS that maps the location, extent, and severity of large fires in the United States at a 30 m grid size. Minor fires (<1000 acres) are not included in the dataset and as such were not considered. Fire severity data were collected from 2000-2014. Fire severity analysis was only monitored after the year 2000, as the amount of beetle-infested area remained small until this time. Fire perimeter data were also collected from 1984-2014 and were used to determine historical burn regions and to ensure control forests analyzed in the study were not recently burned. Fires analyzed in the study differed in size, duration, season, and beetle phase providing a holistic summary of the impacts of MPB infestation on fire severity in the Western US.

Burn severity was found using Landsat imagery before and after each fire to calculate a Normalized Burn Ratio (NBR) and differenced Normalized Burn Ratio (dNBR) within each fire perimeter. The ratios are found through the following equations:

$$NBR = (band\ 4 - band\ 7)/(band\ 4 + band\ 7)$$

$$dNBR = (NBR_{prefire} - NBR_{postfire})$$

Band 7 records middle infrared wavelengths (2.08-2.35 um) that are sensitive to lignose content in non-photosynthetic vegetation, soil/vegetation water content, and is capable of separating dead wood from ash, soil, and charred wood following forest fires. Band 4 records near-infrared wavelengths (0.76-0.90 um) that are sensitive to chlorophyll content in living vegetation (Avery and Berlin, 1992; Elvidge, 1990; Jia et al., 2006; Kokaly et al., 2007). The difference between these two bands has been found to show the largest change between pre-and post-fire images, particularly in forested regions (Lopez Garcia and Caselles, 1991; Miller and Yool, 2002).

Due to concerns of misclassification of fire severity due to variations in pre-fire vegetation and canopy density when using dNBR in beetle infested regions, the relative differenced Normalized Burn Ratio (RdNBR) was also determined. While dNBR measures absolute change between the pre and post fire satellite imagery, RdNBR calculates the relative change based on pre-fire reflectance using the following equation:

$$RdNBR = \frac{NBR_{prefire} - NBR_{postfire}}{\sqrt{abs(\frac{NBRprefire}{1000})}}$$

Although RdNBR may produce more accurate fire severity classifications over a wider range of fires compared to dNBR (Miller and Thode, 2007), recent evidence found dNBR to have a higher classification accuracy than RdNBR both broadly and when evaluating forests with high heterogeneity or areas with low pre-fire canopy closure (Soverel et al., 2010). Regardless, fire severity was analyzed using both dNBR and RdNBR sources for all fires that contained beetle infestation.

3.2.2 Fire Severity Analysis

After the beetle infestation and control layers were processed, the impact of MPB-induced tree mortality on fire severity was analyzed by overlaying tree phase onto fire severity maps. Red phase, grey phase, and unimpacted forest layers were overlain on fire severity maps and the average burn severity for each forest type was quantified for each fire. All map processing and severity analyses were conducted in ArcGIS (*ESRI 2015. ArcGIS Desktop: Release 10.2*). The average burn severity for both beetle phases was then plotted against the unimpacted burn severity for the same host species within the same fire to investigate if burn severity was altered as a result of MPB-induced tree mortality.

dNBR6 severity data was first used which classifies burn severity into 4 categories of unburned to low, low, moderate, or high burn severity using dNBR data. This approach was first utilized to provide a coarser resolution of the influence beetle infestation has on fire severity by restricting the analysis to 4 severity levels instead of having a specific burn severity for each individual 30 m pixel. After overlaying the forest types on the dNBR6 severity layer, the 4 burn severity categories were given a “burn score” to quantify burn severity for each forest type within the fire perimeter. For example, the areal extent of unburned to low severity was multiplied by a value of 1 while the areal extent of high severity was multiplied by a value of 4. The total “burn score” was then summed for all 4 dNBR6 burn severity categories and divided by the total areal extent to provide an average burn severity from a low of 1 to a high of 4 for each forest type within a fire. A similar analysis procedure was then conducted for the raw dNBR data used by MTBS to create the dNBR6 maps and for the raw RdNBR data. For the dNBR and RdNBR data, the burn severity for all pixels in each forest type were summed and divided by the total areal extent to provide an average burn severity value within each fire for each forest type. During the dNBR and RdNBR analyses, fire perimeters that overlapped the unburned edges of another severity map within the same observation year were removed as they caused errors in processing and analysis and only pixels with severity values greater than zero were analyzed.

The average severity for the red and grey phases of infestation was then plotted against the average severity of the unimpacted forest for the same host species for each fire to evaluate differences in burn severity. Besides the influence of fuel variations investigated here, fire behavior is largely dependent on weather and topography (“Glossary of Wildland Fire Terminology,” 2014). These differences are limited using the approach described here by analyzing burn severity within the same fire individually, decreasing differences in topography and weather. Additionally, when evaluating the effects of modeling variables on burn severity, the amount of pre-fire insect damage was found to have the largest influence on burn severity while the effects of aspect, elevation, slope, and topography were found to be minimal in MPB impacted forests (Meigs et al., 2016). Following the quantification of burn severity for each fire, results were compiled using R (R Core Team, 2015) and linear regression was conducted to determine correlations in burn severity for each forest type with the Pearson test determining significant differences for each plot. Plots were analyzed at different minimum area criteria for each forest type to determine if the amount of beetle infestation within a fire influenced the average burn severity within that phase. P-values < 0.05 were considered significant throughout the study. The data sources utilized and the processing steps are highlighted below in Table 3.1.

Table 3.1: Description of geospatial data sources utilized in the study along with processing steps conducted to each geospatial layer and the subsequent severity analysis procedure.

Description of each geospatial data source utilized in the study

Data Layer Type	Data Source	Type	Resolution	Source Location
Forest Cover				
Evergreen Forest	National Land Cover Database	Raster	30 x 30 m	http://mrlc.gov
Specific Forest Species	Gap Analysis Program	Raster	30 x 30 m	http://gapanalysis.usgs.gov
Forest Damage				
Beetle Infestation (2000-2014)	Forest Service Aerial Detection Survey	Polygon	Rasterized to 30 x 30 m	http://foresthealth.fs.usda.gov
Tree Harvest (1999-2012)	LANDFIRE	Raster	30 x 30 m	http://landfire.gov
Fires				
Fire Perimeters (1984-2014)	Monitoring Trends in Burn Severity	Polygon	N/A	http://mtbs.gov
dNBR6, dNBR, & RdNBR Severity Layers (2000-2014)	Monitoring Trends in Burn Severity	Raster	30 x 30 m	http://mtbs.gov

Processing steps conducted for each geospatial layer and the subsequent severity analysis procedure conducted

Land Cover Type	Processing Steps and Analysis
Pine Species (Lodgepole and Ponderosa)	1. Evergreen forest layer was extracted from NLCD 2. Lodgepole and ponderosa species extracted from GAP (Hart et al., 2015) 3. Overlapping areas from NLCD and GAP were clipped to create final lodgepole and ponderosa forest layers
Beetle Infested Forest (Red and Grey Phase)	1. ADS polygons were filtered to only include MPB damage causal agent 2. Polygons were rasterized to 30 x 30 m 3. Layers were clipped by lodgepole and ponderosa forest layers 4. Layers were assigned as red or grey phase for each observation year
Uninfested Control Forest	1. Lodgepole and ponderosa forest layers were clipped to remove areas affected by beetle infestation, wildfires, or tree harvest prior to the observation year
Fire Severity Analysis	1. Severity rasterers were clipped by beetle impacted and control layers for each observation year 2. Average burn severity was compared for control and MPB forested areas for each fire analyzed

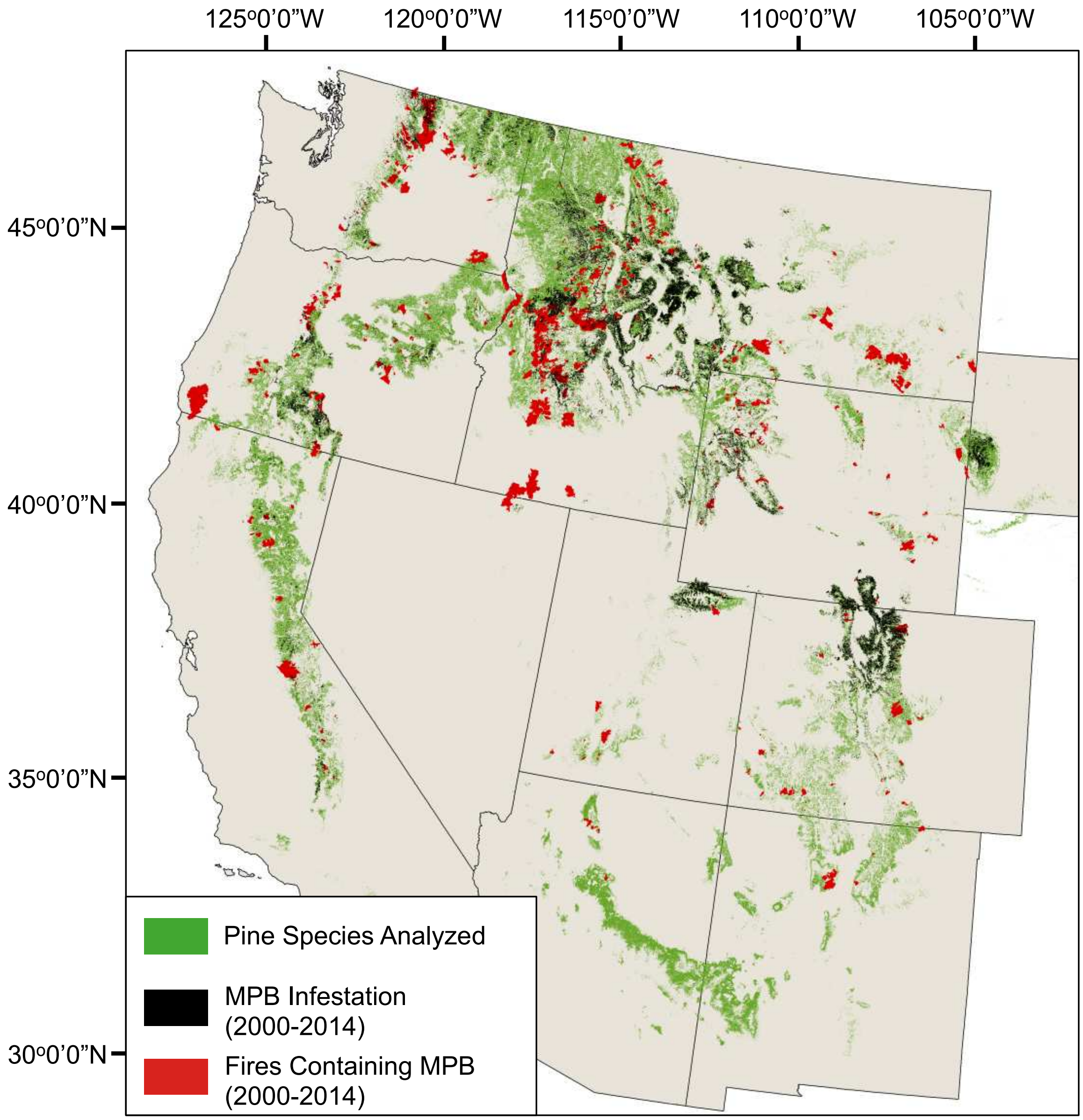

Figure 3.2: Map of fires in the Western US that were found to contain MPB infestation prior to burning and were analyzed in this study.

3.3 Results & Discussion

3.3.1 Fire Severity Analysis Utilizing Categorical dNBR6 Data

Following the data layer processing and overlay analysis, 612 fires in the Western US contained MPB infestation prior to burning between 2000-2014 (Figure 3.2). Forests with only small regions of infestation were not expected to create visible differences in burn severity from satellite imagery; therefore, data analysis was limited to fires that contained at least 0.1 km^2 of each forest type within a fire perimeter for each host species of pine with the focus being on fires that contained at least 0.5 km^2 of each forest type. Out of the original beetle-infested fires, 274 met this condition for lodgepole pine forests while 209 contained the minimum forested areal extent for ponderosa pine forests.

The average burn severity for the infested regions was then plotted against the average burn severity for the control regions of the same pine species for each fire that met the minimum areal criteria. In these plots, a slope lower than one would indicate that red or grey phases of infestation burned less severely than the unimpacted control. Severity analysis was first conducted using categorized differenced Normalized Burn Ratio (dNBR6) data which provides a course burn severity resolution with four categorical severity values ranging from one (unburned to low severity) to four (high severity). Results from the dNBR6 data display that in lodgepole forests, burn severity was 72.4% as intense in red phase forests and 64.5% as intense in the subsequent grey phase compared to unimpacted controls (Figure 3.3). A similar trend was found to occur in ponderosa forests but to a lesser extent, with burn severity in red and grey phases of infestation burning at 90 to 94% severity compared to unimpacted controls, respectively.

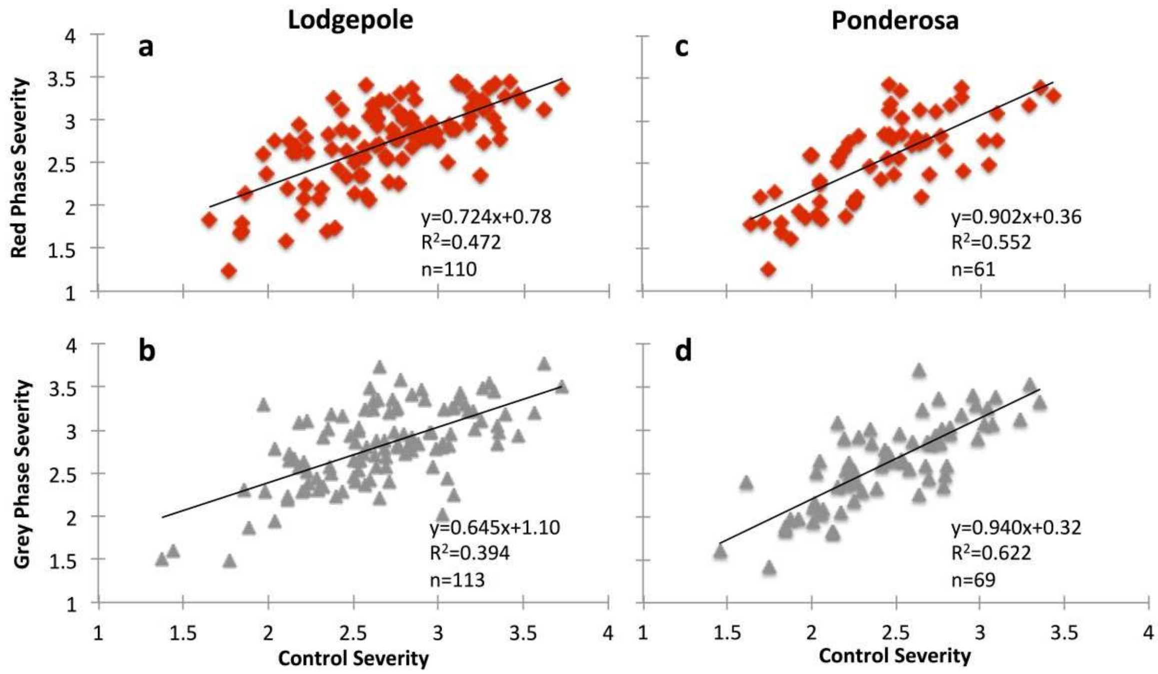

Figure 3.3: Plots of dNBR6 average burn severity comparing red (red diamonds) and grey phases (grey triangles) of beetle infestation to control forests in lodgepole pine (a,b) and ponderosa pine (c,d). Each point represents the average burn severity in both forest types for an individual fire. Values range from a low of 1 indicating the entire forest type burned at the "unburned to low" severity category, to a high of 4 indicating the entire forest type burned at the "high" severity category. Fires were only plotted if they burned at least 0.5 km^2 of each forest type.

Collectively, these data indicate that beetle infestation reduces fire severity in both MPB host species across the Western US. While this overall outcome agrees with previous findings of lower fire severity in MPB and western spruce budworm impacted forests in a smaller regional study of the US Pacific Northwest (Meigs et al., 2016), our results further elucidate questions regarding host species and temporal variations in burn severity while extending the studied domain to the Western US. While burn severity declined in both lodgepole and ponderosa pine forests that experienced MPB infestation, post infestation changes in burn severity are most pronounced in lodgepole pines with burn severity being one quarter to one third as severe as control forests.

The response of infested ponderosa was comparatively modest and burned 5-10% less severely than control forests. Temporal variability in burn severity between phases is also visible between each MPB host species type. While differences in burn severity between infested and control forests remains similar for the red and grey phases of infestation for ponderosa pine forests (< 4% difference), there is a modest decline in lodgepole burn severity associated with the temporal transition from red to grey phases of infestation. Specifically, the grey phase burned 8% less severely than control forests compared to the differences found for the red phase.

Although utilized in several studies to determine links between beetle infestation and the secondary effects that follow (Bearup et al., 2014; Hart et al., 2015; Mikkelson et al., 2013b; Park Williams et al., 2012; Penn et al., 2016), aerial detection survey data used to delineate zones of MPB infestation have limitations. Accuracy assessments reveal 70% agreement between ADS surveys and ground references with zero spatial tolerance and 80% agreement with 50m spatial tolerance for lodgepole pines (Johnson and Ross, 2008). These values exceed the accuracy goals for detection surveys indicating that they are appropriate for analyzing this type of forest disturbance (Hart et al., 2015; Johnson and Ross, 2008). The accuracy of these surveys likely increases after clipping the ADS surveys with maps of MPB host species to remove areas within ADS polygons that do not fit MPB susceptible land cover types as done here; however, a quantitative estimate of this accuracy increase is unknown. Additionally, the coarse resolution of the dNBR6 data offers a way to limit small inaccuracies in MPB location by limiting severity values to 4 categorical values. Through this categorical limitation, pixels located near one another have a high likelihood of having the same burn severity value, creating pockets or mini regions within a fire with the same burn severity and likely the same land cover type. This would decrease result errors from MPB location inaccuracies in a similar manner to the accuracy increase from 70% to 80% when spatial tolerance increases from zero to 50 m (Johnson and Ross, 2008).

3.3.2 Validation of Burn Severity Following MPB Infestation using Raw dNBR and RdNBR Data

As the previous analysis provided a coarse burn severity resolution by limiting each pixel within a fire perimeter to a categorical burn severity value between one and four, the severity analysis was completed again for the raw data used to create dNBR6 (Figure 3.4) as well as for the relative differenced Normalized Burn Ratio (RdNBR) severity data (Figure 3.5). This analysis was conducted to ensure that the categorical values did not influence results and to determine if variations in pre-fire vegetation and canopy density when using differenced data affected the findings compared to relative differenced data. The raw dNBR and RdNBR burn severity data were summed and averaged within each fire instead of the 4 possible categorical values used in the dNBR6 analysis which provided larger averaged variations in severity with an approximate range of 100 to 1,100.

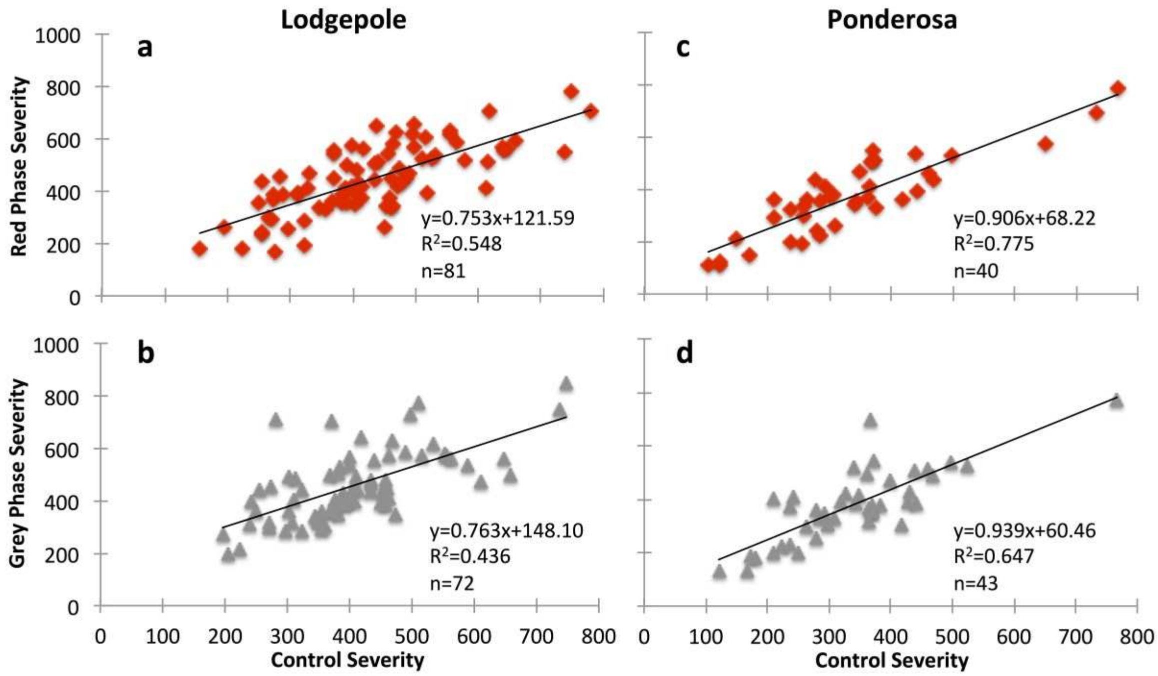

Figure 3.4: Plots of dNBR average burn severity data comparing red (red diamonds) and grey phases (grey triangles) of beetle infestation to control forests in lodgepole pine (a,b) and ponderosa pine (c,d) host species. Each point represents the average burn severity in both forest types for an individual fire. Fires were only plotted if they burned at least 0.5 km^2 of each forest type.

Results for the dNBR data (Figure 3.4) reflect the overall results found in the categorical dNBR6 plots (Figure 3.3). Burn severity in beetle-infested plots were lower than control forests and these differences were again more pronounced in lodgepole pine (red and grey phase severity were 75% and 76% of control severity, respectively) than for ponderosa (red and grey phase severity were 91% and 94% of control severity, respectively). Differences in slope between Figures 3.3 and 3.4 were within three-hundredths with the exception of grey phase lodgepole pine, which had a lower burn severity than the red phase in the dNBR6 data but was nearly the same in the dNBR data. It is not surprising that the results present similar findings, as the categorical dNBR6 values are derived from the dNBR data; however, this provides a convenient control to ensure that the categorical values used in the dNBR6 are both accurate and represents the raw data.

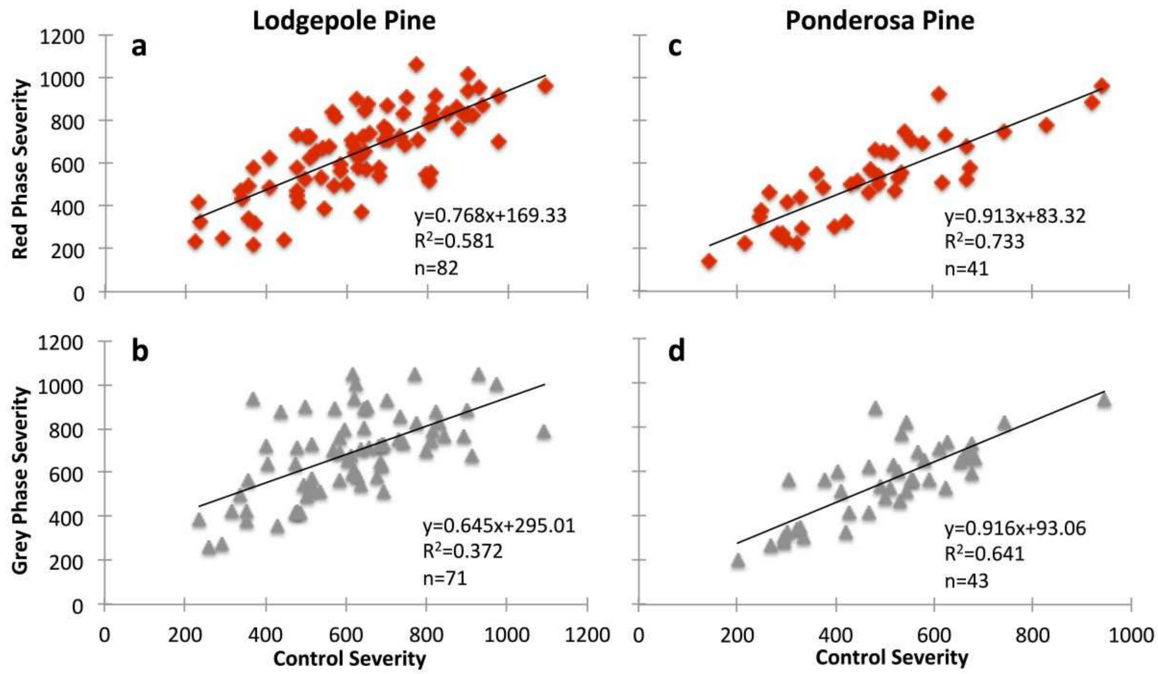

Figure 3.5: Plots of RdNBR average burn severity data comparing red (red diamonds) and grey phases (grey triangles) of beetle infestation to control forests in lodgepole pine (a,b) and ponderosa pine (c,d) host species. Each point represents the average burn severity in both forest types for an individual fire. Fires were only plotted if they burned at least 0.5 km^2 of each forest type.

To investigate possible misclassifications in burn severity due to variations in pre-fire canopy density or vegetation shifts when using dNBR in beetle infested regions, RdNBR was also analyzed which takes into account the absolute change between pre and post fire satellite imagery (Figure 3.5). While burn severity values for all forest types are generally higher in the RdNBR data, the slope of the plotted results displays lower burn severity in beetle infested areas compared to control forests and closely match the results from the dNBR plots negating the concern about using dNBR severity data in disturbed forests. This supports previous results demonstrating that RdNBR data does not estimate burn severity more accurately than dNBR data across diverse fire types with heterogeneous or low canopy land cover (Soverel et al., 2010) and that both fire severity products are viable options for evaluating effects of beetle infestation. The burn severity comparison between grey phase lodgepole and control forests was lower than the red phase severity comparison, which differed from the dNBR data but was similar to the dNBR6 results.

3.3.3 Minimum Area Criteria and Explanatory Severity Mechanisms

Differences in burn severity within a forest are likely minimal in regions containing zones of infestation that only occupy a few 30 m pixels or are masked to satellite imagery products. To ensure that the 0.5 km^2 area criteria focused on for the above analyses did not dictate burn severity differences shown in Figures 3.3-3.5, the same plots were created with 3 different minimum area criteria (Table 3.2). As the minimum area required for each forest type increases, the number of fires that satisfy the criteria decreases, yet the overall slope between beetle infested and control forests remain similar for each burn severity data type. While most correlation slopes stayed within 0.1 of each other regardless of the minimum area requirement and displayed a random pattern of change, the slope for the ponderosa grey phase and control comparison declined consistently by 0.12 to 0.15 for each burn severity data type when the minimum area requirement dropped to 0.1 km^2. Regardless of the minimum required area of each forest type burned, the results still indicate decreased burn severity following beetle infestation compared to control forests with all minimum area requirement trials being significantly different with p-values < 0.001.

Table 3.2: Linear regression results comparing averaged burn severity in red and grey phase MPB impacted forests compared to unimpacted control forests for both host species analyzed. Rows depict variations in slope, coefficient of determination, and number of fires meeting the minimum area required for the control and infested forests within each individual fire perimeter declines.

Lodgepole Pine Forests

Minimum area of each forest type within individual fire perimeters (km^2)	dNBR6			dNBR			RdNBR		
Red phase and uninfested control	Slope	R^2	N	Slope	R^2	N	Slope	R^2	N
1.00	0.711	0.533	72	0.747	0.606	54	0.736	0.606	54
0.50*	0.724	0.472	110	0.753	0.548	81	0.768	0.581	82
0.25	0.778	0.441	152	0.753	0.484	109	0.764	0.479	110
0.10	0.781	0.455	195	0.771	0.470	145	0.817	0.528	144
Minimum area of each forest type within individual fire perimeters (km^2)	dNBR6			dNBR			RdNBR		
Grey phase and uninfested control	Slope	R^2	N	Slope	R^2	N	Slope	R^2	N
1.00	0.741	0.511	77	0.880	0.614	48	0.770	0.526	48
0.50*	0.645	0.393	113	0.763	0.436	72	0.645	0.372	71
0.25	0.734	0.446	146	0.812	0.482	96	0.660	0.385	95
0.10	0.741	0.409	190	0.780	0.400	123	0.721	0.369	122

Ponderosa Pine Forests

Minimum area of each forest type within individual fire perimeters (km^2)	dNBR6			dNBR			RdNBR		
Red phase and uninfested control	Slope	R^2	N	Slope	R^2	N	Slope	R^2	N
1.00	0.827	0.560	42	0.880	0.740	26	0.948	0.757	27
0.50*	0.902	0.552	61	0.906	0.775	40	0.913	0.733	41
0.25	0.921	0.579	81	0.947	0.767	55	0.960	0.748	55
0.10	0.912	0.505	128	0.940	0.667	86	0.978	0.697	83
Minimum area of each forest type within individual fire perimeters (km^2)	dNBR6			dNBR			RdNBR		
Grey phase and uninfested control	Slope	R^2	N	Slope	R^2	N	Slope	R^2	N
1.00	0.964	0.686	52	0.942	0.748	31	0.962	0.767	32
0.50*	0.940	0.622	69	0.939	0.647	43	0.916	0.641	43
0.25	0.918	0.596	105	0.892	0.608	65	0.836	0.577	65
0.10	0.789	0.413	147	0.749	0.419	91	0.712	0.414	92

Note:
*Values depict the same results plotted in Figures 3-5 but are included for visual comparison
All correlation coefficients are statistically significant with p-values <0.001

Several mechanisms may be responsible for the observed reductions in fire severity following MPB-induced tree mortality. The reduced severity in the grey phase is likely due to reduced fuel loads in the canopy. Additionally, revegetation and fallen trees may not actively increase ladder fuels to the canopy in the grey phase or the lack of fuel in the canopy prevents these ladder fuels from creating severe crown fires (Hicke et al., 2012). The reduction in fire severity in the red phase is more ambiguous. One possible explanation may be that although red needles still exist in the canopy that are more flammable than green needles of unimpacted trees (Hicke et al., 2012; Jenkins et al., 2014), the degradation of these needles along with the reduction in sap content, photosynthates, and extractives (McDowell et al., 2011; Woo et al., 2007) throughout the tree or other mechanisms that follow tree mortality decrease the fuel available during a fire, reducing burn severity after infestation regardless of phase. Additionally, although canopy moisture content decreases following beetle-induced tree mortality (Jenkins et al., 2014), crown fires are so intense that differences in moisture content between control and impacted stands may have little effect on overall burn severity.

Although burn severity was lower in red and grey phases of ponderosa pine compared to unimpacted controls, differences were limited with beetle infested burn severity being between 90 to 94% as severe as control forests. Burn severity variations between beetle infested and control forests were more pronounced in fires burning lodgepole pines with red and grey phases of infestation burning approximately 65 to 77% as severely as control forests depending on the data source used. Differences in burn severity between MPB host species likely occur due to ecological and fuel structure differences between lodgepole and ponderosa pine forests. Lodgepole pine forests are typically dense monocultures with limited undergrowth (*2008 Report: The Health of Colorado's Forests*, 2008), while ponderosa pine forests are not as dense and allow more undergrowth to occur (Graham and Jain, 2005). Additionally, the high tree density and elevated leaf area index in lodgepole pine forests compared to ponderosa pine (Fule et al., 1997; Pierce and Running, 1988; Ryan and Waring, 1992) likely create higher fuel loads in the canopy and more severe fires. Evidence of these differences can be seen in the burn severity data with infested and control lodgepole pine forests burning at a higher severity than ponderosa pine forests (Figure 3.4, 3.5). Therefore, shifts in canopy structure or fuel loads that alter burn severity as a result of beetle infestation are more apparent in lodgepole pines. Due to the significantly lower burn severity in MPB infested lodgepole pine, our recommendation is to avoid tree removal in this forest type as a management objective to reduce fire severity. This host species has been the most susceptible to MPB infestation across the Rocky Mountains with mortality approaching 100% in some regions (Collins et al., 2011). MPB impacted ponderosa forests have not burned to the extent of impacted lodgepole forests (Hart et al., 2015) and due to the similar burn severity between beetle infested ponderosa and control stands, infested ponderosa are likely not as strong of a natural fire buffer compared to impacted lodgepole forests.

3.4 Conclusions

Overall, the data presented here indicates that beetle-infested forests burn less severely than uninfested forests. Complementary studies evaluating differences in fire severity after insect infestation using a similar approach as described here for the US Pacific Northwest (Meigs et al., 2016) or those focusing on detailed field data from seven discrete fires in Montana, Idaho, and Wyoming,(Harvey et al., 2013, 2014) rather than the larger areal data presented here, also found beetle outbreak to decrease burn severity or be unrelated to most field measures of fire severity. Our findings focusing on burn severity across the Western US over the duration of the current bark beetle epidemic add to an increasing body of scientific literature (Hart et al., 2015; Harvey et al., 2014; Meigs et al., 2016) to conclude that contrary to public perception (Kotack, 2016; Poppleton, 2008), forest fire risk decreases following bark beetle infestation.

Climate change is clearly increasing forest disturbances with drought stress being a large contributor and predictor of wildfires (Park Williams et al., 2012; Westerling, 2006; Williams et al., 2010). Although drought conditions have also expanded bark beetle habitat and caused ecohydrological, biogeochemical, and forest fuel structure changes (Hicke et al., 2012; Mikkelson et al., 2013a, 2013c), the direct perturbations from beetle infestation do not disproportionally appear to have contributed to increases in fire severity. Due to recent findings that have highlighted the influence of insect induced-tree mortality on altering water quality (Mikkelson et al., 2013b), carbon uptake (Kurz et al., 2008), and climate feedbacks (Maness et al., 2012), future research should focus on these secondary effects of expansive forest die-off.

Several studies have quantified fire behavior dynamics after beetle infestation through discrete plot analysis or modeling; however, our study used a robust empirical dataset of observed fire and MPB epidemic data coupled to elucidate whether these forest changes impact fire severity. The quantity of fires analyzed and overall agreement between the three data types (dNBR6, dNBR, and RdNBR) employed in the study provides further validation of the data processing and severity analysis procedure utilized along with the overall conclusion of reduced fire severity following beetle infestation. Additionally, the approach used in this study can be valuable for investigating other natural global disturbances. Although modeling and detailed plot analysis help elucidate the mechanisms or perturbations in natural systems resulting from a changing climate, large-scale temporal analysis of observed data similar to the approach described here can more holistically synthesize these findings and establish correlations to other observable secondary effects (*i.e.* water quality changes). Analyzing other climatically distinct regions experiencing increases in vegetation mortality and wildfires such as British Columbia (Gillett, 2004; Maness et al., 2012) or Europe (Seidl et al., 2011) could also be used to establish whether there are geographical limitations to these findings.

While the spatial and temporal approach utilized here allowed characterization of numerous fires to display that burn severity declines following infestation and that severity is approximately equal between the red and subsequent grey phases for each tree species analyzed, further work is needed to elucidate this phenomenon. While the reduction of fuel in the canopy likely leads to the decreased burn severity found in grey phase trees, differences in fuel availability and burn intensity following tree death is still unclear and elucidation of the subsequent mechanisms responsible for lower burn severity in the red phase is needed. An increasing concern in the future will be the need to analyze shifts in burn severity during the old phase when extended tree fall occurs (Figure 3.1) as fallen trees can affect burn patterns (Kulakowski and Velben, 2007), complicate fire suppression, and impact firefighter safety (Alexander and Stam, 2003). While our analysis extends 15 years and captures areas experiencing windthrow of beetle infested-trees, millions of hectares of forests will continue to fall and understory regrowth will occur increasing surface and ladder fuels that complicate burn severity (Hicke et al., 2012).

Due to the expansive threats forest fires have on property and public health, wildfire concerns are driving policy and forest management decisions toward removal of impacted trees. For example, through the assumption linking expansive beetle-induced tree mortality and subsequent increases in dead fuels to elevated fire threats, $200 million was designated from the 2014 US Farm Bill to support fuel reduction strategies and mitigate wildfires risk in US National forests affected by insect infestation and disease (*Agricultural Act of 2014, Public Law 113-791*, 2014; Hart et al., 2015). Besides threats to property or human well-being, fire also impacts water quality and water management through increased erosion and sediment transport (Smith et al., 2011). Municipal water providers whose watersheds are located in forested regions containing beetle-infested forests have removed dead trees as a mechanism to reduce increases in assumed fire risk (Poppleton, 2008). The results demonstrated here indicate that beetle infestation actually reduces fire severity and that tree removal efforts to decrease fire risk may in fact be eliminating a natural fire buffer with ancillary and unanticipated repercussions. Tree harvest has been shown to adversely impact drinking water and may lead to other secondary effects such as elevated nutrient concentrations or erosion impacts to streams (Aust and Blinn, 2004). The removal of trees may therefore cause additional impacts to water quality in an attempt to reduce an imaginary wildfire risk.

There is also an economic incentive to harvest dead trees for commercial products, non-structural lumber, or biofuels (Poppleton, 2008; Zhou et al., 2013); however, wildfire suppression and prevention costs upward of ten million dollars annually in many National Forests in the Western US (Thompson et al., 2015). Our findings suggest that policy decisions regulating tree removal for economic incentives should therefore weigh the costs of removing dead trees that provide a natural reduction in fire severity. As shifts in weather patterns and fuel sources occur in arid regions in this period of climatic change, continued analysis of wildfire drivers is needed to enhance fire prediction ability, forest management, and appropriate mitigation strategies. However, a growing body of scientific literature suggests that large-scale bark beetle infestation may provide a natural buffer as an outgrowth of these same climatic drivers.

CHAPTER 4

SEVERITY OF TREE MORTALITY INFLUENCES SOIL BIOGEOCHEMICAL RESPONSE IN A BEETLE-INFESTED CONIFEROUS FOREST

Modified from a manuscript submitted for publication

Brent M. Brouillard[1,2], Kristin M. Mikkelson[1,3], Chelsea M. Bokman[1], Erin Berryman[4], Jonathan O. Sharp[1,3]

Abstract

Recent increases in the magnitude and occurrence of bark beetle-induced tree mortality are disrupting evergreen forests globally. To resolve potentially conflicting ecosystem responses, we investigated whether surrounding trees exert compensatory effects on biogeochemical signatures following beetle infestation. To this end, we surveyed plots containing a range of tree mortality (from 9-91% of standing trees) in the Colorado Rocky Mountains and sampled near-surface soil horizons under plot-centered live (green) and beetle-killed (grey) lodgepole pines. Sampling over two consecutive summers with variable moisture conditions revealed that net soil respiration was 18-28% lower beneath beetle infested trees and correlated to elevated dissolved organic carbon aromaticity. Surrounding live trees and associated subsurface processes were found to buffer this effect with significant increases in respiration associated with increased numbers of surrounding live trees. In addition to respiration, other soil properties such as

[1] Department of Civil and Environmental Engineering, Colorado School of Mines
[2] Principal researcher and author of this manuscript
[3] Hydrologic Science and Engineering Program, Colorado School of Mines
[4] United States Geological Survey, Geosciences and Environmental Change Science Center

leachable carbon and nitrogen species were correlated to mortality phase (green vs grey) and severity of surrounding tree mortality. While certain edaphic parameters including pH and water content were elevated below grey compared to green trees, other biogeochemical responses required a high severity of surrounding mortality to overcome compensatory effects of neighboring live trees. For instance, C:N ratios declined with increased severity of surrounding tree mortality, while the proportion of ammonium displayed a threshold effect increasing primarily after surrounding tree mortality exceeded ~ 40%. Overall, the biogeochemical response to tree death was most prominent in the mineral horizon where cessation of root processes following mortality and an increase in top-down nutrient flux from degrading material had the largest effect on carbon recalcitrance and the enrichment of nitrogen species. These results can be used to predict fluctuating nutrient cycles that have implications for emergent growth and biogeochemical feedbacks to the atmosphere and hydrosphere as global forest mortality continues and ecosystems evolve.

4.1 Introduction

While past studies have investigated seasonal and inter-annual variability of terrestrial biogeochemical cycling during forest recovery (Ferrenberg et al., 2014; Mikkelson et al., 2016b; Norton et al., 2015; Štursová et al., 2014), few have investigated variability due to the severity of beetle infestation (Cigan et al., 2015). In chapter four, we aim to better understand and resolve variable and potentially conflicting biogeochemical responses after beetle infestation to enhance predictions of soil respiration and nutrient shifts following this form of forest mortality. Motivation came from a precedent established following logging disturbance, which suggests that geochemical responses are muted until a threshold of surrounding tree mortality is surpassed (Parsons et al., 1994; Prescott et al., 2003) presumably because adjacent live trees exert a compensatory effect on ecosystem disruption. While tree harvesting has notable differences from that of mortality caused by bark beetles (Adams et al., 2012; Mikkelson et al., 2013a), we hypothesized that an analogous threshold of localized tree mortality must be exceeded before a pronounced disruption of terrestrial carbon and nitrogen cycling is observed. To enable this inquiry, we focused our study on lodgepole pines (*Pinus contorta*) infested by bark beetles in the Colorado Rocky Mountains. Plots were surveyed that contained a range of beetle-induced tree mortality ranging from 9-91% of standing trees affected. A suite of soil biogeochemical parameters (i.e. soil respiration, C and N species, pH) were then compared to mortality phase (healthy vs. deceased) and related to the severity of tree mortality within each plot. Sampling was conducted during two subsequent summers with variable moisture scenarios to provide temporal reproducibility and validation across different inter-annual climatic conditions. Our findings provide a foundation to better understand how and when terrestrial biogeochemical processes may change in association with this type of large-scale ecosystem disruption.

4.2 Methods

4.2.1 Site Selection and Characterization

The study was performed in the White River National Forest approximately 5 km southwest of Frisco, Colorado (39.5427° N, 106.1460° W) in the summer of 2015 and 2016. This site was chosen for its range of localized tree mortality severity, accessibility, relative homogeneity of vegetation, and uniform slope and aspect (Table B.1). The forest is dominated by lodgepole pine (*Pinus contorta*) (USDA, 2017), which experienced mountain pine beetle infestation beginning between 2007 and 2008. This study focused on comparisons between the ‘green’ phase, when a tree is alive, healthy, and transpiring, and the ‘grey’ phase, with an onset 3-5 years after initial infestation when the dead tree has dropped its needles (Mikkelson et al., 2013a). No recent anthropogenic or natural forest disturbance aside from bark beetle infestation has occurred at the site.

Thirty-eight, 8 meter radius plots were established, each centered on a green phase (n=7) or grey phase (n=31) sample tree. Plot-level severity of tree mortality was defined as percentage of dead trees relative to total number of trees in the plot and ranged from 9 to 91%. In the northern Rocky Mountains, lodgepole pine roots may extend 4 meters from the trunk (Parsons et al., 1994); therefore, an 8-meter radius plot size was selected to include trees that may partially overlap with the root system of the sample tree. Only trees with diameter at breast height > 7 cm were included in mortality measures. Surveyed neighboring trees were primarily lodgepole pine with an occasional aspen (Figure B.1). All plots were located on the same hillslope and care was taken to account for and reduce heterogeneity in slope, aspect, soil type, land cover, tree circumference, and sun exposure while capturing a range of surrounding tree mortality (Table B.1). The aspect at each sample tree was East-Southeast with slopes ranging from 8 to 27%.

4.2.2 Soil Respiration Analysis

Respiration and soil horizon sampling was conducted during three consecutive days in mid-July of 2015 and again in early August 2016. Soil respiration was measured at three polyvinyl chloride (PVC) collars positioned ~ 0.5 m from the trunk of each plot-center tree using a closed dynamic chamber (LI-8100 survey soil gas flux system, LI-COR Biosciences). Collars were installed 24 hours prior to conducting soil respiration measurements to allow gas equilibration following installation. Care was taken to collect samples from three distinct locations around the tree trunk during the second summer that were free from disturbance arising from the previous year's sampling event. Two CO_2 flux measurements were collected consecutively from each of the three collars around each sample tree. These measurements were then averaged, providing one soil respiration value per tree to examine effects of tree phase and surrounding tree mortality. No correlations were found between soil respiration and soil temperature or water content; therefore, no temperature or moisture corrections were performed on the respiration data.

4.2.3 Collection of Soil Horizon Samples

Immediately following respiration measurements, samples were collected from the litter, organic, and mineral horizon within each respiration collar, providing a reproducible zone of collection and a consistent sampling procedure (Figure B.1). Approximately equal volumes of horizon sample were obtained from the three collars around each tree (1 L total) and hand homogenized to create a representative sample for each tree. After collecting litter and organic layer samples within each ring, the ring was removed and a small hole (20 cm diameter) was dug using a hand trowel for mineral soil collection. Due to variable litter depth, mineral horizon samples were collected 15 cm below the interface between the mineral and organic horizon.

During the first sampling season (2015), mineral soil samples were collected at all 38 plot-center trees, whereas organic and litter samples were collected at a subset of plot-center trees (n=25; 5 green and 20 grey phase trees) to enable sufficient processing time for time sensitive variables (i.e. N species). To confirm temporal reproducibility and investigate whether differences in moisture conditions influenced biogeochemical response, additional samples were collected from all three horizons at plot-center trees in a subset of the original plots in 2016 (n=26; 6 green and 20 grey phase trees). Furthermore, 2016 mineral soil samples from each respiration collar were analyzed individually (as opposed to homogenization of the samples as conducted in 2015) to specifically associate each mineral soil sample to a respiration measurement. Mineral soil results for each respiration collar were then averaged together to produce a single value for each plot when analyzing geochemical trends in relation to plot tree mortality. Samples for geochemical analyses were put on ice and immediately transported to the lab and stored in the dark at 4 ^{o}C. Analyses were performed in less than 2 weeks.

Daily precipitation data were obtained from two National Climatic Data Center gauges that were both located within 13.5 km of the study site for the week prior to collection through the 3rd (final) day of sampling. Sampling during 2015 resembled moist conditions, while the 2016 sampling event occurred under substantially drier summer conditions.

4.2.4 Geochemical Analyses

Mineral soil, organic layer, and litter layer samples were analyzed for pH (2015 only), soil moisture, organic matter content, dissolved organic carbon (DOC), ultraviolet absorbance at 254 nm (UV_{254}), total nitrogen (TN), nitrate (NO_3^-), ammonium (NH_4^+). Mineral samples were sieved through 2 mm mesh to remove large soil aggregates and all samples were thoroughly homogenized prior to analysis. Moisture was determined gravimetrically and organic matter content was measured using loss-on-ignition method

(Ball, 1964). Samples were dried at 105 ^{o}C for 24 hours and then placed in a 375 ^{o}C oven for 16 hours. Geochemical digests were performed following one hour of shaking in 1:5 solid mass:liquid volume ratio (g/mL) for mineral and organic horizon samples and a 1:8 ratio for litter samples. Measures of extractable DOC, UV_{254}, TN, and ammonium were determined by digestion in 0.5 M K_2SO_4 solution (Ferrenberg et al., 2013). Extractions were filtered through 0.45 um polyethersulfone filters prior to aqueous analysis. DOC and TN were then determined using a Shimadzu TOC-550A Total Organic Carbon Analyzer after acidifying with HCl acid. UV_{254} was measured using a DU 800 spectrophotometer. Specific UV absorbance (SUVA) was calculated by dividing UV_{254} by DOC concentration to evaluate differences in aromatic structure (Drewes and Croue, 2002). Ammonium concentrations were measured using the sodium salicylate method and absorbance at 650 nm with a DR 3900 Hach Spectrometer (Sparks et al., 1996). Measures of NO_3^- and pH were determined following deionized water digests during 2015 (Ferrenberg et al., 2013). In 2016, NO_3^- analysis was conducted following the same K_2SO_4 digests as for other nitrogen species to enable a more accurate mass balance. While deionized water digests were found to leach similar concentrations of nitrate as K_2SO_4 digests for mineral horizon samples, deionized water mobilized higher average concentrations of NO_3^- in the litter and organic horizons (38 and 51% higher than K_2SO_4 digests, respectively). Nonetheless, overall trends were consistent between digests. Nitrate concentrations were determined using the dimethylphenol method and absorbance at 345 nm with a DR 3900 Hach Spectrometer (Moorcroft et al., 2001). The concentration of dissolved organic nitrogen was calculated through mass balance by subtracting the sum of nitrate and ammonium from the TN concentration (Kaňa et al., 2012, 2015). Geochemical results were normalized by kg of dry sample and C:N ratios were calculated as molar ratios of DOC:TN.

4.2.5 Statistical Analyses

Mann-Whitney rank abundance tests were used to compare biogeochemical parameters between plot-centered trees classified as green versus grey. Spearman and Pearson tests were used to assess nonlinear and linear correlations between geochemical results and two different plot mortality indices. Respiration trends were compared to the number of live trees as respiring root systems and associated live root processes play a significant role in overall soil respiration (Bhupinderpal-Singh et al., 2003). All other biogeochemical trends were related to surrounding tree mortality (number of surrounding grey trees/total trees) as the amount of infested trees drives geochemical shifts occurring from altered litterfall, nutrient/water uptake, and canopy closure (Mikkelson et al., 2013a). Segmented linear regression was used to test for threshold relationships (Muggeo, 2003) between biogeochemical parameters and plot tree mortality severity using R (R Core Team, 2014). P-values less than 0.05 were considered significant.

4.3 Results

To investigate the relationship between shifting biogeochemical parameters in relation to the degree of local beetle infestation, soil respiration and horizon samples were collected below green and grey trees with varying severity of surrounding tree mortality that ranged from 9-91%. Distinct biogeochemical signatures were found when comparing parameters beneath green and grey trees along with trends related to the degree of surrounding tree mortality (calculated as the number of dead trees/total trees). These biogeochemical results for the mineral layer are depicted in Table 4.1 (page 73) for both sampling years while similar statistical results for the litter and organic layer are displayed in Appendix B (Tables B.2-B.3). We found that some biogeochemical signatures were linked to plot tree mortality severity, while others were disrupted under beetle-killed trees regardless of mortality severity.

The 2015 results represent geochemical differences under wetter conditions as averaged cumulative precipitation between two local gauges displayed more than 4 times as much cumulative rainfall prior to and during the sampling event when contrasted with 2016 (37.6 and 8.9 mm; respectively, over 9 days). This resulted in average mineral soil moisture conditions that were 33% greater under green trees and 58% greater below grey trees when contrasting these wet and dry periods (Table 4.1). Aside from soil respiration results, significant geochemical differences and trends were typically consistent for both years analyzed, although higher N and C concentrations were found in the litter and organic horizons during the drier 2016 conditions.

4.3.1 Altered Soil Respiration Following Tree Mortality

Root respiration ceases following tree die-off and shifts in nutrient cycling may affect microbial respiration in the subsurface. To explore the implications of these changes, soil respiration was analyzed to determine differences below tree phases and to elucidate trends linked to surrounding tree mortality. Overall, respiration was elevated during wet conditions (2015) compared to dry conditions (2016) for both tree phases. Average soil respiration below grey trees was 18 and 28% lower than green trees during the 2015 and 2016 sampling events (respectively); however, this difference was only significant during 2016 (Table 4.1, Figure 4.1).

Table 4.1: Changes in mineral layer biogeochemical properties as a function of tree stage and sampling year. Significant differences are denoted in bold with an asterisk (p-value < 0.05).

Parameter	2015 (Wet Conditions) Green Average (SD)[1]	Grey Average (SD)[1]	Mann-Whitney U[2]	Spearman rho[3]	2016 (Dry Conditions) Green Average (SD)[1]	Grey Average (SD)[1]	Mann-Whitney U[2]	Spearman rho[3]
pH	5.04 (±0.17)	5.52 (±0.31)	**16.5***	-0.045	-	-	-	-
Water Content (% wet weight)	7.85 (±2.64)	12.49 (±3.66)	**32***	-0.193	5.89 (±0.60)	7.92 (±2.40)	**26***	0.164
DOC (mg-C/kg dry sample)	137 (±68)	95 (±48)	65	-0.160	117 (±18)	104 (±49)	33	-0.180
SUVA (kg dry sample/mg*M)	0.50 (±0.10)	0.57 (±0.07)	66	**0.361***	0.47 (±0.08)	0.57 (±0.08)	**24***	**0.687***
Organic Matter (%)	3.39 (±1.57)	3.27 (±1.55)	92	-0.038	3.47 (±0.68)	3.80 (±1.19)	53	0.192
Total Nitrogen (mg-N/kg dry sample)	5.15 (±1.02)	6.37 (±2.02)	64	0.093	4.62 (±0.56)	5.56 (±1.90)	40	0.317
NO_3^- (mg-N/kg dry sample)	1.06 (±0.61)	1.38 (±0.47)	61	-0.011	0.98 (±0.28)	1.24 (±0.88)	52	0.361
NH_4^+ (mg-N/kg dry sample)	0.31 (±0.09)	1.22 (±1.14)	**42***	**0.428***	0.37 (±0.10)	1.14 (±1.08)	**18***	**0.705***
Organic Nitrogen (mg-N/kg dry sample)	3.78 (±0.56)	3.77 (±1.36)	82	-0.151	3.27 (±0.41)	3.21 (±0.59)	53	-0.364
NO_3^-/TN	0.19 (±0.07)	0.23 (±0.07)	79	-0.167	0.21 (±0.05)	0.21 (±0.10)	58	0.299
NH_4^+/TN	0.06 (±0.02)	0.18 (±0.13)	**55***	**0.406***	0.08 (±0.02)	0.18 (±0.10)	**21***	**0.666***
Organic N/TN	0.74 (±0.06)	0.60 (±0.11)	**27***	**-0.409***	0.71 (±0.03)	0.61 (±0.15)	37	**-0.630***
C:N (molar ratio)	29.71 (±9.03)	17.70 (±6.39)	**32***	-0.232	29.77 (±5.42)	22.22 (±7.90)	**22***	**-0.517***
Soil Respiration[4] ($umol/m^2*sec$)	4.52 (±1.27)	3.69 (±0.84)	54	**0.499***	3.66 (±0.73)	2.65 (±0.69)	**19***	0.018

Year 1 (wet conditions): n=31 grey, 7 green
Year 2 (dry conditions): n=20 grey, 6 green
[1] Average parameter ± their standard deviation (SD)
[2] Difference between green and grey phase trees
[3] Nonlinear correlation between parameter under grey phase trees and plot-level severity of tree mortality (different for respiration, see below)
[4] Collected above undisturbed horizons prior to sampling. Spearman correlation found between respiration under grey phase trees and number of surrounding green trees

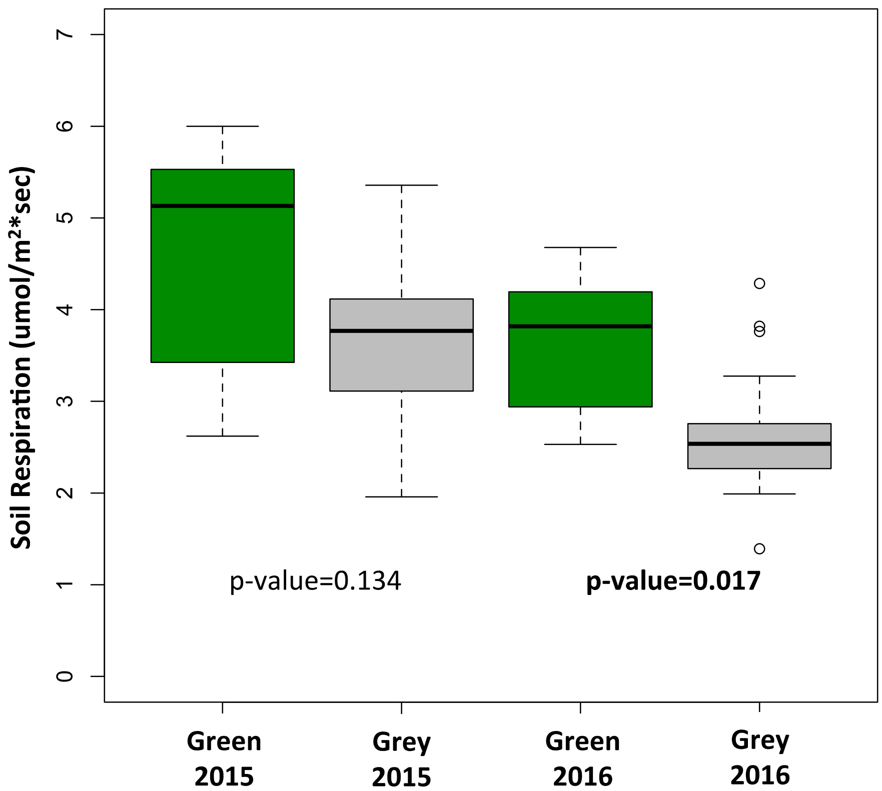

Figure 4.1: Changes in soil respiration below green and grey phase trees during the 2015 (wet conditions) and 2016 (dry conditions) sampling events. Boxes are representative of the upper and lower quartiles and whiskers represent the maximum and minimum values. Points represent outliers.

When evaluating links between soil respiration and plot mortality indices, soil respiration was found to correlate strongest with the number of live tress within each plot. Although average soil respiration beneath grey trees was found to be lower than under green trees, soil respiration rates below grey trees approached those of green trees as the number of surrounding healthy trees within the plots increased in 2015 (Figure 4.2, Table 4.1). A similar trend was not found during the dry 2016 conditions.

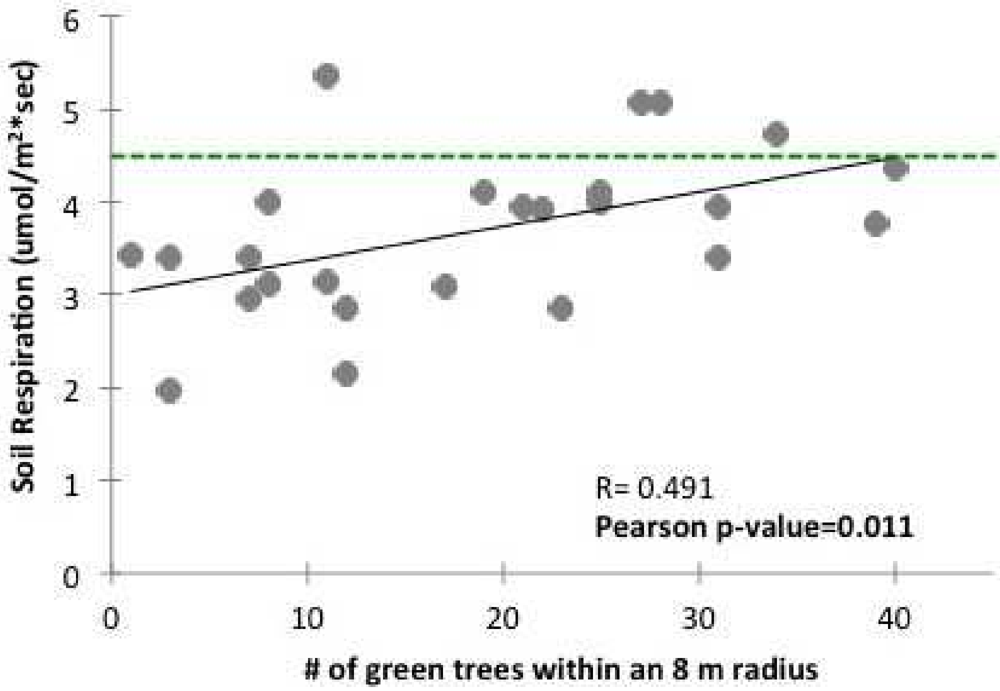

Figure 4.2: Soil respiration beneath grey phase trees during the 2015 (wet conditions) sampling event compared to the number of surrounding green trees within 8m. For comparison, the dashed green line shows the average soil respiration under green trees during 2015.

As respiration increased with number of surrounding live trees in 2015 potentially due to root derived nutrients that shift soil respiration, trends were evaluated between mineral layer nutrients (C and N) and soil respiration for each collar individually in 2016. Although a relationship between soil respiration and DOC or N-species concentrations was not found, soil respiration significantly declined with increased SUVA in the mineral layer (Figure B.2). This trend of decreased respiration with elevated carbon aromaticity was found both when SUVA and respiration were determined individually for each ring (2016) and when SUVA was calculated from the binned samples and compared to the average soil respiration beneath each tree (2015).

4.3.2 Edaphic Shifts Under Beetle-killed Trees

Analogous to soil respiration, geochemical parameters were found to differ depending on tree phase. Specifically, water content was significantly higher in the organic and mineral horizons and pH was significantly higher in all three horizons when comparing soils under grey compared to green phase trees. However, despite differences in these parameters under grey phase trees, there was no correlation to the severity of surrounding tree mortality (Tables 4.1, B.2 – B.3). Soil organic matter content, on the other hand, was not significantly different under green versus grey phase trees in any soil horizon (Table 4.1, B.2 – B.3).

As N speciation can be sensitive to and vary with forest disturbance (Mikkelson et al., 2013a), we analyzed the primary components of the soil TN pool (organic N, ammonium, and nitrate) relative to tree phase and surrounding tree mortality. The concentration of TN was not significantly different between tree phases and did not associate with surrounding tree mortality except in the litter horizon in 2016, where it increased modestly in conjunction with surrounding tree mortality and exhibited differences between green and grey trees (Tables 4.1, B.2 – B.3). Similarly, organic N and nitrate concentrations were not significantly different between green and grey trees and did not consistently shift with increasing tree mortality (Tables 4.1, B.2 – B.3). Ammonium, on the other hand, was found to be significantly higher under grey compared to green trees in the mineral horizon and was found to increase with the level of surrounding tree mortality in all horizons (Tables 4.1, B.2 – B.3). While the majority of trends related to the concentration of nitrogen species were not compelling, in all sampled horizons and across both time points there was a marked change in the N species composition of the TN pool as severity of tree mortality increased (Figure 4.3).

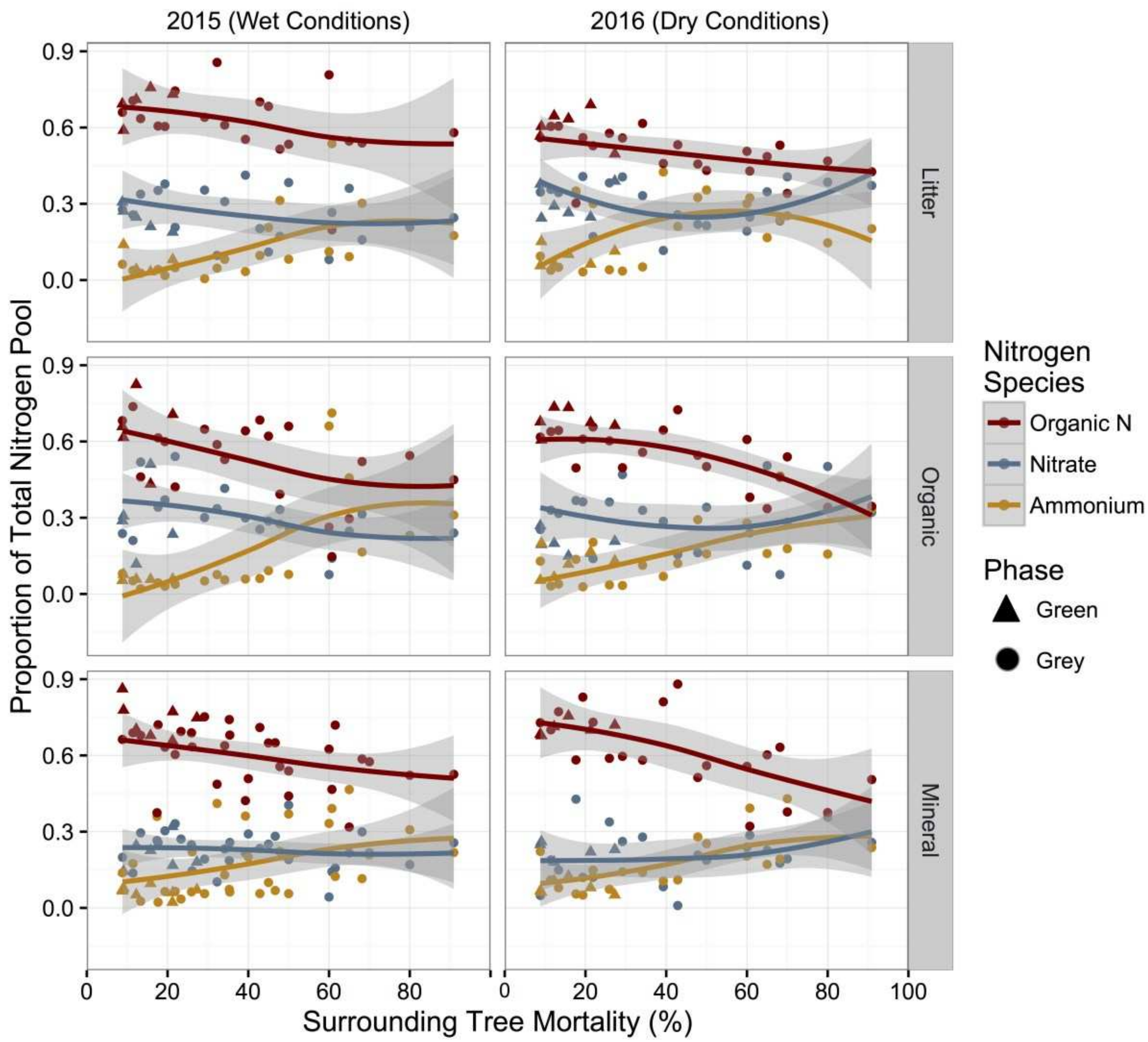

Figure 4.3: Changing composition of the total nitrogen pool relative to surrounding tree mortality. LOESS smoothing indicated by the solid lines was conducted on N species under grey phase trees. Green trees are excluded from the smoothing regression but are included graphically for comparison. Shaded area represents the 95% confidence interval.

Organic N dominated in all soil horizons and was typically higher under green trees, constituting an average of 61-70%, 65-68%, and 71-74% of the TN pool in the litter, organic, and mineral horizons, respectively for both years. Under grey phase trees organic N still dominated the TN pool but at lower percentages (50-61%, 52-54%, and 60% in the litter, organic, and mineral horizons; respectively) for both years. The relative proportion of organic N under grey phase trees also decreased as surrounding tree mortality increased (Figure 4.3; Tables 4.1, B.2 – B.3; p-value < 0.05 for all horizons in both years). In contrast, the proportion of nitrate in the TN pool was not significantly different between grey and green phase trees in any horizon and was unaffected by surrounding tree mortality (Figure 4.3; Tables 4.1, B.2 – B.3).

In investigating the proportion of ammonium in the TN pool across both years, ammonium generally increased in all horizons in association with the severity of surrounding mortality (Figure 4.4; Tables 4.1, B.2 – B.3; p-value < 0.05). Interestingly, the proportion primarily increased when surrounding tree mortality surpassed a threshold of approximately 40%. For grey phase trees surrounded by less than 40% tree mortality, the proportion of ammonium was typically low and comparable to that observed under green trees.

We also investigated the concentration and character of the leachable DOC pool. The concentration of DOC did not significantly differ between green and grey trees nor was it related to plot-mortality severity (Tables 4.1, B.2 – B.3). However, carbon aromaticity, and by association recalcitrance, was elevated below grey phase trees compared to green trees in the mineral horizon in 2016, with SUVA increasing by an average of 21% under grey phase trees (Table 4.1). Analyzing variations in SUVA between green and grey phase trees also suggests differences in recalcitrance in the upper horizons for both years, with averaged p-values approaching statistical significance (p-value: organic horizon=0.054, litter horizon=0.096). Furthermore, SUVA increased significantly with elevated surrounding tree mortality in the mineral horizon for both years (Table 4.1; p-value < 0.05).

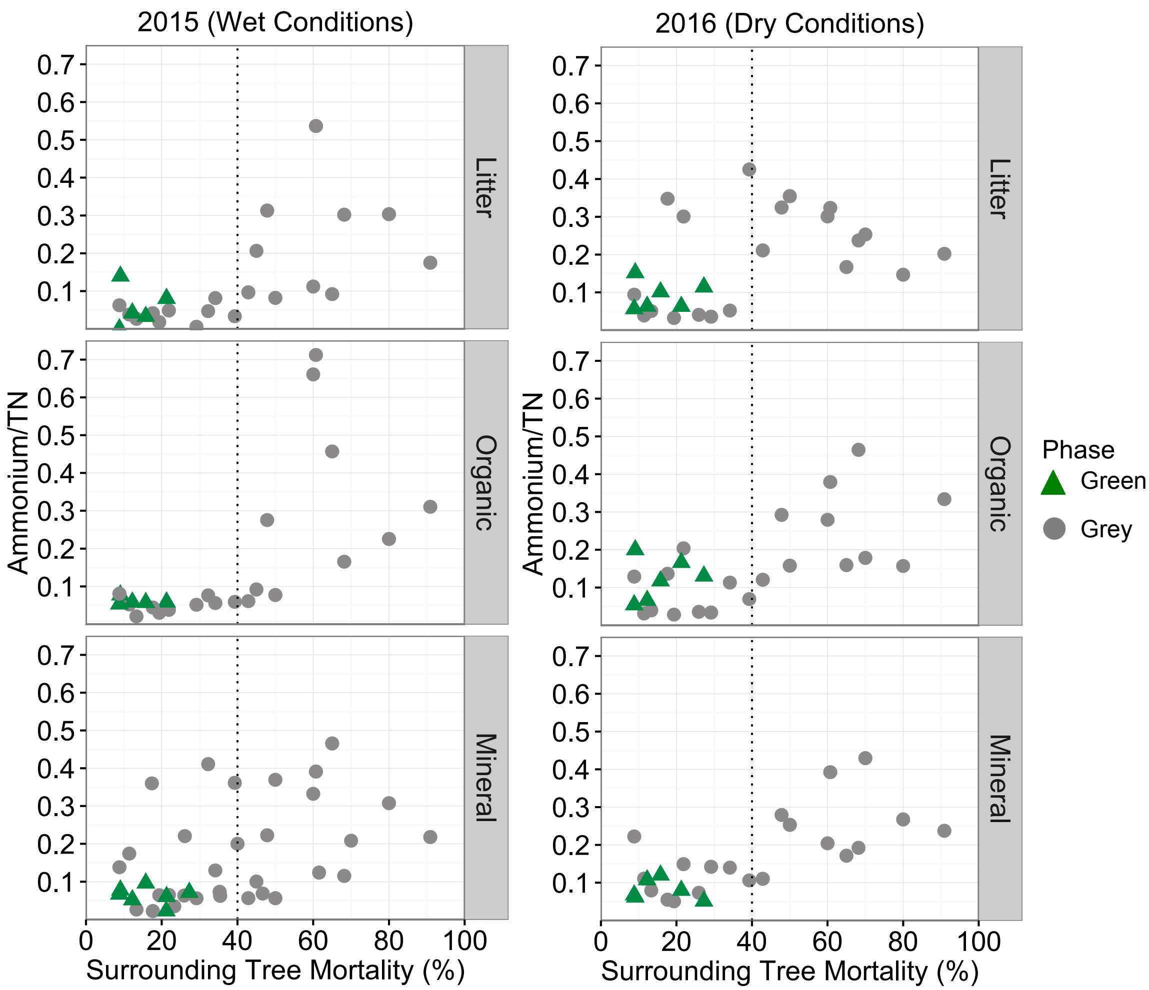

Figure 4.4: The proportion of ammonium under green and grey phase trees surrounded by varying levels of tree mortality in each horizon. The dotted black line represents the approximate threshold of tree mortality (40%) for an ammonium response in each horizon (with the exception of the mineral horizon in 2015 and two outliers in the litter horizon during 2016).

4.3.3 Shifts in C:N Ratio Linked to Surrounding Tree Mortality

Given their interrelated feedbacks, the relative abundance of C versus N (C:N ratio) was used to examine the relationship between relevant biogeochemical processes after bark beetle impact. In the lower two horizons (organic layer and mineral soil), C:N ratios were significantly reduced under grey trees when contrasted to green trees (Tables 4.1, B.3; p-value <0.05). For example, averaged C:N ratios were 22-40% lower under grey compared to green trees in the mineral horizon (Table 1). In addition, C:N ratios decreased as the severity of surrounding tree mortality increased in all horizons except the mineral horizon in 2015 (Figure 4.5; Tables 4.1, B.2 – B.3; p-value <0.05).

In building upon these trends, ammonium concentrations were coupled to C:N ratios across all soil horizons (Figure 4.6, page 82). Ammonium concentrations typically began to rise once the C:N ratio declined past a quantifiable breakpoint; however, the value of this breakpoint differed by soil horizon. The C:N ratio for this transition from baseline to elevated ammonium concentrations decreased in the lower horizons in 2015, from 29:1 in the litter, to 18:1 in the organic and mineral horizons. This segmented breakpoint trend was also displayed during 2016 with values of 29:1 in the litter and 26:1 in the mineral horizons. In the organic horizon, however; even though ammonium was still found to significantly increase as the C:N ratio declined, there was no significant breakpoint. Collectively, these trends demonstrated that the accumulation of ammonium typically occurred when the abundance of C relative to N was below a particular level in each soil horizon.

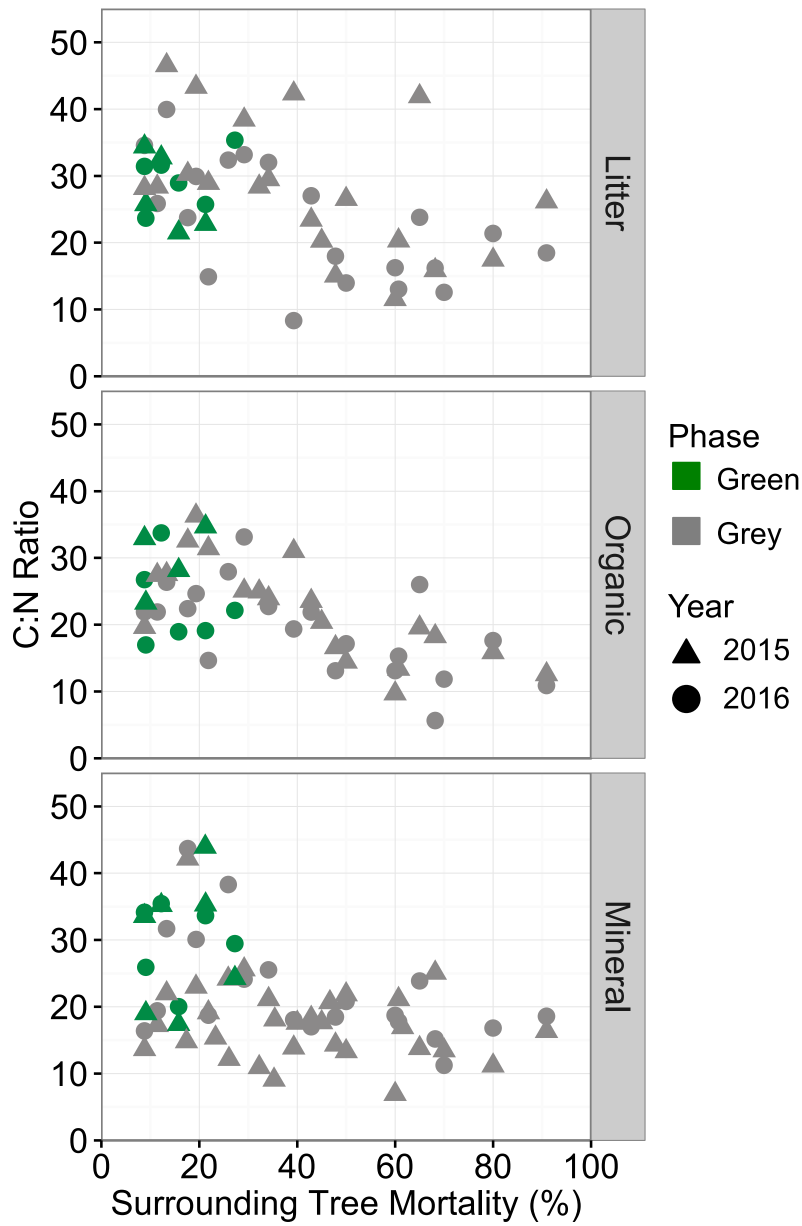

Figure 4.5: The C:N ratio under green and grey phase trees surrounded by varying levels of tree mortality in each horizon during the 2015 and 2016 sampling events.

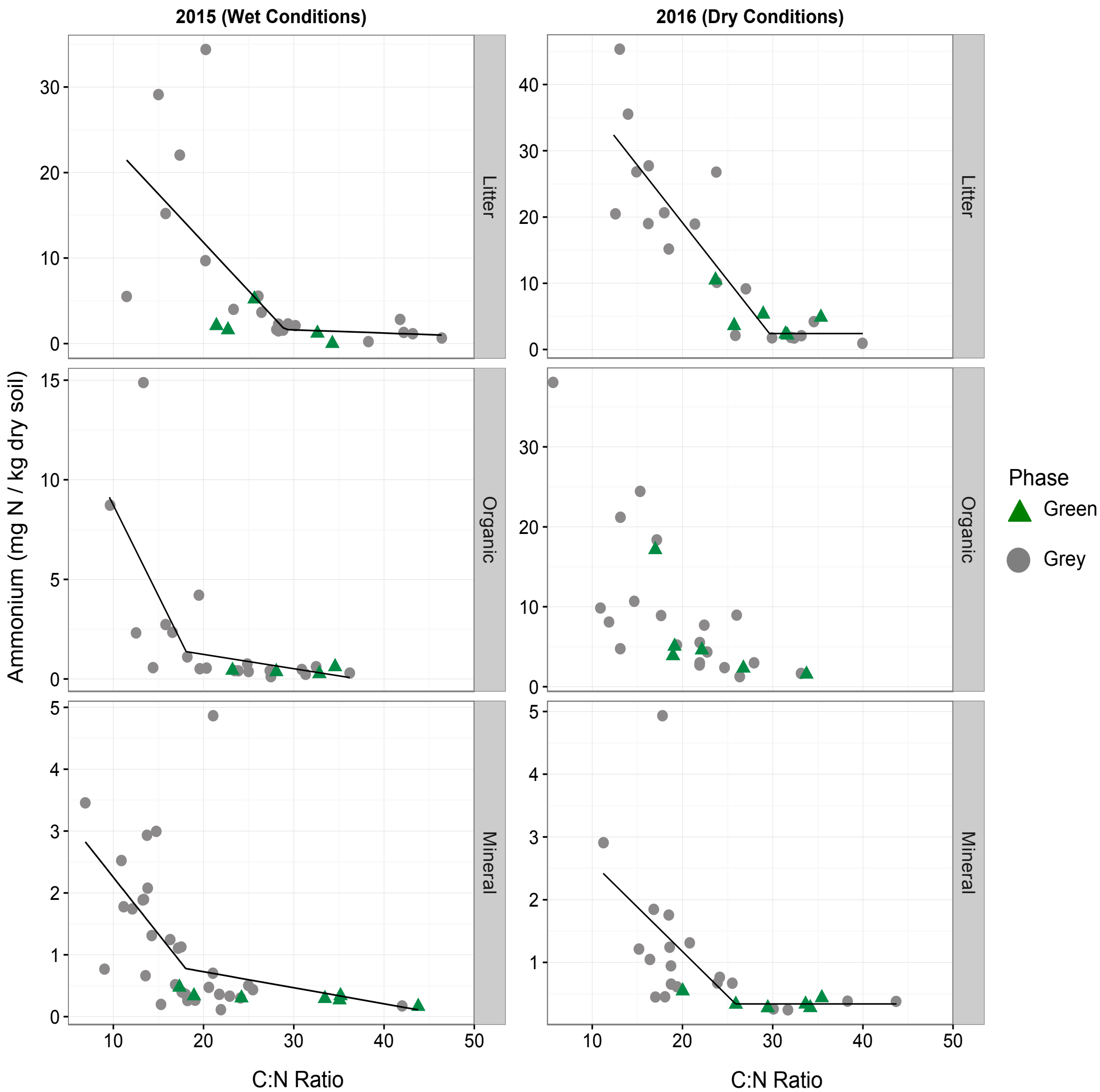

Figure 4.6: The relationship between the concentration of ammonium and C:N ratio under green and grey phase trees in the litter, organic, and mineral horizon. The vertical axes scale differently between horizons and years. One data point with C:N = 79 from the organic horizon in 2015 and one data point with an ammonium concentration of 98 mg N/kg dry soil from the litter horizon in 2016 were omitted to improve data visualization, but follow overall trends.

4.4 Discussion

By studying changes to soil biogeochemical parameters along a continuum of tree mortality, we gained insights into mechanisms associated with larger-scale C and N cycling. Previous studies typically compared biogeochemical response between an unimpacted versus a beetle-impacted plot (Bearup et al., 2014; B. M. Brouillard et al., 2016; Mikkelson et al., 2016b), which may introduce geographic biases occurring from differences in elevation, soil type, vegetation, and aspect between sites. Additionally, these paired-plot studies provide biogeochemical results for one level of infestation and ignore the potential for adjacent surviving trees to mitigate post-infestation terrestrial response. The work herein provides a different perspective by analyzing biogeochemical perturbations beneath trees with a range of surrounding tree mortality (plot-level severity=9-91%) located on the same hillslope to minimize biases (Table B.1). In doing so, it also brings insight into conflicting results regarding shifts in carbon and nitrogen cycling following beetle infestation that may have arisen from differences in tree mortality levels. Our results depict physicochemical shifts both as a function of surrounding mortality and tree phase to allow predictive insights into when and where biogeochemical shifts are expected following beetle-induced tree mortality.

In the case of bark beetle infestation, nutrient inputs to the soil are altered as rhizodeposition ceases followed by enhanced litter fall enriched with N and recalcitrant C (Morehouse et al., 2008). As the canopy diminishes following accelerated needle fall, soil properties such as water content and pH can change with reported trends being fairly consistent across studies (Kaňa et al., 2012; Mikkelson et al., 2013a). Similar to other beetle-killed forests (Kaňa et al., 2012; Xiong et al., 2011), we found higher pH values under grey phase trees in all sampled horizons regardless of the acidic needle drop. We also observed higher water content under grey phase trees in the mineral horizon during both annual moisture condition sampling events, presumably due to limited canopy interception and decreased root uptake (Mikkelson et al., 2013a). These broad findings agree with previous results depicting elevated pH and soil moisture with beetle-induced lodgepole mortality in mineral soils in western Canada (Cigan et al., 2015) and were not dependent on the level of surrounding tree mortality.

Unlike alterations to soil moisture and pH after beetle infestation, reported changes to soil respiration are variable following tree mortality (Binkley et al., 2006; Hogberg et al., 2001; Moore et al., 2013; Morehouse et al., 2008; Speckman et al., 2015). While beetle infestation may exacerbate climate feedbacks, previous studies investigating total carbon fluxes disagree, with some predicting a switch from a C sink to a C source (Kurz et al., 2008) and other monitoring studies showing a muted response (Speckman et al., 2015) or a decline in respiration (Moore et al., 2013). We propose that severity of tree mortality is an essential component to take into consideration when estimating the impact on CO_2 flux. Respiration below grey trees declined by 18-28% compared to green trees (Figure 4.1), which is likely attributed to the cessation of root respiration following mortality. However, a compensatory effect from surrounding live trees was found to increase respiration rates to those comparable to green trees during wet conditions once the number of surrounding green trees reached approximately 40 within an 8m radius (Figure 4.2). This trend likely occurred due to respiration associated with root systems from adjacent green trees that can extend below grey trees in these typically dense lodgepole pine forests (Parsons et al., 1994). Symbiotic microbial communities associated with tree roots decline following tree mortality (Štursová et al., 2014), which likely decreases soil microbial respiration; however, surrounding live root systems may provide additional root exudates that maintain microbial respiration at pre-infestation levels once a certain density of green trees is reached. The higher soil moisture found under grey trees, particularly during the wetter sampling event, may further increase the mobility of these root exudates and make them more accessible to microbial communities. This may also help explain the larger variance in soil respiration below grey trees in the wet year (2015) compared to the dry year (2016). During dry conditions, soil respiration rates below grey trees varied little from plot to plot. In contrast, soil respiration was more variable below grey trees in the wetter 2015 conditions as different concentrations of root exudates from surviving root systems were mobilized depending on the number of surrounding live trees. Similar to prior work, respiration was elevated during wet conditions for both tree phases, which may occur due to suppression of microbial activity during dry conditions (Allison and Treseder, 2008; Orchard and Cook, 1983).

Further evidence of the importance of labile root exudates in maintaining root respiration below grey phase trees emerged when analyzing trends between carbon aromaticity and soil respiration (Figure B.2). As carbon aromaticity increased in the mineral horizon below grey trees, soil respiration declined. Recalcitrant carbon from degrading plant material is not as easily utilized as labile carbon from root exudates, possibly decreasing microbial respiration. While this study did not differentiate the proportion of CO_2 flux that was derived from root respiration compared to microbial respiration, future work should be directed toward determining the shifts and drivers that impact respiration partitioning following tree mortality. Prior work has found soil respiration to remain stable after beetle infestation in spruce forests in the Rocky Mountains (Speckman et al., 2015); however, the work herein suggests that respiration at the ground surface declines after beetle infestation in lodgepole forests. Additionally, soil respiration under beetle-infested trees was dependent on the number of surrounding green trees during moist conditions, providing evidence of a compensatory effect and the potential for regrowth to increase soil respiration. Discrepancies in previous studies may stem from differences in the density of live trees between sites or moisture conditions that enhance heterotrophic respiration in the subsurface (Berryman et al., 2013).

Unlike soil respiration, tree-scale leachable-carbon concentrations did not significantly differ between green and grey phase trees or correlate with degree of surrounding tree mortality. Conversely, elevated carbon recalcitrance was associated with increased severity of plot mortality. Prior work has also found increases in carbon recalcitrance following beetle infestation in soil digests in European Spruce forests (Kaňa et al., 2015). However, shifts in surface water quality and carbon recalcitrance were not found in the Colorado Rocky Mountain region until greater than 50% of a watershed was beetle-impacted (B. M. Brouillard et al., 2016). This provides further support to our guiding hypothesis that biogeochemical shifts are tied to the level of impact and can be mitigated by compensatory effects from surviving trees in forested regions experiencing lower severities of mortality.

Analogous to soil respiration variations following tree mortality, reported changes to terrestrial nitrogen cycling are variable (Biederman et al., 2016; Cigan et al., 2015; Edburg et al., 2012; Ferrenberg et al., 2014; Griffin et al., 2011; Huber, 2005; Kaňa et al., 2015; Mikkelson et al., 2013a, 2016b; Morehouse et al., 2008; Norton et al., 2015) and our study lends insight into these discrepancies. Lodgepole pine forests in the Rocky Mountains are typically N-limited (Stump and Binkley, 1993); however, the elevated proportion of ammonium and altered C:N ratio observed in this study suggest that organic decay and changing carbon properties are influencing nitrogen availability. Interestingly, accumulation of the ammonium proportion was most pronounced when grey phase trees were surrounded by at least 40% tree mortality. This pattern suggests that N-speciation is buffered until a threshold of surrounding tree mortality is surpassed. When evaluating the ammonium proportion individually by year, the 40% threshold is still pronounced with the exception of the mineral layer in 2015 and the litter layer in 2016 (Figure 4.4; Tables 4.1, B.2 – B.3). The elevated proportion of ammonium below grey trees in some of the 2015 mineral samples may be due to the higher moisture conditions, which could mobilize N sourced from decaying tree material in the upper horizons down to the mineral layer. Additionally, the litter horizon had aged an additional year by 2016, which may have impacted the proportion of ammonium within the needles and prevented a visible threshold effect comparable to what was seen in 2015.

The relative enrichment in ammonium associated with the extent of surrounding tree mortality could be the result of several mechanisms that are consistent with the observed increases in SUVA and elevated ammonium concentrations under grey phase trees with decreasing C:N. Nitrification may be limited by the cessation of easily utilizable root exudates that decreases microbial activity as remaining carbon stores become more refractory. Annual fluxes of N from litter fall have been found to more than double following beetle infestation (Kaňa et al., 2012), not only increasing N in the litter horizon but subsequently the deeper horizons as woody material is degraded and nutrients are mobilized. This alteration to the nitrogen pool is intensified by a lack of nutrient uptake by the now inactive tree system (Mikkelson et al., 2013a).

We observed lower C:N ratios beneath grey compared to green phase trees, indicating that N becomes more abundant relative to C in the mineral and organic horizons and changes were magnified as the severity of mortality increased (Figure 4.5; Tables 4.1, B.2 – B.3). Furthermore, ammonium accumulation primarily occurred after a certain C:N breakpoint value, potentially indicating when N-saturation begins to occur in each horizon relative to C (Figure 4.6). The TN pool transitioned from being predominantly organic N (a result of decaying plant biomass, rhizodeposits and microbial biomass) to being comprised of more inorganic ammonium produced by N mineralization as surrounding tree mortality increased. This shift in the organic N proportion may also suggest less of the total N pool is microbially assimilated. Microorganisms can adapt to nutrient availability shifts through community structure fluctuations following beetle infestation (Mikkelson et al., 2016a, 2016b) as competitive advantages change and by altered nitrogen use efficiency (NUE) where microbes waste excess N in the form of ammonium (Mooshammer et al., 2014). Furthermore, net ammonification and carbon recalcitrance have previously been found to increase under beetle-impacted spruce stands (Kaňa et al., 2015), providing validation of the links between elevated ammonium, increased microbial-N mineralization, and carbon recalcitrance. These results suggest that NUE is altered and bioavailable carbon is scarce relative to nitrogen under grey phase trees, enhancing net ammonification, decreasing nitrification, and further contributing to ammonium accumulation.

Unlike systemically N-saturated European forests, increased nitrate accumulation after bark beetle infestation does not appear to be happening in the comparatively nitrogen limited Colorado Rocky Mountains. With the largest solubility and repulsive interactions with positively charged soil particles (Tate, 1995), nitrate may exit the soil system rapidly in the aqueous form; however, prior work has not found increased leaching of nitrate in these forests following infestation (Biederman et al., 2016; Rhoades et al., 2013). Alternatively, nitrate may be transformed through denitrification and exit the system as N_2, N_2O, and/or NO as was observed in response to beetle infestation in the Rocky Mountains four years after initial infestation (Norton et al., 2015) and following tree girdling experiments in Swiss forests (Krause et al., 2013). Alarmingly, this suggests that widespread beetle infestation may lead to increased flux of the potent greenhouse gas N_2O from the soil.

Shifts in nutrient and edaphic parameters below grey phase trees were most pronounced in the mineral layer due to both top down inputs of nutrients from the upper horizons and the cessation of root exudates (largely composed of labile C) in the mineral horizon where fine root hair structures in lodgepole pines are localized (Walker et al., 2003). Following mortality, this loss of rhizodeposits can help explain the lower C:N ratios under grey phase trees in this horizon. Although not statistically significant, average DOC concentrations declined and TN concentrations increased in the mineral horizon of grey phase trees (Table 4.1) during both sampling years, which supports this interpretation and corroborates findings from other beetle-killed forests (Mikkelson et al., 2016b). The litter and organic horizon on the other hand appear to be primarily affected by top down inputs of recalcitrant C- and N-enriched litter from surrounding beetle-killed trees, which is mobilized through litter decay and altered leaching processes (Mikkelson et al., 2013a).

Our study lends insight into why the same biogeochemical response is not always observed in different beetle-killed forests. While certain biogeochemical signatures significantly differed between green and grey phase trees regardless of surrounding tree mortality, many parameters were found to shift with the severity of mortality within each plot. This dependency on the severity level of infestation demonstrates the ability of live tree root systems to buffer edaphic shifts at low severity levels and it would be insightful to determine if similar shifts are observed in other N-limited forest types; for example, spruce (*Picea spp.*) do not have the same root structure, tree density, or temporal deposition of needles following beetle infestation as the investigated lodgepole pines do. These results support prior findings where forests with low levels of infestation experienced minimal shifts in edaphic parameters and water quality compared to highly infested forests (B. M. Brouillard et al., 2016; Mikkelson et al., 2016b) demonstrating the resiliency of a forest during low-severity insect disturbances and highlighting the ability of increased woody debris and nutrient flux from the canopy to alter biogeochemical cycling with elevated mortality levels.

Determining disturbance effects on biogeochemical cycling is often difficult due to unpredictable weather conditions or shifts in nutrient cycles with time. Our study captured two contrasting moisture regimes and found consistent trends related to tree mortality phase and severity of plot mortality across both years. Furthermore, while the bulk of previous research investigated shifts in biogeochemical parameters that occurred within the first few years of infestation (Mikkelson et al., 2013a), we found altered soil respiration and C/N shifts nearly a decade after impact. This demonstrates the long-term implications associated with forest mortality even after labile portions of impacted trees have degraded (Prescott et al., 2000). Nitrogen cycling in particular appears significantly altered when this Rocky Mountain ecosystem has a high level of tree mortality, although our study suggests that the proportions of the TN pool are more likely to change as opposed to the total amount of nitrogen. Collectively, these biogeochemical shifts could lead to this N-limited ecosystem experiencing a relative enrichment in nutrient availability that could favorably influence emergent growth and ecosystem rebound following beetle infestation. While the work herein focused on tree-scale C and N cycling, future studies could investigate the threshold biogeochemical response at the watershed or regional scale to enable better ecological predictions after forest disturbance as recent findings have shown that large forest disturbances can have global repercussions (Garcia et al., 2016).

CHAPTER 5

CONCLUDING REMARKS AND FUTURE DIRECTIONS

Collectively, the research presented in this thesis analyzed the biogeochemical and ecological impacts following bark beetle infestation in the Rocky Mountains over the last two decades. While elevated forest drought stress has caused unprecedented insect infestation and subsequent mortality of coniferous forests across Western North America, diseases and insect infestations are also occurring in both coniferous and deciduous forests in the Eastern United States (Herms and McCullough, 2014; Vendettuoli et al., 2015). Furthermore, analogous infestations and disease are occurring in regions of Europe and Asia that are likely driving similar shifts in water quality and biogeochemical cycling (Štursová et al., 2014; Tokuchi et al., 2004). Conducting similar analyses to the ones presented here can aid in the management and prediction of the secondary effects that occur following these forest disturbances. As forest drought stress continues over the next century, global forest mortality is predicted to continue (McDowell et al., 2015; Park Williams et al., 2012) and the findings presented here can be used to infer biogeochemical and ecological impacts associated with these future incidences of insect-induced tree mortality.

As seen in chapter two, surface waters utilized for municipal purposes may be impacted as increased aromatic carbon loading from degrading tree material elevates DBP formation following chlorine disinfection at water treatment facilities. However, this trend was primarily found in watersheds with >50% areal infestation, demonstrating the ability for low-impacted watersheds to mitigate alterations in carbon cycling.

Elevated carbon loading in impacted watersheds primarily occurred after hydrologic events (runoff, high precipitation) and was exacerbated in the summer and fall months potentially due to increased carbon mobilization with elevated water tables in high-impacted watersheds. Although increased carbon loading and aromatic character in beetle infested watersheds was found to increase DBP formation, other physical and chemical mechanisms associated with climate change and forest mortality may also be elevating DBP formation and deserve further investigation. For example, increased water temperatures can increase the formation of DBPs (Nikolaou and Lekkas, 2001) and future work can elucidate whether climate change or other drivers that elevate water temperature can help explain increases in DBPs within Rocky Mountain watersheds. Additionally, increases in pH can elevate THM production but decreases HAA formation (Nikolaou and Lekkas, 2001). Many studies along with the results from chapter 4 have found elevated pH under beetle-impacted trees (Cigan et al., 2015; Mikkelson et al., 2016b). If this translates to elevated pH in surface waters, this may help explain why historical increases in TTHM concentrations following beetle infestation were found (Figure 2.2) while HAA5 concentrations didn't increase over a similar timeframe.

Due to public concern regarding heightened wildfire risk following beetle infestation, chapter three evaluated the links between wildfire severity and beetle infestation. Counter to this intuition, mountain pine beetle-impacted lodgepole and ponderosa pine forests were found to burn less severely than unimpacted forests. These findings contribute to a growing body of research suggesting that wildfire occurrence and severity does not increase following bark beetle infestation (Hart et al., 2015; Meigs et al., 2016). Additionally, this research can help aid future forest management and prevent costs associated with removal of beetle-infested trees due to this perceived wildfire threat. Finally, chapter four investigated the potential for live trees to buffer biogeochemical shifts following infestation. While some edaphic parameters including pH and water content were significantly different between green and grey phase trees, others responded with the severity of surrounding tree mortality (proportion of nitrogen species, C:N ratio, and carbon aromaticity). These conclusions help to resolve and explain observations from prior work, demonstrating why the same biogeochemical differences may not occur in sites experiencing low rates of tree mortality compared to sites with higher severities of beetle-induced tree mortality (Mikkelson et al., 2016b).

Although regions most susceptible to mountain pine beetle infestation have been impacted in the Rocky Mountain Region and new incidences of infestation have dramatically declined (Figure 2.1), many of the biogeochemical responses and water quality effects presented here have persisted for nearly a decade. This demonstrates the long-term impacts associated with this form of tree die-off and future work should continue to monitor these shifts, particularly those that have human health implications (DBP formation). Increased water quality monitoring particularly during peaks in DBP precursor mobilization during hydrologic events can help predict when DBP formation may exceed MCLs and can be used to mitigate altered water quality by informing potential alternative treatment processes that reduce DBP precursor levels. While increased nitrate release has not occurred in the nitrogen-limited Rocky Mountain ecosystems that forms the foundation of this work compared to beetle infested regions in nitrogen saturated European forests (Biederman et al., 2016; Rhoades et al., 2013), nitrate may be leaving forested soils through denitrification to N_2O (Norton et al., 2015).

Increased release of this potent greenhouse gas may produce positive feedbacks toward a warming climate. Low C:N ratios and associated increases in ammonium (Figures 4.5, 4.6) below grey phase trees with high surrounding tree mortality indicates an enrichment in N, and future work could investigate if this elevates N_2O flux during wet conditions. Additionally, as nitrogen speciation appears particularly sensitive following tree death as seen in chapter four, additional research could focus on elucidating nitrogen species transformations and transport through a forested watershed and determine fluxes to the hydrosphere and atmosphere.

As bark beetle infestation within North America has caused unprecedented mortality of lodgepole pine forests, prior work and the research presented in this thesis evaluating shifts in biogeochemical and hydrologic cycling following mountain pine beetle infestation has focused on this tree species. Although many of the overarching principals found through this work can be translated to other coniferous species following insect-induced mortality, changes in tree structure or the variable timing of mortality phases (i.e. litterfall rates) can create differences in biogeochemical and ecological response. For instance, the decreased canopy density between lodgepole and ponderosa pine may explain the differences in fire severity between these two species and their unimpacted controls (chapter three). Future research could determine whether threshold biogeochemical responses similar to the ones observed here are evident in other coniferous species that contain different root structures, needle fall rates, and needle chemistries.

Work has recently begun within our laboratory group that will focus on nutrient flux rates from coniferous needles and to elucidate how needle degradation processes following beetle infestation impact biogeochemical cycling. This field study located in Crested Butte, Colorado will investigate degradation rates of two species of coniferous needles along with monitoring subsequent mobilization of C and N species through gaseous and soil-water sampling. Additionally, by importing and deploying needles at different elevations and inducing early snowmelt, this study will investigate how variable moisture and temperature regimes will affect degradation rates and nutrient fluxes which can be used to predict biogeochemical response in an altered climate. The needle plots were deployed in the fall of 2016 and will be monitored over the following two years (Figure 5.1).

Spruce needles from trees recently impacted by bark beetle infestation were deployed in PVC rings along with naturally senesced spruce and lodgepole pine needles. As needle litter from beetle-killed trees has an altered chemical composition compared to naturally-senesced litter (Griffin et al., 2011; Morehouse et al., 2008), measuring degradation and nutrient flux rates between these needle types can better inform biogeochemical shifts discussed in this thesis. Some plots also contain twice the mass of impacted needles as others, which will elucidate the extent that increased litterfall rates have in altering subsurface and atmospheric C and N fluxes. In addition to investigating needle degradation processes, extensive expansion of spruce beetle is occurring in proximal regions of southwest Colorado (Colorado State Forest Service, 2017) allowing threshold hypotheses similar to the ones investigated in chapter four to be analyzed in a different forest type to see if consistent biogeochemical responses are observed in relation to the severity of spruce beetle infestation.

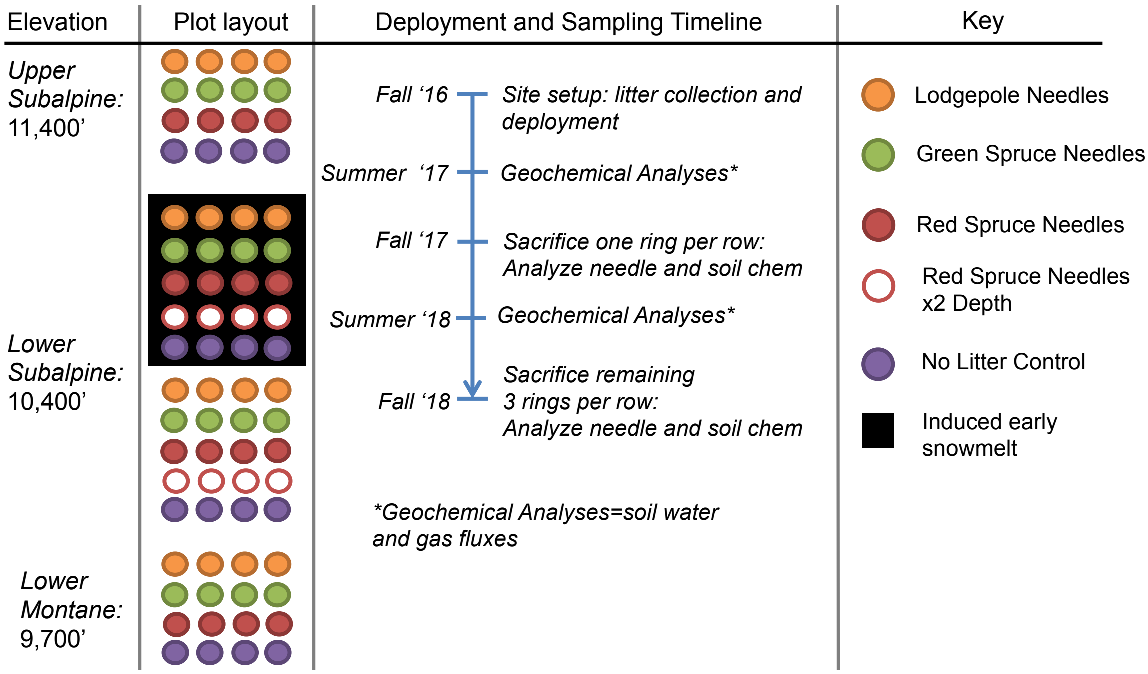

Figure 5.1: Diagram depicting the plot layout and sampling schedule for the coniferous needle degradation project implemented during the fall of 2016 in Crested Butte, CO.

REFERENCES

A burning issue for insurers? [WWW Document], 2013. . Lloyd's. URL http://www.lloyds.com/~/media/lloyds/reports/emerging%20risk%20reports/wildfire%20final.pdf (accessed 10.10.14).

Adams, H.D., Luce, C.H., Breshears, D.D., Allen, C.D., Weiler, M., Hale, V.C., Smith, A.M.S., Huxman, T.E., 2012. Ecohydrological consequences of drought- and infestation- triggered tree die-off: insights and hypotheses. Ecohydrology 5, 145–159. doi:10.1002/eco.233

Agricultural Act of 2014, Public Law 113-791, 2014.

Agriculture, Hydrology and Water Quality, 2002. . CABI.

Alexander, M.A., Stam, J.C., 2003. Safety alert for wildland firefighters: fuel conditions in spruce-beetle-killed forests of Alaska. Fire Manag. Tody 63, 25.

Allison, S.D., Treseder, K.K., 2008. Warming and drying suppress microbial activity and carbon cycling in boreal forest soils. Glob. Change Biol. 14, 2898–2909. doi:10.1111/j.1365-2486.2008.01716.x

Areas with tree mortality from bark beetles, 2014. . United States Forest Service.

Aust, M., Blinn, C., 2004. Forestry best management practices for timber harvesting and site preparation in the eastern United States: An overview of water quality and productivity research during the past 20 years (1982-2002). Water Air Soil Pollut. Focus 4, 5–36.

Avery, T.E., Berlin, G.L., 1992. Fundamentals of remote sensing and airphoto interpretation. Prentice Hall, Upper Saddle River, NJ.

Baker, M.A., Valett, H.M., Dahm, C.N., 2000. Organic Carbon Supply and Metabolism in a Shallow Groundwater Ecosystem. Ecology 81, 3133. doi:10.2307/177406

Bakker, M., Strack, D.L., 1996. Capture zone delineation in two-dimensional groundwater flow models. Water Resour. Res. 32, 1309–1315.

Ball, D., 1964. Loss ‐ on ‐ ignition as an estimate of organic matter and organic carbon in non ‐ calcareous soils. J. Soil Sci. 15, 84–92. doi:10.1111/j.1365-2389.1964.tb00247.x

Barrena, I., Menéndez, S., Duñabeitia, M., Merino, P., Florian Stange, C., Spott, O., González-Murua, C., Estavillo, J.M., 2013. Greenhouse gas fluxes (CO2, N2O and CH4) from forest soils in the Basque Country: Comparison of different tree species and growth stages. For. Ecol. Manag. 310, 600–611. doi:10.1016/j.foreco.2013.08.065

Bauch, N., Bails, J., 2004. Water-quality characteristics and ground-water quantity of the Fraser River Watershed, Grand County, Colorado, 1998-2001 (No. 03–4275), Water-Resources Investigations. U.S. Geological Survey.

Bearup, L.A., Maxwell, R.M., Clow, D.W., McCray, J.E., 2014. Hydrological effects of forest transpiration loss in bark beetle-impacted watersheds. Nat. Clim. Change 4, 481–486. doi:10.1038/nclimate2198

Bebi, P., Kulakowski, D., Veblen, T.T., 2003. Interactions between fire and spruce beetles in a subalpine Rocky Mountain forest landscape. Ecology 84, 362–371. doi:10.1890/0012-9658(2003)084[0362:IBFASB]2.0.CO;2

Beggs, K.M.H., Summers, R.S., 2011. Character and Chlorine Reactivity of Dissolved Organic Matter from a Mountain Pine Beetle Impacted Watershed. Environ. Sci. Technol. 45, 5717–5724. doi:10.1021/es1042436

Berryman, E., Marshall, J.D., Rahn, T., Litvak, M., Butnor, J., 2013. Decreased carbon limitation of litter respiration in a mortality-affected piñon–juniper woodland. Biogeosciences 10, 1625–1634. doi:10.5194/bg-10-1625-2013

Bhupinderpal-Singh, Nordgren, A., Ottosson, M., M, H., Mellander, P., Hogberg, P., 2003. Tree root and soil heterotrophic respiration as revealed by girdling of boreal Scots pine forest- extending observations beyond the first year.pdf. Plant Cell Environ. 26, 1287–1296.

Biederman, J.A., Brooks, P.D., Harpold, A.A., Gochis, D.J., Gutmann, E., Reed, D.E., Pendall, E., Ewers, B.E., 2012. Multiscale observations of snow accumulation and peak snowpack following widespread, insect-induced lodgepole pine mortality: Snowpack following insect-induced pine mortality. Ecohydrology 7, 150–162. doi:10.1002/eco.1342

Biederman, J.A., Meixner, T., Harpold, A.A., Reed, D.E., Gutmann, E.D., Gaun, J.A., Brooks, P.D., 2016. Riparian zones attenuate nitrogen loss following bark beetle-induced lodgepole pine mortality: RIPARIAN CONTROL OF BARK BEETLE N LOSS. J. Geophys. Res. Biogeosciences 121, 933–948. doi:10.1002/2015JG003284

Bieroza, M., Baker, A., Bridgeman, J., 2009. Relating freshwater organic matter fluorescence to organic carbon removal efficiency in drinking water treatment. Sci. Total Environ. 407, 1765–1774. doi:10.1016/j.scitotenv.2008.11.013

Binkley, D., Stape, J.L., Takahashi, E.N., Ryan, M.G., 2006. Tree-girdling to separate root and heterotrophic respiration in two Eucalyptus stands in Brazil. Oecologia 148, 447–454. doi:10.1007/s00442-006-0383-6

Bond, T., Goslan, E.H., Parsons, S.A., Jefferson, B., 2011. Treatment of disinfection by‐product precursors. Environ. Technol. 32, 1–25. doi:10.1080/09593330.2010.495138

Brennan, C., Aguilar, J., 2013. Eight days, 1,000-year rain, 100-year flood. Boulder Dly. Camera.

Brouillard, B., Dickenson, E., Mikkelson, K., Sharp, J., 2016. Water quality following extensive beetle-induced tree mortality: Interplay of aromatic carbon loading, disinfection byproducts, and hydrologic drivers. Sci. Total Environ.

Brouillard, B.M., Dickenson, E.R.V., Mikkelson, K.M., Sharp, J.O., 2016. Water quality following extensive beetle-induced tree mortality: Interplay of aromatic carbon loading, disinfection byproducts, and hydrologic drivers. Sci. Total Environ. 572, 649–659. doi:10.1016/j.scitotenv.2016.06.106

Burke, M.P., Hogue, T.S., Kinoshita, A.M., Barco, J., Wessel, C., Stein, E.D., 2013. Pre- and post-fire pollutant loads in an urban fringe watershed in Southern California. Environ. Monit. Assess. 185, 10131–10145. doi:10.1007/s10661-013-3318-9

Burns, D.A., Murdoch, P.S., 2005. Effects of a clearcut on the net rates of nitrification and N mineralization in a northern hardwood forest, Catskill Mountains, New York, USA. Biogeochemistry 72, 123–146. doi:10.1007/s10533-004-0355-z

Calkin, D.E., Cohen, J.D., Finney, M.A., Thompson, M.P., 2014. How risk management can prevent future wildfire disasters in the wildland-urban interface. Proc. Natl. Acad. Sci. 111, 746–751. doi:10.1073/pnas.1315088111

Chen, W., Westerhoff, P., Leenheer, J.A., Booksh, K., 2003. Fluorescence Excitation−Emission Matrix Regional Integration to Quantify Spectra for Dissolved Organic Matter. Environ. Sci. Technol. 37, 5701–5710. doi:10.1021/es034354c

Cigan, P.W., Karst, J., Cahill, J.F., Sywenky, A.N., Pec, G.J., Erbilgin, N., 2015. Influence of bark beetle outbreaks on nutrient cycling in native pine stands in western Canada. Plant Soil 390, 29–47. doi:10.1007/s11104-014-2378-0

Coble, P., 1996. Characterization of marine and terrestrial DOM in seawater using excitation-emission matrix spectroscopy. Mar. Chem. 51, 325–346.

Collins, B.J., Rhoades, C.C., Hubbard, R.M., Battaglia, M.A., 2011. Tree regeneration and future stand development after bark beetle infestation and harvesting in Colorado lodgepole pine stands. For. Ecol. Manag. 261, 2168–2175. doi:10.1016/j.foreco.2011.03.016

Colorado State Forest Service, 2015 Aerial Survey. http://csfs.colostate.edu/forest-management/common-forest-insects-diseases/spruce-bark-beetle (accessed 02.01.17)

Comprehensive Disinfectants and Disinfection Byproducts Rules (Stage 1 and Stage 2): Quick Reference Guide, 2010. . US Environmental Protection Agency.

Custodio, E.D. Groundwater Protection and Contamination.

Davidson, E.A., Janssens, I.A., 2006. Temperature sensitivity of soil carbon decomposition and feedbacks to climate change. Nature 440, 165–173. doi:10.1038/nature04514

Dawson, J.J.C., Soulsby, C., Tetzlaff, D., Hrachowitz, M., Dunn, S.M., Malcolm, I.A., 2008. Influence of hydrology and seasonality on DOC exports from three contrasting upland catchments. Biogeochemistry 90, 93–113. doi:10.1007/s10533-008-9234-3

Drewes, J.E., Croue, J.-P., 2002. New approaches for structural characterization of organic matter in drinking water and wastewater effluents. Water Sci. Technol. Water Supply 2, 1–10.

Edburg, S.L., Hicke, J.A., Brooks, P.D., Pendall, E.G., Ewers, B.E., Norton, U., Gochis, D., Gutmann, E.D., Meddens, A.J., 2012. Cascading impacts of bark beetle-caused tree mortality on coupled biogeophysical and biogeochemical processes. Front. Ecol. Environ. 10, 416–424. doi:10.1890/110173

Elvidge, C.D., 1990. Visible and near infrared reflectance characteristics of dry plant materials. Int. J. Remote Sens. 11, 1775–1795. doi:10.1080/01431169008955129

ESRI 2015. ArcGIS Desktop: Release 10.2, n.d. . Redlands, CA: Environmental Systems Research Institute.

Falkowski, P., Scholes, R., Boyle, E., Canadell, J., Canfield, D., Elser, J., Gruber, N., Hibbard, K., Hogberg, P., Linder, S., 2000. The Global Carbon Cycle: A Test of Our Knowledge of Earth as a System. Science 290, 291–296. doi:10.1126/science.290.5490.291

Feller, M.C., Kimmins, J.P., 1984. Effects of clearcutting and slash burning on streamwater chemistry and watershed nutrient budgets in southwestern British Columbia. Water Resour. Res. 20, 29–40.

Ferrenberg, S., Knelman, J.E., Jones, J.M., Beals, S.C., Bowman, W.D., Nemergut, D.R., 2014. Soil bacterial community structure remains stable over a 5-year chronosequence of insect-induced tree mortality. Front. Microbiol. 5. doi:10.3389/fmicb.2014.00681

Ferrenberg, S., O'Neill, S.P., Knelman, J.E., Todd, B., Duggan, S., Bradley, D., Robinson, T., Schmidt, S.K., Townsend, A.R., Williams, M.W., others, 2013. Changes in assembly processes in soil bacterial communities following a wildfire disturbance. ISME J. 7, 1102–1111.

Foran, J., Brosnan, T., Connor, M., Delfino, J., DePinto, J., Dickson, K., Humphrey, H., Novotny, V., Smith, R., Sobsey, M., others, 2000. A framework for comprehensive, integrated, watershed monitoring in New York City. Environ. Monit. Assess. 62, 147–167.

Fule, P.Z., Covington, W.W., Moore, M.M., 1997. Determining Reference Conditions for Ecosystem Management of Southwestern Ponderosa Pine Forests. Ecol. Appl. 7, 895. doi:10.2307/2269441

Furniss, M.J., 2011. Water, climate change, and forests: watershed stewardship for a changing climate. DIANE Publishing.

Garcia, E.S., Swann, A.L.S., Villegas, J.C., Breshears, D.D., Law, D.J., Saleska, S.R., Stark, S.C., 2016. Synergistic Ecoclimate Teleconnections from Forest Loss in Different Regions Structure Global Ecological Responses. PLOS ONE 11, e0165042. doi:10.1371/journal.pone.0165042

Gillett, N.P., 2004. Detecting the effect of climate change on Canadian forest fires. Geophys. Res. Lett. 31. doi:10.1029/2004GL020876

Glossary of Wildland Fire Terminology [WWW Document], 2014. . Natl. Wildl. Coord. Group. URL http://gacc.nifc.gov/nrcc/dc/idgvc/dispatchforms/glossary.pdf (accessed 9.7.14).

Graham, R.T., Jain, T.B., 2005. Ponderosa pine ecosystems, in: Proceedings of the Symposium on Ponderosa Pine: Issues, Trends, and Management, Gen. Tech. Rep. PSW-GTR-198. Albany CA: Pacific Southwest Research Station, Forest Service, US Department of Agriculture, Klamath Falls, OR. Citeseer, pp. 1–32.

Grayston, S., Vaughan, D., Jones, D., 1997. Rhizosphere carbon flow in trees, in comparison with annual plants- the importance of root exudation and its impact on microbial activity and nutrient availability. Appl. Soil Ecol. 5, 29–56.

Griffin, J.M., Turner, M.G., Simard, M., 2011. Nitrogen cycling following mountain pine beetle disturbance in lodgepole pine forests of Greater Yellowstone. For. Ecol. Manag. 261, 1077–1089. doi:10.1016/j.foreco.2010.12.031

Grünwald, A., Šť astnỳ, B., Slavíčková, K., Slavíček, M., 2002. Formation of haloforms during chlorination of natural waters. Acta Polytech. 42.

Haldane, M., 2013. Insurers, government grapple with costs of growth in wildland-urban interface [WWW Document]. Insur. J. URL http://www.insurancejournal.com/news/national/2013/08/15/301833.htm (accessed 12.20.14).

Hart, S.J., Schoennagel, T., Veblen, T.T., Chapman, T.B., 2015. Area burned in the western United States is unaffected by recent mountain pine beetle outbreaks. Proc. Natl. Acad. Sci. 112, 4375–4380. doi:10.1073/pnas.1424037112

Harvey, B.J., Donato, D.C., Romme, W.H., Turner, M.G., 2013. Influence of recent bark beetle outbreak on fire severity and postfire tree regeneration in montane Douglas-fir forests. Ecology 94, 2475–2486. doi:10.1890/13-0188.1

Harvey, B.J., Donato, D.C., Turner, M.G., 2014. Recent mountain pine beetle outbreaks, wildfire severity, and postfire tree regeneration in the US Northern Rockies. Proc. Natl. Acad. Sci. 111, 15120–15125. doi:10.1073/pnas.1411346111

Herms, D.A., McCullough, D.G., 2014. Emerald Ash Borer Invasion of North America: History, Biology, Ecology, Impacts, and Management. Annu. Rev. Entomol. 59, 13–30. doi:10.1146/annurev-ento-011613-162051

Hicke, J.A., Johnson, M.C., Hayes, J.L., Preisler, H.K., 2012. Effects of bark beetle-caused tree mortality on wildfire. For. Ecol. Manag. 271, 81–90. doi:10.1016/j.foreco.2012.02.005

Hoffman, C.M., Morgan, P., Mell, W., Parsons, R., Strand, E., Cook, S., 2013. Surface Fire Intensity Influences Simulated Crown Fire Behavior in Lodgepole Pine Forests with Recent Mountain Pine Beetle-Caused Tree Mortality. For. Sci. 59, 390–399. doi:10.5849/forsci.11-114

Hogberg, P., Nordgren, A., Buchmann, N., Taylor, A., Ekblad, A., Hogberg, M., Nyberg, G., Ottosson-Lofvenius, M., Read, D., 2001. Large-scale forest girdling shows that current photosynthesis drives soil respiration. Nature 411, 789–792.

Homer, C., Dewitz, J., Fry, J., Coan, M., Hossain, N., Larson, C., Herold, N., McKerrow, A., VanDriel, J.N., Wickham, J., 2007. Completion of the 2001 National Land Cover Database for the Conterminous United States. Photogramm. Eng. Remote Sens. 73, 337–341.

Hood, E., Williams, M.W., McKnight, D.M., 2005. Sources of dissolved organic matter (DOM) in a Rocky Mountain stream using chemical fractionation and stable isotopes. Biogeochemistry 74, 231–255. doi:10.1007/s10533-004-4322-5

Houze, R.A., 2012. Orographic effects on precipitating clouds. Rev. Geophys. 50. doi:10.1029/2011RG000365

Hua, G., Kim, J., Reckhow, D.A., 2014. Disinfection byproduct formation from lignin precursors. Water Res. 63, 285–295. doi:10.1016/j.watres.2014.06.029

Hua, G., Reckhow, D.A., 2007. Characterization of Disinfection Byproduct Precursors Based on Hydrophobicity and Molecular Size. Environ. Sci. Technol. 41, 3309–3315. doi:10.1021/es062178c

Hubbard, R.M., Rhoades, C.C., Elder, K., Negron, J., 2013. Changes in transpiration and foliage growth in lodgepole pine trees following mountain pine beetle attack and mechanical girdling. For. Ecol. Manag. 289, 312–317. doi:10.1016/j.foreco.2012.09.028

Huber, C., 2005. Long Lasting Nitrate Leaching after Bark Beetle Attack in the Highlands of the Bavarian Forest National Park. J. Environ. Qual. 34, 1772. doi:10.2134/jeq2004.0210

Huber, C., Baumgarten, M., Göttlein, A., Rotter, V., 2004. Nitrogen turnover and nitrate leaching after bark beetle attack in mountainous spruce stands of the Bavarian Forest National Park. Water Air Soil Pollut. Focus 4, 391–414.

Jandl, R., Lindner, M., Vesterdal, L., Bauwens, B., Baritz, R., Hagedorn, F., Johnson, D.W., Minkkinen, K., Byrne, K.A., 2007. How strongly can forest management influence soil carbon sequestration? Geoderma 137, 253–268. doi:10.1016/j.geoderma.2006.09.003

Jardine, P.M., Wilson, G.V., McCarthy, J.F., Luxmoore, R.J., Taylor, D.L., Zelazny, L.W., 1990. Hydrogeochemical processes controlling the transport of dissolved organic carbon through a forested hillslope. J. Contam. Hydrol. 6, 3–19.

Jenkins, M.J., Runyon, J.B., Fettig, C.J., Page, W.G., Bentz, B.J., 2014. Interactions among the Mountain Pine Beetle, Fires, and Fuels. For. Sci. 60, 489–501. doi:10.5849/forsci.13-017

Jia, G.J., Burke, I.C., Goetz, A.F.H., Kaufmann, M.R., Kindel, B.C., 2006. Assessing spatial patterns of forest fuel using AVIRIS data. Remote Sens. Environ. 102, 318–327. doi:10.1016/j.rse.2006.02.025

Johnson, E., Ross, J., 2008. Quantifying error in aerial survey data. Aust. For. 71, 216–222.

Jolly, W.M., Parsons, R.A., Hadlow, A.M., Cohn, G.M., McAllister, S.S., Popp, J.B., Hubbard, R.M., Negron, J.F., 2012. Relationships between moisture, chemistry, and ignition of Pinus contorta needles during the early stages of mountain pine beetle attack. For. Ecol. Manag. 269, 52–59. doi:10.1016/j.foreco.2011.12.022

Jung, C.-W., Son, H.-J., 2008. The relationship between disinfection by-products formation and characteristics of natural organic matter in raw water. Korean J. Chem. Eng. 25, 714–720.

Kalbitz, K., Geyer, W., Geyer, S., 1999. Spectroscopic properties of dissolved humic substances—a reflection of land use history in a fen area. Biogeochemistry 47, 219–238.

Kalbitz, K., Glaser, B., Bol, R., 2004. Clear-cutting of a Norway spruce stand: implications for controls on the dynamics of dissolved organic matter in the forest floor. Eur. J. Soil Sci. 55, 401–413.

Kalbitz, K., Kaiser, K., Bargholz, J., Dardenne, P., 2006. Lignin degradation controls the production of dissolved organic matter in decomposing foliar litter. Eur. J. Soil Sci. 57, 504–516. doi:10.1111/j.1365-2389.2006.00797.x

Kaňa, J., Tahovská, K., Kopáček, J., 2012. Response of soil chemistry to forest dieback after bark beetle infestation. Biogeochemistry 113, 369–383. doi:10.1007/s10533-012-9765-5

Kaňa, J., Tahovská, K., Kopáček, J., Šantrůčková, H., 2015. Excess of Organic Carbon in Mountain Spruce Forest Soils after Bark Beetle Outbreak Altered Microbial N Transformations and Mitigated N-Saturation. PLOS ONE 10, e0134165. doi:10.1371/journal.pone.0134165

Kenney, D.S., Goemans, C., Klein, R., Lowrey, J., Reidy, K., 2008. Residential Water Demand Management: Lessons from Aurora, Colorado [1]. JAWRA J. Am. Water Resour. Assoc. 44, 192–207. doi:10.1111/j.1752-1688.2007.00147.x

Kitis, M., Karanfil, T., Kilduff, J., Wigton, A., 2001. The reactivity of natural organic matter to disinfection by- products formation and its relation to specific ultraviolet absorbance. Water Sci. Technol. 43, 9–16.

Kitis, M., Karanfil, T., Kilduff, J.E., 2004. The reactivity of dissolved organic matter for disinfection by-product formation. Turk. J. Eng. Environ. Sci. 28, 167–180.

Kokaly, R.F., Rockwell, B.W., Haire, S.L., King, T.V.V., 2007. Characterization of post-fire surface cover, soils, and burn severity at the Cerro Grande Fire, New Mexico, using hyperspectral and multispectral remote sensing. Remote Sens. Environ. 106, 305–325. doi:10.1016/j.rse.2006.08.006

Kotack, M., 2016. Even indoor kids should worry about California's 30 million dead trees. Wired Sci.

Krause, K., Niklaus, P.A., Schleppi, P., 2013. Soil-atmosphere fluxes of the greenhouse gases CO2, CH4 and N2O in a mountain spruce forest subjected to long-term N addition and to tree girdling. Agric. For. Meteorol. 181, 61–68. doi:10.1016/j.agrformet.2013.07.007

Kulakowski, D., Velben, T., 2007. Effect of Prior Disturbances on the Extent and Severity of Wildfire in Colorado Subalpine Forests. Ecology 88, 759–769. doi:10.1890/06-0124

Kurz, W.A., Dymond, C.C., Stinson, G., Rampley, G.J., Neilson, E.T., Carroll, A.L., Ebata, T., Safranyik, L., 2008. Mountain pine beetle and forest carbon feedback to climate change. Nature 452, 987–990. doi:10.1038/nature06777

Lal, R., 2005. Forest soils and carbon sequestration. For. Ecol. Manag. 220, 242–258. doi:10.1016/j.foreco.2005.08.015

Likens, G.E., Bormann, F.H., Johnson, N.M., Fisher, D.W., Pierce, R.S., 1970. Effects of Forest Cutting and Herbicide Treatment on Nutrient Budgets in the Hubbard Brook Watershed-Ecosystem. Ecol. Monogr. 40, 23. doi:10.2307/1942440

Lopez Garcia, M.J., Caselles, V., 1991. Mapping burns and natural reforestation using Thematic Mapper data. Geocarto Int. 1, 31–37.

Lu, J., Zhang, T., Ma, J., Chen, Z., 2009. Evaluation of disinfection by-products formation during chlorination and chloramination of dissolved natural organic matter fractions isolated from a filtered river water. J. Hazard. Mater. 162, 140–145. doi:10.1016/j.jhazmat.2008.05.058

Lynch, H.J., Renkin, R.A., Crabtree, R.L., Moorcroft, P.R., 2006. The Influence of Previous Mountain Pine Beetle (Dendroctonus ponderosae) Activity on the 1988 Yellowstone Fires. Ecosystems 9, 1318–1327. doi:10.1007/s10021-006-0173-3

Maness, H., Kushner, P.J., Fung, I., 2012. Summertime climate response to mountain pine beetle disturbance in British Columbia. Nat. Geosci. doi:10.1038/ngeo1642

McDowell, N.G., Beerling, D.J., Breshears, D.D., Fisher, R.A., Raffa, K.F., Stitt, M., 2011. The interdependence of mechanisms underlying climate-driven vegetation mortality. Trends Ecol. Evol. 26, 523–532. doi:10.1016/j.tree.2011.06.003

McDowell, N.G., Williams, A.P., Xu, C., Pockman, W.T., Dickman, L.T., Sevanto, S., Pangle, R., Limousin, J., Plaut, J., Mackay, D.S., Ogee, J., Domec, J.C., Allen, C.D., Fisher, R.A., Jiang, X., Muss, J.D., Breshears, D.D., Rauscher, S.A., Koven, C., 2015. Multi-scale predictions of massive conifer mortality due to chronic temperature rise. Nat. Clim. Change 6, 295–300. doi:10.1038/nclimate2873

McGuire, K.J., McDonnell, J.J., Weiler, M., Kendall, C., McGlynn, B.L., Welker, J.M., Seibert, J., 2005. The role of topography on catchment-scale water residence time: Catchment-scale water residence time. Water Resour. Res. 41, n/a-n/a. doi:10.1029/2004WR003657

McKnight, D.M., Boyer, E.W., Westerhoff, P.K., Doran, P.T., Kulbe, T., Andersen, D.T., 2001. Spectrofluorometric characterization of dissolved organic matter for indication of precursor organic material and aromaticity. Limnol. Oceanogr. 46, 38–48.

Mei, Y., Hornberger, G.M., Kaplan, L.A., Newbold, J.D., Aufdenkampe, A.K., 2012. Estimation of dissolved organic carbon contribution from hillslope soils to a headwater stream: Dissolved organic carbon from soils to stream. Water Resour. Res. 48, n/a-n/a. doi:10.1029/2011WR010815

Meigs, G.W., Campbell, J.L., Zald, H.S., Bailey, J.D., Shaw, D.C., Kennedy, R.E., 2015. Does wildfire likelihood increase following insect outbreaks in conifer forests? Ecosphere 6, art118.

Meigs, G.W., Zald, H.S.J., Campbell, J.L., Keeton, W.S., Kennedy, R.E., 2016. Do insect outbreaks reduce the severity of subsequent forest fires? Environ. Res. Lett. 11, 45008. doi:10.1088/1748-9326/11/4/045008

Metcalf, M.J., Robbins, G.A., 2013. Natural Buffering of Groundwater Contaminants Related to Development in Fractured Rock. Groundw. Monit. Remediat. 33, 89–99.

Michalzik, B., Matzner, E., 1999. Dynamics of dissolved organic nitrogen and carbon in a Central European Norway spruce ecosystem. Eur. J. Soil Sci. 50, 579–590.

Mikkelson, K., Bearup, L.A., Maxwell, R.M., Stednick, J.D., McCray, J.E., Sharp, J.O., 2013a. Bark beetle infestation impacts on nutrient cycling, water quality and interdependent hydrological effects. Biogeochemistry 115, 1–21. doi:10.1007/s10533-013-9875-8

Mikkelson, K., Bokman, C.M., Sharp, J.O., 2016a. Rare Taxa Maintain Microbial Diversity and Contribute to Terrestrial Community Dynamics throughout Bark Beetle Infestation. Appl. Environ. Microbiol. 82, 6912–6919. doi:10.1128/AEM.02245-16

Mikkelson, K., Dickenson, E.R.V., Maxwell, R.M., McCray, J.E., Sharp, J.O., 2013b. Water-quality impacts from climate-induced forest die-off. Nat. Clim. Change 3, 218–222. doi:10.1038/nclimate1724

Mikkelson, K., Lozupone, C.A., Sharp, J.O., 2016b. Altered edaphic parameters couple to shifts in terrestrial bacterial community structure associated with insect-induced tree mortality. Soil Biol. Biochem. 95, 19–29. doi:10.1016/j.soilbio.2015.12.001

Mikkelson, K., Maxwell, R.M., Ferguson, I., Stednick, J.D., McCray, J.E., Sharp, J.O., 2013c. Mountain pine beetle infestation impacts: modeling water and energy budgets at the hill-slope scale: Pine Beetle Impacts On the Water and Energy Budget. Ecohydrology 6, 64–72. doi:10.1002/eco.278

Mikkelson, K.M., Lozupone, C.A., Sharp, J.O., 2015. Altered edaphic parameters couple to shifts in terrestrial bacterial community structure associated with insect-induced tree mortality. Press Soil Biol. Biogeochem.

Miller, J.D., Thode, A.E., 2007. Quantifying burn severity in a heterogeneous landscape with a relative version of the delta Normalized Burn Ratio (dNBR). Remote Sens. Environ. 109, 66–80. doi:10.1016/j.rse.2006.12.006

Miller, J.D., Yool, S.R., 2002. Mapping forest post-fire canopy consumption in several overstory types using multi-temporal Landsat TM and ETM data. Remote Sens. Environ. 82, 481–496. doi:10.1016/S0034-4257(02)00071-8

Moorcroft, M.J., Davis, J., Compton, R.G., 2001. Detection and determination of nitrate and nitrite: a review. Talanta 54, 785–803.

Moore, D., Trahan, N., Wilkes, P., Quaife, T., Stephens, B., Elder, K., Desai, A., Negron, J., Monson, R., 2013. Persistent reduced ecosystem respiration after insect disturbance in high elevated forests. Ecol. Lett. 16, 731–737.

Mooshammer, M., Wanek, W., Hämmerle, I., Fuchslueger, L., Hofhansl, F., Knoltsch, A., Schnecker, J., Takriti, M., Watzka, M., Wild, B., Keiblinger, K.M., Zechmeister-Boltenstern, S., Richter, A., 2014. Adjustment of microbial nitrogen use efficiency to carbon:nitrogen imbalances regulates soil nitrogen cycling. Nat. Commun. 5. doi:10.1038/ncomms4694

Morehouse, K., Johns, T., Kaye, J., Kaye, M., 2008. Carbon and nitrogen cycling immediately following bark beetle outbreaks in southwestern ponderosa pine forests. For. Ecol. Manag. 255, 2698–2708. doi:10.1016/j.foreco.2008.01.050

Muggeo, V.M., 2003. Estimating regression models with unknown break-points. Stat. Med. 22, 3055–3071.

Neff, J.C., Asner, G.P., 2001. Dissolved Organic Carbon in Terrestrial Ecosystems: Synthesis and a Model. Ecosystems 4, 29–48. doi:10.1007/s100210000058

Nikolaou, A., Lekkas, T., 2001. The role of natural organic matter during formation of chlorination by products_a review.pdf. Acta Hydroch Hydrob 29, 63–77.

Norton, U., Ewers, B.E., Borkhuu, B., Brown, N.R., Pendall, E., 2015. Soil nitrogen five years after bark beetle infestation in lodgepole pine forests. Soil Sci. Soc. Am. J. 79, 282–293.

Orchard, V.A., Cook, F.J., 1983. Relationship between soil respiration and soil moisture. Soil Biol. Biochem. 15, 447–453.

Page, W.G., Jenkins, M.J., Runyon, J.B., 2012. Mountain pine beetle attack alters the chemistry and flammability of lodgepole pine foliage. Can. J. For. Res. 42, 1631–1647. doi:10.1139/x2012-094

Park Williams, A., Allen, C.D., Macalady, A.K., Griffin, D., Woodhouse, C.A., Meko, D.M., Swetnam, T.W., Rauscher, S.A., Seager, R., Grissino-Mayer, H.D., Dean, J.S., Cook, E.R., Gangodagamage, C., Cai, M., McDowell, N.G., 2012. Temperature as a potent driver of regional forest drought stress and tree mortality. Nat. Clim. Change 3, 292–297. doi:10.1038/nclimate1693

Parsons, W.F.J., Knight, D.H., Miller, S.L., 1994. Root Gap Dynamics in Lodgepole Pine Forest: Nitrogen Transformations in Gaps of Different Size. Ecol. Appl. 4, 354. doi:10.2307/1941939

Penn, C.A., Bearup, L.A., Maxwell, R.M., Clow, D.W., 2016. Numerical experiments to explain multiscale hydrological responses to mountain pine beetle tree mortality in a headwater watershed. Water Resour. Res. n/a-n/a. doi:10.1002/2015WR018300

Pierce, L.L., Running, S.W., 1988. Rapid Estimation of Coniferous Forest Leaf Area Index Using a Portable Integrating Radiometer. Ecology 69, 1762–1767. doi:10.2307/1941154

Poppleton, J., 2008. A good intention gone wrong. Headwaters Colo. Found. Water Educ. 19–23.

Postel, S.L., Thompson, B.H., 2005. Watershed protection: Capturing the benefits of nature's water supply services. Nat. Resour. Forum 29, 98–108.

Prescott, C.E., Hope, G.D., Blevins, L.L., 2003. Effect of gap size on litter decomposition and soil nitrate concentrations in a high-elevation spruce fir forest. Can. J. For. Res. 33, 2210–2220.

Prescott, C.E., Zabek, L.M., Staley, C.L., Kabzems, R., 2000. Decomposition of broadleaf and needle litter in forests of British Columbia: influences of litter type, forest type, and litter mixtures. Can. J. For. Res. 30, 1742–1750.

Pugh, E., Gordon, E., 2013. A conceptual model of water yield effects from beetle-induced tree death in snow-dominated lodgepole pine forests. Hydrol. Process. 27, 2048–2060. doi:10.1002/hyp.9312

R Core Team, 2015. R: A language and environment for statistical computing. R Foundation for Statistical Computing, Vienna, Austria.

R Core Team, 2014. . R Foundation for Statistical Computing, Vienna, Austria.

Raffa, K.F., Aukema, B.H., Bentz, B.J., Carroll, A.L., Hicke, J.A., Turner, M.G., Romme, W.H., 2008. Cross-scale drivers of natural disturbances prone to anthropogenic amplification: the dynamics of bark beetle eruptions. Bioscience 58, 501–517.

Rhoades, C.C., McCutchan, J.H., Cooper, L.A., Clow, D., Detmer, T.M., Briggs, J.S., Stednick, J.D., Veblen, T.T., Ertz, R.M., Likens, G.E., others, 2013. Biogeochemistry of beetle-killed forests: Explaining a weak nitrate response. Proc. Natl. Acad. Sci. 110, 1756–1760.

Richardson, S.D., Postigo, C., 2011. Drinking Water Disinfection By-products, in: Barceló, D. (Ed.), Emerging Organic Contaminants and Human Health. Springer Berlin Heidelberg, Berlin, Heidelberg, pp. 93–137.

Ryan, M.G., Waring, R.H., 1992. Maintenance Respiration and Stand Development in a Subalpine Lodgepole Pine Forest. Ecology 73, 2100–2108. doi:10.2307/1941458

Schimel, J., Bennett, J., 2004. Nitrogen mineralization- challenges of a changing paradigm. Ecology 85, 591–602.

Schoennagel, T., Veblen, T.T., Negron, J.F., Smith, J.M., 2012. Effects of Mountain Pine Beetle on Fuels and Expected Fire Behavior in Lodgepole Pine Forests, Colorado, USA. PLoS ONE 7, e30002. doi:10.1371/journal.pone.0030002

Schwalm, C.R., Williams, C.A., Schaefer, K., Baldocchi, D., Black, T.A., Goldstein, A.H., Law, B.E., Oechel, W.C., Paw U, K.T., Scott, R.L., 2012. Reduction in carbon uptake during turn of the century drought in western North America. Nat. Geosci. 5, 551–556. doi:10.1038/ngeo1529

Seidl, R., Schelhaas, M.-J., Lexer, M.J., 2011. Unraveling the drivers of intensifying forest disturbance regimes in Europe: Drivers of Forest Disturbance Intensification. Glob. Change Biol. 17, 2842–2852. doi:10.1111/j.1365-2486.2011.02452.x

Simard, M., Romme, W.H., Griffin, J.M., Turner, M.G., 2011. Do mountain pine beetle outbreaks change the probability of active crown fire in lodgepole pine forests? Ecol. Monogr. 81, 3–24. doi:10.1890/10-1176.1

Smith, H.G., Sheridan, G.J., Lane, P.N.J., Nyman, P., Haydon, S., 2011. Wildfire effects on water quality in forest catchments: A review with implications for water supply. J. Hydrol. 396, 170–192. doi:10.1016/j.jhydrol.2010.10.043

Soverel, N.O., Perrakis, D.D.B., Coops, N.C., 2010. Estimating burn severity from Landsat dNBR and RdNBR indices across western Canada. Remote Sens. Environ. 114, 1896–1909. doi:10.1016/j.rse.2010.03.013

Sparks, D., Page, A., Helmke, P., Loeppert, R., Soltanpour, P., Tabatabai, M., Johnston, C., Sumner, M., 1996. Methods of soil analysis. Part 3-Chemical Methods. Soil Science Society of America Inc.

Speckman, H.N., Frank, J.M., Bradford, J.B., Miles, B.L., Massman, W.J., Parton, W.J., Ryan, M.G., 2015. Forest ecosystem respiration estimated from eddy covariance and chamber measurements under high turbulence and substantial tree mortality from bark beetles. Glob. Change Biol. 21, 708–721. doi:10.1111/gcb.12731

Stump, L., Binkley, D., 1993. Relationships between litter quality and nitrogen availability in Rocky Mountain forests. Can. J. For. Res. 23, 492–502.

ŠturSová, M., Šnajdr, J., Cajthaml, T., Bárta, J., Šantrůčková, H., Baldrian, P., 2014. When the forest dies: the response of forest soil fungi to a bark beetle-induced tree dieback. ISME J. 8, 1920–1931. doi:10.1038/ismej.2014.37

Tate, R., 1995. Soil Microbiology. Wiley & Sons, New York.

Thompson, M.P., Haas, J.R., Finney, M.A., Calkin, D.E., Hand, M.S., Browne, M.J., Halek, M., Short, K.C., Grenfell, I.C., 2015. Development and application of a probabilistic method for wildfire suppression cost modeling. For. Policy Econ. 50, 249–258. doi:10.1016/j.forpol.2014.10.001

Thurman, E.M., 1985. Organic Geochemistry of Natural Waters. Springer Netherlands, Dordrecht.

Tokuchi, N., Ohte, N., Hobara, S., Kim, S.-J., Masanori, K., 2004. Changes in biogeochemical cycling following forest defoliation by pine wilt disease in Kiryu experimental catchment in Japan. Hydrol. Process. 18, 2727–2736. doi:10.1002/hyp.5578

Tong, S.T.Y., Chen, W., 2002. Modeling the relationship between land use and surface water quality. J. Environ. Manage. 66, 377–393. doi:10.1006/jema.2002.0593

Trahan, N.A., Dynes, E.L., Pugh, E., Moore, D.J.P., Monson, R.K., 2015. Changes in soil biogeochemistry following disturbance by girdling and mountain pine beetles in subalpine forests. Oecologia 177, 981–995. doi:10.1007/s00442-015-3227-4

United States Forest Service. 2008 Report: The Health of Colorado's Forests, 2008. http://static.colostate.edu/client-files/csfs/pdfs/894651_08FrstHlth_www.pdf (accessed 7.10.16)

USDA, 2017. The PLANTS Database.

Vendettuoli, J.F., Orwig, D.A., Krumins, J.A., Waterhouse, M.D., Preisser, E.L., 2015. Hemlock woolly adelgid alters fine root bacterial abundance and mycorrhizal associations in eastern hemlock. For. Ecol. Manag. 339, 112–116.

Vitousek, P., Gosz, J., Grier, C., Melillo, J., Reiners, W., Todd, R., 1979. Nitrate losses from disturbed ecosystems. Science 204, 469–474.

Walker, T., Bais, H., Grotewold, E., Vivanco, J., 2003. Root exudation and rhizosphere biology. Plant Physiol. 132, 44–51.

Wear, D.N., Coulston, J.W., 2015. From sink to source: Regional variation in U.S. forest carbon futures. Sci. Rep. 5, 16518. doi:10.1038/srep16518

Weintraub, M.N., Scott-Denton, L.E., Schmidt, S.K., Monson, R.K., 2007. The effects of tree rhizodeposition on soil exoenzyme activity, dissolved organic carbon, and nutrient availability in a subalpine forest ecosystem. Oecologia 154, 327–338. doi:10.1007/s00442-007-0804-1

Westerling, A.L., 2006. Warming and Earlier Spring Increase Western U.S. Forest Wildfire Activity. Science 313, 940–943. doi:10.1126/science.1128834

Whitworth, K.L., Baldwin, D.S., Kerr, J.L., 2012. Drought, floods and water quality: Drivers of a severe hypoxic blackwater event in a major river system (the southern Murray–Darling Basin, Australia). J. Hydrol. 450–451, 190–198. doi:10.1016/j.jhydrol.2012.04.057

Williams, A.P., Allen, C.D., Millar, C.I., Swetnam, T.W., Michaelsen, J., Still, C.J., Leavitt, S.W., 2010. Forest responses to increasing aridity and warmth in the southwestern United States. Proc. Natl. Acad. Sci. 107, 21289–21294. doi:10.1073/pnas.0914211107

Woo, K.L., Watson, P., Mansfield, S.D., 2007. The effects of mountain pine beetle attack on lodgepole pine wood morphology and chemistry: Implications for wood and fiber quality. Wood Fiber Sci. 37, 112–126.

Xie, Y., 2003. Disinfection byproducts in drinking water: Formation, analysis, and control. CRC Press, Boca Raton, FL.

Xiong, Y., D'Atri, J.J., Fu, S., Xia, H., Seastedt, T.R., 2011. Rapid soil organic matter loss from forest dieback in a subalpine coniferous ecosystem. Soil Biol. Biochem. 43, 2450–2456. doi:10.1016/j.soilbio.2011.08.013

Xu, N., Saiers, J.E., 2010. Temperature and Hydrologic Controls on Dissolved Organic Matter Mobilization and Transport within a Forest Topsoil. Environ. Sci. Technol. 44, 5423–5429. doi:10.1021/es1002296

Yavitt, J.B., Fahey, T.J., 1986. Litter Decay and Leaching from the Forest Floor in Pinus Contorta (Lodgepole Pine) Ecosystems. J. Ecol. 74, 525. doi:10.2307/2260272

Zhou, H., Zhu, J.Y., Luo, X., Leu, S.-Y., Wu, X., Gleisner, R., Dien, B.S., Hector, R.E., Yang, D., Qiu, X., Horn, E., Negron, J., 2013. Bioconversion of Beetle-Killed Lodgepole Pine Using SPORL: Process Scale-up Design, Lignin Coproduct, and High Solids Fermentation without Detoxification. Ind. Eng. Chem. Res. 52, 16057–16065. doi:10.1021/ie402873y

Zimmermann, L., Moritz, K., Kennel, M., Bittersohl, J., 2000. Influence of bark beetle infestation on water quantity and quality in the Grosse Ohe catchment(Bavarian Forest National Park). Silva Gabreta 4, 51–62.

APPENDIX A

SUPPLEMENTAL INFORMATION TO CHAPTER 2

Table A.1: Watershed characteristics.

Water Treatment Facility	Infestation Level	Surface Water Source	Mean Basin Elevation (m)	Watershed Area (km^2)
Steamboat Springs	High	Fish Creek	2969	66
Granby		Fraser River	3021	755
Gypsum	Moderate	Gypsum Creek	2935	171
Glenwood Springs		Grizzly/No Name Creek	3139/2993	139
Carbondale	Low	Nettle Creek	2835	10
Aspen		Castle/Maroon Creek	3383/3414	288

Table A.2: Historical trends in total organic carbon (TOC) and total trihalomethane (TTHM) concentrations from 2004-2014 for all watersheds analyzed.

Watershed	Infestation Level	TOC Slope from 2004-2014 ($mg\ L^{-1}\ yr^{-1}$)	P-value for TOC Trend	TTHM Slope from 2004-2014 ($mg\ L^{-1}\ yr^{-1}$)	P-value for TTHM Trend
Steamboat Springs	High	0.05	0.001	2.22	0.014
Granby		0.03	<0.001	2.53	<0.001
Gypsum	Moderate	0.04	0.944	N/A	N/A
Glenwood Springs		0.00	0.507	N/A	N/A
Carbondale	Low	0.00	0.087	N/A	N/A
Aspen		0.01	0.052	-0.09	0.152

Missing TTHM slopes and p-values are a result of missing data when municipalities switched to a reduced monitoring schedule

Table A.3: Historic quarterly five haloacetic acid (HAA5) and total trihalomethane (TTHM) concentration samples collected from the distribution system for Environmental Protection Agency reporting. Units are ug/L.

HAA5	2011				2012				2013				2014			
	Q1	Q2	Q3	Q4	Q1	Q2	Q3	Q4	Q1	Q2	Q3	Q4	Q1	Q2	Q3	Q4
Steamboat Springs	18.40	37.30	60.95*	49.30	21.10	8.50	53.75*	42.90	30.30	62.10	39.05*	45.40*	45.30	36.15	40.05	62.55
Granby	0.00	23.90	34.90	14.10	21.90	21.30	36.50	13.10	0.00	2.50	22.20	18.60	20.60	31.90	23.10	20.70
Gypsum			0.65*				2.60*				1.05*				1.60*	
Glenwood Springs			26.60				11.90	10.10			11.80	19.35	8.05*	43.00*	21.50*	12.45*
Carbondale			3.07*				1.67*				1.07*				2.80*	
Aspen	5.40*	8.32*	3.54*	4.66*	2.95*	10.60*	6.21*	3.31*	2.49*	19.85*	7.46*	5.54*	3.45*	14.00*	9.07*	7.27*

TTHM	2011				2012				2013				2014			
	Q1	Q2	Q3	Q4	Q1	Q2	Q3	Q4	Q1	Q2	Q3	Q4	Q1	Q2	Q3	Q4
Steamboat Springs	12.60	21.70	74.45*	26.60	14.30	6.90	67.35*	29.60	28.40	35.10	54.70*	95.05*	50.75*	30.35*	51.90*	108.80
Granby	51.10	28.10	26.30	46.80	48.40	40.80	56.60	47.40	57.20	45.40	38.10	85.80	44.40	48.00	32.50	73.80
Gypsum			5.95*				7.50*				11.40*				12.95*	
Glenwood Springs			33.10				19.70	20.30			22.90*	25.40*	8.90*	42.50*	37.48*	23.55*
Carbondale			6.43*				5.70*				8.50*				7.50*	
Aspen	6.95*	13.35*	7.13*	6.49*	5.56*	16.30*	5.32*	11.08*	3.16*	15.90*	13.30*	11.40*	5.93*	17.95*	11.15*	9.96*

* =average of 2 samples or more

=At least one sample within 80% of MCL

=At least one sample over MCL

Gypsum, Carbondale, and Glenwood Springs are on a reduced monitoring schedule.

Regulatory maximum contaminant levels for HAA5 = 60 ug/L

Regulatory maximum contaminant levels for TTHM = 80 ug/L

Q1, Q2, Q3 and Q4 represent quarters 1,2,3 and 4 respectively.

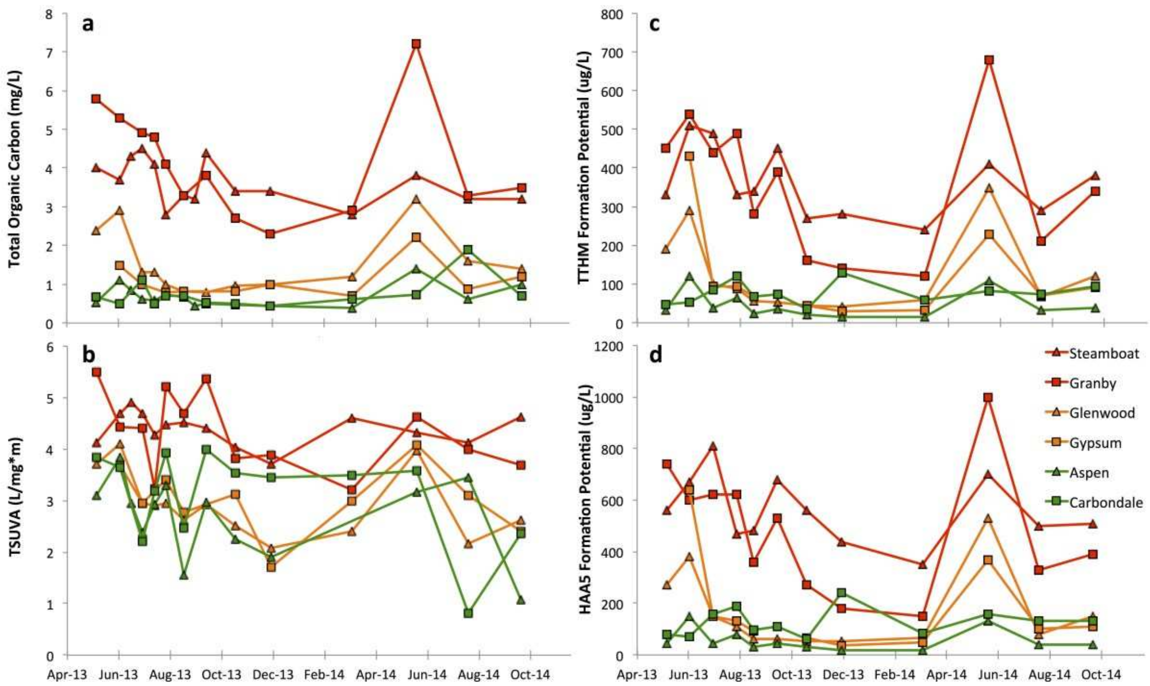

Figure A.1: Water quality parameters for each individual watershed during 2013 and 2014 surface water sampling with panels displaying **a.** total organic carbon **b.** total specific ultraviolet absorbance (TSUVA) **c.** total trihalomethane (TTHM) formation potential and **d.** five haloacetic acid (HAA5) formation potential.

A.1 Additional Carbon Character Analysis Information

Fluorescence index was calculated from the ratio of intensities at emission wavelengths 470 and 520 nm (both at an excitation wavelength of 370 nm) (McKnight et al., 2001). Maximum intensities for Peak A were found between 240-270 nm excitation and 380-460 nm emission and Peak C maximum intensities were found between 300-360 nm excitation and 400-480 nm emission (Coble, 1996). Fluorescence regional integration was also found for five regions in the EEMs which were defined as: aromatic protein Region I (ex: 240-250 nm; em: 280-330 nm); aromatic protein Region II (ex: 240-250 nm; em: 331-380 nm); fulvic acid-like Region III (ex: 240-250 nm; em:381-580 nm);

soluble microbial byproduct-like Region IV (ex: 252.5-450 nm; em:280-380 nm); and humic acid-like Region V (ex: 252.5-450 nm; em:381-580 nm) (Chen et al., 2003). Due to instrument limitations with the lowest excitation wavelengths beginning at 240 nm creating smaller Regions I-III compared to what is typical, most attention was given to Region IV and V. As some samples were damaged in transport or were lost in shipping, the fluorescence index, specific peak intensity, and fluorescence regional integration results displayed below represent the averaged values for eight sampling dates when all watershed samples were tested to prevent bias. Standard deviation values are shown for temporal variability.

A.2 Additional Climatic and Vegetative Difference Analyses

Historical analysis of precipitation data exhibited either insignificant (two watersheds) or drying trends (3 watersheds) during the analysis period with a maximum slope of -1.42 mm yr $^{-1}$. Although the watersheds displaying a decreasing precipitation trend were high or moderate impact watersheds, drier conditions aren't expected to be the culprit for the observed increasing TOC or TTHMs slopes; rather, it supports the link between drought and expanding insect infestation (Raffa et al., 2008; Williams et al., 2010). Specifically, peaks in TOC concentration and DBP precursor levels occur during flushing events in spring and summer months as snow melts (Figure 3.3). Therefore, decreasing precipitation should lower TOC degradation and transport, yet an increasing trend still occurs in high impacted sites. Historical temperature data were available for three watersheds analyzed in the study, which also displayed limited trends during the analysis period with Aspen being the only watershed displaying a significant slope of -0.07 ^{o}C yr $^{-1}$. Precipitation normals between all 6 watersheds were found to be significantly different, presumably due to watershed location and orographic effects (Houze, 2012) with annual rates ranging from 0.29 to 0.663 m/yr while temperature normals between watersheds were not significant. When comparing 30-year precipitation normals for two watersheds at a time it is clear that precipitation rates are not a primary control on water quality differences across infestation bins as normal precipitation rates were not significantly different between Aspen and Steamboat (P-value=1.00) or Granby and Glenwood Springs (P-value=0.095).

The majority of evergreen forest watersheds in the Rocky Mountain region are now beetle impacted. This limited control watersheds to those containing more area above tree line where rock outcrops, talus slopes, and other regions free of vegetation are found. Vegetation differences likely contribute to the higher TOC and DBP precursor levels in the moderate and high impact sites compared to control facilities (Hood et al., 2005), but this does not explain the historical increasing trends seen following beetle infestation as vegetated area remained constant, suggesting differences in organic carbon concentration is associated with beetle-induced forest die-off. Additionally, the percent of each watershed classified as developed in the NLCD revealed no or insignificant changes between 2001 and 2011, negating the possibility of increased development driving TOC historical trends in the high impact sites (Table A.4).

Table A.4: Percentage of each watershed developed in 2001 and 2011.

Analysis Year	Development Type	Steamboat	Granby	Glenwood Springs	Gypsum	Carbondale	Aspen
2001	Open space	0.20	0.99	0.00	0.00	0.00	0.00
	Low Intensity	0.01	0.57	0.00	0.00	0.00	0.00
	Medium Intensity	0.00	0.11	0.00	0.00	0.00	0.00
	High Intensity	0.00	0.01	0.00	0.00	0.00	0.00
2011	Open space	0.20	1.03	0.00	0.00	0.00	0.00
	Low Intensity	0.01	0.57	0.00	0.00	0.00	0.00
	Medium Intensity	0.00	0.18	0.00	0.00	0.00	0.00
	High Intensity	0.00	0.02	0.00	0.00	0.00	0.00

Table A.5: Precipitation rates for each watershed shown as a percentage compared to the 30-year average monthly rate, with all watersheds displaying precipitation rates of approximately 200% of the 30-year average during September 2013.

Site	Infestation Level	April	May	June	July	August	September	October
Steamboat Springs	High	101.6	131.8	6.2	195.3	61.0	232.4 (129.3)	167.1
Granby		164.3	146.2	0.9	116.3	110.2	196.4 (80.3)	75.2
Glenwood Springs	Moderate	160.3	114.4	4.0	80.9	134.9	214.6 (106.3)	212.2
Gypsum		280.3	150.2	0.0	81.6	60.0	190.0 (69.0)	148.0
Aspen	Low	155.3	114.7	9.0	126.1	124.5	208.4 (108.5)	96.3

Absolute precipitation rates in millimeters are shown in parentheses for September

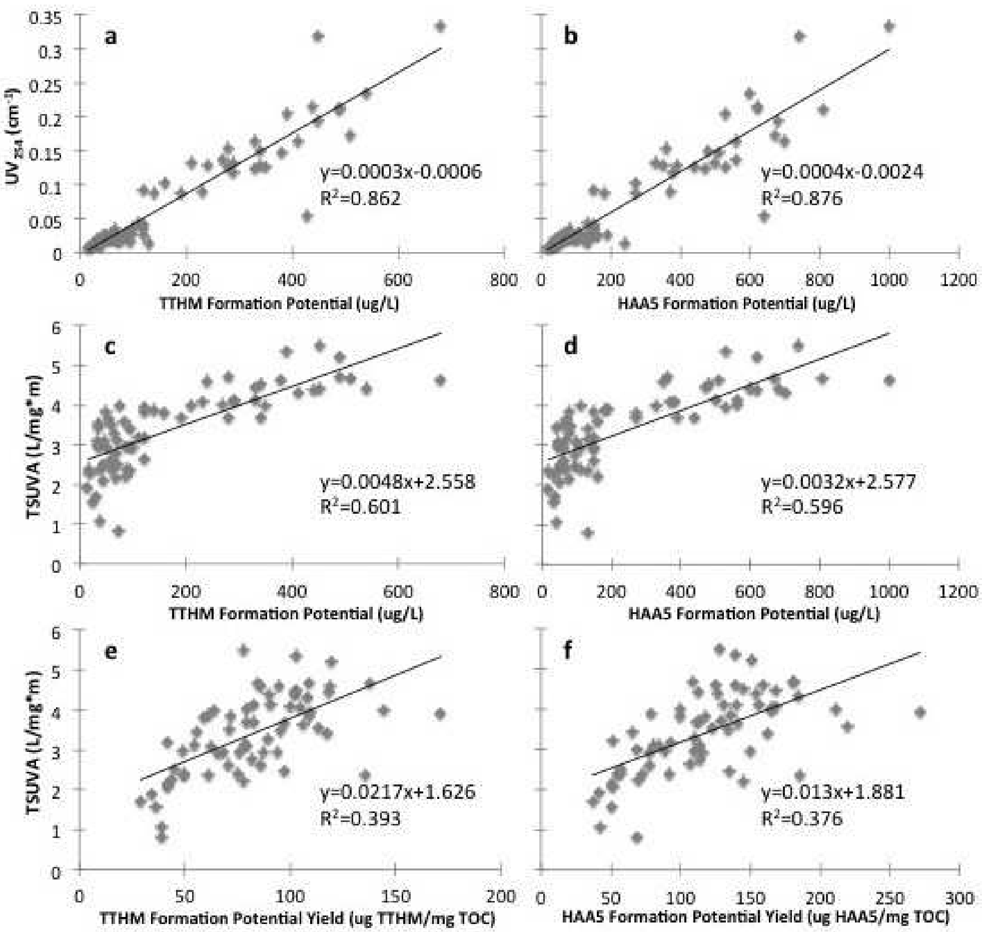

Figure A.2: Linear trends and correlations for ultraviolet absorbance spectroscopy at 254 nm versus **(a)** total trihalomethane (TTHM) or **(b)** five haloacetic acid (HAA5) formation potential. Linear trends and correlations for total specific ultraviolet absorbance (TSUVA) versus **(c)** TTHM or **(d)** HAA5 formation potential. Linear trends and correlations for total specific ultraviolet absorbance (TSUVA) versus **(e)** carbon normalized TTHM formation potential or **(f)** carbon normalized HAA5 formation potential. The data presented encompasses 2013-2014 surface water sampling results across all sites. Significance was established with p-values for all plots being < 0.001.

APPENDIX B

SUPPLEMENTAL INFORMATION TO CHAPTER 4

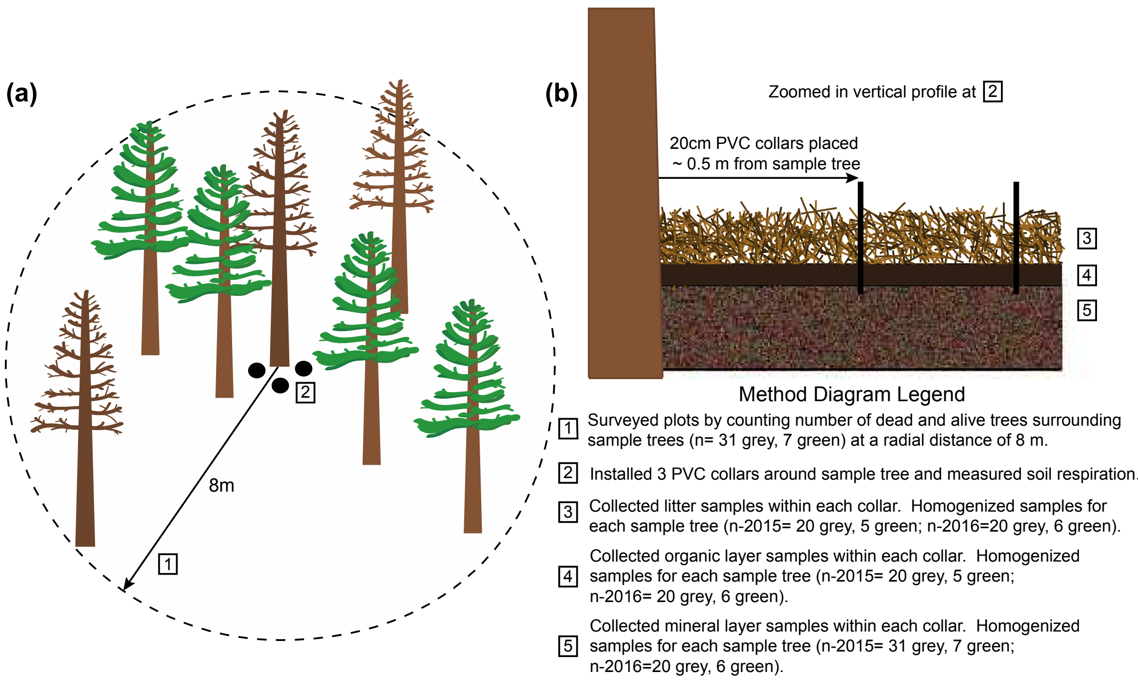

Figure B.1: Diagram depicting (a) survey methods quantifying severity of plot mortality and (b) biogeochemical sampling methods.

Table B.1: Table of site descriptive characteristics. Grey-centered tree plots are binned by percent of surrounding tree mortality.

	Green Trees Mean (SD)	Grey Trees 0-25% Mean (SD)	Grey Trees 25-40% Mean (SD)	Grey Trees 40-59% Mean (SD)	Grey Trees >59% Mean (SD)
n	7	7	8	8	8
Diameter (cm)	22.1 (2.6)	25.4 (2.7)	24.3 (3.6)	26.0 (3.4)	28.4 (3.4)
Elevation (m)	2959 (51)	2984 (50)	2934 (75)	3057 (45)	3016 (55)
Slope (degrees)	17.8 (5.2)	17.7 (3.2)	14.1 (4.5)	19.9 (2.3)	19.0 (5.5)
Aspect (degrees)	116.6 (10.9)	111.3 (10.6)	114.0 (6.5)	113.4 (11.8)	117.9 (4.9)
Density (trees/m^2)	0.19 (0.05)	0.16 (0.03)	0.18 (0.06)	0.11 (0.04)	0.09 (0.03)

Notes:
SD: Standard deviation
n: Number of trees in bin

Table B.2: Changes in litter layer biogeochemical properties as a function of tree stage and sampling year. Significant differences are denoted in bold with an asterisk (p-value < 0.05).

Parameter	2015 (Wet Conditions)				2016 (Dry Conditions)			
	Green Average (SD)[1]	Grey Average (SD)[1]	Mann-Whitney U[2]	Spearman rho[3]	Green Average (SD)[1]	Grey Average (SD)[1]	Mann-Whitney U[2]	Spearman rho[3]
pH	4.77 (±0.23)	5.19 (±0.42)	**18***	-0.206	-	-	-	-
Water Content (% wet weight)	40.75 (±8.87)	41.88 (±8.37)	40	-0.420	28.22 (±6.32)	26.66 (±6.47)	53	-0.020
DOC (mg-C/kg dry sample)	820 (±253)	1034 (±395)	35	-0.171	1220 (±155)	1280 (±359)	60	-0.032
SUVA (kg dry sample/mg*M)	0.20 (±0.03)	0.25 (±0.06)	25	0.383	0.20 (±.03)	0.23 (±0.03)	32	0.134
Organic Matter (%)	47.59 (±17.69)	56.78 (±16.32)	37	0.224	86.68 (4.82)	88.64 (±7.22)	37	-0.202
Total Nitrogen (mg-N/kg dry sample)	36.20 (±14.91)	45.87 (±16.73)	29	0.350	49.65 (±11.63)	78.61 (±45.47)	**27***	**0.543***
NO_3^- (mg-N/kg dry sample)	8.80 (±3.23)	11.38 (±5.32)	37	-0.014	14.55 (±2.29)	21.70 (±9.55)	28	**0.477***
NH_4^+ (mg-N/kg dry sample)	2.02 (±1.74)	7.33 (±9.72)	29	**0.790***	4.80 (±2.80)	19.41 (±21.89)	41	0.424
Organic Nitrogen (mg-N/kg dry sample)	25.38 (±11.77)	27.16 (±9.56)	41	0.011	30.30 (±8.47)	37.49 (±19.91)	45	0.382
NO_3^-/TN	0.24 (±0.04)	0.26 (±0.10)	45	-0.266	0.30 (±0.06)	0.30 (±0.09)	59	-0.029
NH_4^+/TN	0.06 (±0.05)	0.13 (±0.13)	32	**0.776***	0.09 (±0.03)	0.20 (±0.13)	40	0.358
Organic N/TN	0.70 (±.06)	0.61 (±0.13)	25	**-0.550***	0.61 (±0.06)	0.50 (±0.08)	**17***	**-0.586***
C:N (molar ratio)	27.33 (±5.20)	28.04 (±9.81)	49	**-0.591***	29.45 (±3.89)	22.78 (±8.59)	35	**-0.585***

Year 1 (wet conditions): n=20 grey, 5 green
Year 2 (dry conditions): n=20 grey, 6 green
[1] Average parameter ± their standard deviation (SD)
[2] Difference between green and grey phase trees
[3] Nonlinear correlation between parameter under grey phase trees and plot-level severity of tree mortality

Table B.3: Changes in organic layer biogeochemical properties as a function of tree stage and sampling year. Significant differences are denoted in bold with an asterisk (p-value < 0.05).

Parameter	2015 (Wet Conditions)				2016 (Dry Conditions)			
	Green Average (SD)[1]	Grey Average (SD)[1]	Mann-Whitney U[2]	Spearman rho[3]	Green Average (SD)[1]	Grey Average (SD)[1]	Mann-Whitney U[2]	Spearman rho[3]
pH	4.97 (±0.11)	5.52 (±0.34)	**3***	-0.014	-	-	-	-
Water Content (% wet weight)	10.70 (±3.84)	17.54 (±3.73)	**11***	-0.104	26.58 (±5.91)	28.77 (±11.06)	53	-0.152
DOC (mg-C/kg dry sample)	245 (±146)	167 (±75)	35	-0.386	770 (±266)	974 (±528)	47	-0.400
SUVA (kg dry sample/mg*M)	0.45 (±0.11)	0.58 (±0.08)	21	0.371	0.32 (±0.06)	0.42 (±0.10)	28	0.212
Organic Matter (%)	5.31 (±1.01)	7.28 (±3.11)	29	**0.522***	45.98 (±12.14)	54.60 (±20.89)	43	-0.370
Total Nitrogen (mg-N/kg dry sample)	7.02 (±1.96)	9.07 (±3.56)	28	0.278	41.84 (20.50)	58.65 (±25.07)	37	-0.117
NO_3^- (mg-N/kg dry sample)	1.97 (±0.85)	2.51 (±0.87)	32	-0.195	8.34 (±4.44)	17.82 (±10.56)	**27***	-0.159
NH_4^+ (mg-N/kg dry sample)	0.42 (±0.11)	2.10 (±3.53)	30	**0.746***	5.75 (±5.24)	9.50 (±9.10)	40	**0.577***
Organic Nitrogen (mg-N/kg dry sample)	4.63 (±1.83)	4.46 (±1.52)	43	-0.260	27.75 (±11.42)	31.32 (±15.13)	52	**-0.462***
NO_3^-/TN	0.29 (±0.13)	0.30 (±0.11)	45	-0.421	0.20 (±0.04)	0.30 (±0.12)	29	-0.095
NH_4^+/TN	0.06 (±0.01)	0.18 (±0.20)	37	**0.795***	0.12 (±0.05)	0.17 (±0.12)	53	**0.690***
Organic N/TN	0.65 (±0.13)	0.52 (±0.15)	27	**-0.504***	0.68 (±0.04)	0.54 (±0.11)	**11***	**-0.651***
C:N (molar ratio)	39.51 (±20.08)	22.13 (±7.18)	**16***	**-0.780***	22.95 (±0.57)	19.38 (±6.58)	44	**-0.623***

Year 1 (wet conditions): n=20 grey, 5 green
Year 2 (dry conditions): n=20 grey, 6 green
[1] Average parameter ± their standard deviation (SD)
[2] Difference between green and grey phase trees
[3] Nonlinear correlation between parameter under grey phase trees and plot-level severity of tree mortality

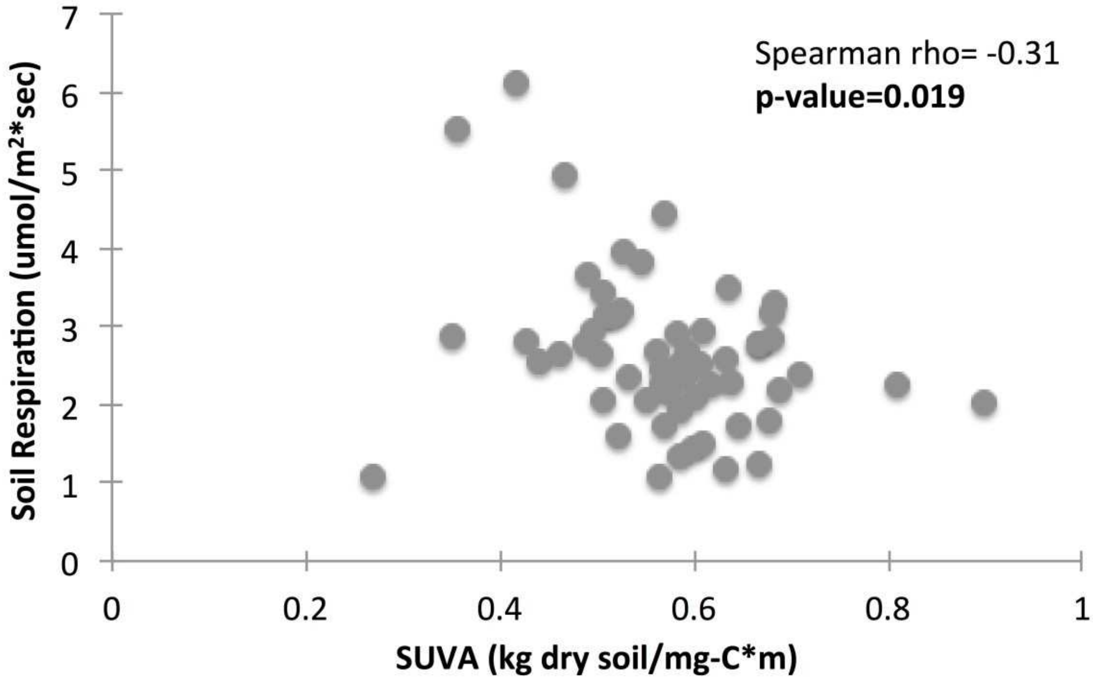

Figure B.2: Averaged soil respiration at each of the three PVC rings below grey phase trees compared to the carbon normalized specific ultraviolet absorbance (SUVA) at 254nm in the mineral layer during 2016. A similar declining trend in soil respiration with increasing SUVA was also found below grey phase trees in 2015.

APPENDIX C

COPYRIGHT PERMISSIONS

Appendix C contains the permission from Licensed Publisher-Elsevier for reprinting the manuscript within this Thesis.

Copyright Clearance Center RightsLink®

Home | Account Info | Help

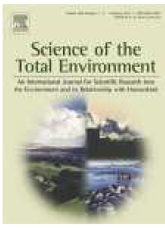

Title: Water quality following extensive beetle-induced tree mortality: Interplay of aromatic carbon loading, disinfection byproducts, and hydrologic drivers

Author: Brent M. Brouillard,Eric R.V. Dickenson,Kristin M. Mikkelson,Jonathan O. Sharp

Publication: Science of The Total Environment

Publisher: Elsevier

Date: 1 December 2016

Logged in as:
brent brouillard
LOGOUT

Order Completed

Thank you for your order.

This Agreement between brent brouillard ("You") and Elsevier ("Elsevier") consists of your license details and the terms and conditions provided by Elsevier and Copyright Clearance Center.

Your confirmation email will contain your order number for future reference.

Printable details.

License Number	4032570313053
License date	Jan 19, 2017
Licensed Content Publisher	Elsevier
Licensed Content Publication	Science of The Total Environment
Licensed Content Title	Water quality following extensive beetle-induced tree mortality: Interplay of aromatic carbon loading, disinfection byproducts, and hydrologic drivers
Licensed Content Author	Brent M. Brouillard,Eric R.V. Dickenson,Kristin M. Mikkelson,Jonathan O. Sharp
Licensed Content Date	1 December 2016
Licensed Content Volume	572
Licensed Content Issue	n/a
Licensed Content Pages	11
Type of Use	reuse in a thesis/dissertation
Portion	full article
Format	both print and electronic
Are you the author of this Elsevier article?	Yes
Will you be translating?	No
Order reference number	
Title of your thesis/dissertation	Biogeochemical and Ecological Impacts Resulting From Beetle-Induced Forest Mortality
Expected completion date	Feb 2017
Estimated size (number of pages)	140
Elsevier VAT number	GB 494 6272 12

Requestor Location	brent brouillard 1500 Illinois St. GOLDEN, CO 80401 United States Attn: brent brouillard
Total	0.00 USD

ORDER MORE CLOSE WINDOW